Study on Some Elastodynamic Problems in Materials with Microstructure and with Reinforced Fibres

A

Thesis

submitted in fulfillment of the requirement

for the award of the degree

of

Doctor of Philosophy

in

Mathematics

by

Tanupreet Kaur

(Registration No. : 901211006)

School of Mathematics

Thapar University - 147 004 (Punjab), India

October-2016

DEDICATED

TO

THE ALMIGHTY

&

MY PARENTS

Certificate

This is to certify that the thesis entitled, "Study on Some Elastodynamic Problems in Materials with Microstructure and with Reinforced Fibres," submitted by Ms. Tanupreet Kaur in the fulfillment of the requirement for the award of the degree of Doctor of Philosophy in School of Mathematics, Thapar University, Patiala, is a record of candidates own work carried out by her under my supervision and guidance.

The matter presented in this thesis has not been submitted in part or full for the award of any degree in any other University or Institute.

Attestation by supervisor

Dr. Satish Kumar Sharma
Assistant Professor
School of Mathematics
Thapar University
Patiala-147004
INDIA

Declaration

I hereby declare that the research work presented in this thesis entitled, "Study on Some Elastodynamic Problems in Materials with Microstructure and with Reinforced Fibres," submitted for the award of the degree of Doctor of Philosophy in School of Mathematics, Thapar University, Patiala is an authenticated record of my own research work carried out under the supervision of Dr. Satish Kumar Sharma (School of Mathematics) and refers other researcher's work are duly listed in the bibliography section.

The matter embodied in this thesis has not been submitted in part or full to any other university or institute for the award of any degree.

Tanupreet Kaur

Attestation by supervisor

Dr. Satish Kumar Sharma
Assistant Professor
School of Mathematics
Thapar University
Patiala-147004
INDIA

Acknowledgements

The work presented in this thesis would not have been possible without my close association with many people who were always there to extend their support. I take this opportunity to acknowledge them and extend my sincere gratitude towards all those who made this Ph.D thesis possible.

First and foremost, I would like to express my genuine regards and acknowledgement to my supervisor Dr. Satish Kumar Sharma, Assistant Professor, School of Mathematics, Thapar University, Patiala for his precious recommendations, guidance and continuous inspiration throughout the period of research work. I am eternally grateful to Dr. Abhishek Kumar Singh, Assistant Professor, Indian School of Mines, Dhanbad, Jharkhand for his valuable assistance, motivation, immense knowledge as well as wholehearted support without any ulterior motives that played a significant role throughout the course of my research work.

I am highly thankful to Dr. A.K. Lal, Head of School of Mathematics for the motivation and inspiration. I would also like to thank Prof. S.S. Bhatia, Dr. Amit Kumar and all other faculty members of School of Mathematics for their valuable advice. I am also thankful to all members of doctoral committee and non-teaching staff of School of Mathematics for their kind support.

I also impart my thanks to Dr. Parkash Gopalan, Director, Thapar University for providing necessary infrastructure and resources to accomplish my research work.

I am also indebted to Dr. O.P. Pandey, Dean of Research and Sponsored Project, for his never ending motivation that was of immense value in the completion of this thesis.

I am gratified to my good friends Saravmangla, Harwinder, Jeevan, Komal, Sandeep, Gourav, Jagdeep, Jasdeep, Tina, Bikram, Sukhpreet, Sukhbir, Sam, Santan, Raman, Tarun and all other research scholars of School of Mathematics for their help and support. My friends have been an encouragement every time and their motivation helped me to reach here. I am very grateful to all the people I have met along the way and have contributed to the development of my research work.

I would like to express my special indebtedness to my parents and grandmother who has always stood by me like a pillar in times of need and to whom I owe my life for their constant love, encouragement, moral support and blessings. They are my true virtue for the fulfillment of this task. I would like to offer my specialized as well as extraordinary grace to my brother for his monotonous confidence and moral strength that was of great importance in the fruition of the work.

Above all, I bow down the invincible God, who bestowed upon me the strength to carry out this work.

Patiala **Tanupreet Kaur**

Date: October 3, 2016

Abstract

Theoretical problems involving analysis of elastic wave propagation in complex media is an integral part of geophysics and Earth sciences. It presents fascinating tool to examine Earth's interior. In this light, the present research contributes to the study of some elastodynamic problems like wave propagation and moving load problems in mediums with various material properties and geometry. Graphical user interface (GUI) software in MATLAB has been developed for several problems. The thesis is structured in six chapters dealing with different problems. Major contributions and conclusions of the chapters are as follows:

Chapter 1

This chapter contains evolution and historical overview of elasticity, micro-continuum theories and anisotropic materials. Recent developments in the fields have been recorded along with the basic governing equations and constitutive relations.

Chapter 2

This chapter consists of two problems highlighting the effect of moving load on the stresses produced in an irregular half-space. First problem of this chapter studies the stresses produced in an irregular fibre-reinforced half-space due to a normal moving load on a free surface. The closed form expression of stresses has been obtained. Three different cases of irregularity viz. rectangular, parabolic and

no irregularity have been discussed and compared. It is distinctly marked out that the stresses produced due to normal moving load are affected by depth of half-space, depth and type of irregularity. Also, these effects are highlighted through numerical illustrations. Second problem of this chapter presents a theoretical model to study the response of moving load on an irregular micropolar half-space. The expression of stresses produced due to moving load have been obtained in closed form. The irregularity has been taken in three different forms viz. rectangular, parabolic and no irregularity. Effects of frictional coefficient, microstructure and irregularity on stresses have been studied and depicted by means of graphs for various cases.

Chapter 3

This chapter includes a comprehensive study of surface wave propagation in an anisotropic medium. Secular equation for the propagation of Rayleigh-type surface waves in self-reinforced half-space under the influence of gravity and liquid loading has been derived in closed form. The effect of reinforcement, gravity and liquid loading on the phase velocity of Rayleigh-type waves has been distinctly observed. Graphical demonstration has been carried out to highlight the important peculiarities of the problem. Moreover, the comparative study has been made of reinforced over reinforced-free case to unravel the reinforcement effect. Also, the effect of absence of liquid loading on propagation of Rayleigh-type waves is analysed.

Chapter 4

This chapter deals with propagation of SH-wave in vertically heterogeneous viscoelastic layer lying over a micropolar elastic half-space. Dispersion equation and damping equation are obtained in closed form and are plotted for different variations in relevant parameters of heterogeneity, viscoelasticity and micropolarity.

The heterogeneity in viscoelastic layer is caused by consideration of exponential variation in rigidity, internal friction and density. The dispersion equation has been matched with classical Love wave equation as a special case of the problem when the isotropic layer is lying over an isotropic half-space. Moreover, a comparative study is made to study the impact of presence and absence of micropolarity in the medium of elastic half-space.

Chapter 5

We have examined two problems of shear wave propagation in elastic medium with imperfect bonding between layer and half-space in this chapter. In first problem of this chapter, propagation behaviour of horizontally polarized shear wave in layered structure consisting of a vertically heterogeneous fibre-reinforced layer imperfectly bonded to a micropolar elastic half-space is studied. An analytical expression of dispersion equation has been obtained in closed form. The exponential form of heterogeneity is considered in fibre-reinforced layer. The significant effects of imperfectness, heterogeneity, reinforcement, micropolarity and coupling factor have been studied and shown graphically. The second problem in this chapter discuss the propagation of shear wave in micropolar elastic half-space imperfectly bonded with a heterogeneous viscoelastic layer. In said model, dispersion equation and damping equation are obtained in closed form. The effect of imperfect common interface, heterogeneity present in layer, internal friction associated with viscoelastic layer and micropolarity associated with half-space have been investigated and graphical demonstration has been performed to highlight these effects.

Chapter 6

This chapter emerges with the study of horizontally polarized shear wave propagation in a heterogeneous fibre-reinforced layer lying over an initially stressed isotropic elastic half-space. The interface between layer and half-space is considered as corrugated and loosely bonded. The heterogeneity in the layer is caused due to exponential variation of depth. The dispersion relation has been found analytically in closed form. The effect of presence and absence of the corrugated common surface with loose bonding on the dispersion curves has been meticulously examined. Moreover, the substantial effect of reinforcement, anisotropy, heterogeneity, initial stress, undulation parameter and position parameter on phase velocity of SH-wave have been remarkably traced out. Comparative study is also performed to compare reinforced (anisotropic) case with reinforced-free (isotropic) case, heterogeneous case with homogeneous case and loosely bonded corrugated interface case with perfectly bonded planar interface case. Numerical computation along with graphical demonstration has been carried out for the problem to unravel the hidden facts.

List of Papers

1. **Tanupreet Kaur**, Abhishek Kumar Singh, Amares Chattopadhyay, and Satish Kumar Sharma. "Dynamic response of normal moving load on an irregular fiber-reinforced half-space." Journal of Vibration and Control 22 (1): 77-88, 2016. **(SCI, impact factor: 1.643)**.

2. **Tanupreet Kaur**, Satish Kumar Sharma, and Abhishek Kumar Singh. "Dynamic response of a moving load on a micropolar half-space with irregularity." Applied Mathematical Modelling 40 (5-6): 3535-3549, 2016. **(SCI, impact factor: 2.291)**.

3. **Tanupreet Kaur**, Satish Kumar Sharma, and Abhishek Kumar Singh. "Effect of reinforcement, gravity and liquid loading on Rayleigh-type wave propagation." Meccanica 51 (10): 2449-2458, 2016.**(SCI, impact factor: 1.828)**.

4. **Tanupreet Kaur**, Satish Kumar Sharma, and Abhishek Kumar Singh. "Influence of imperfectly bonded micropolar elastic half-space with non-homogeneous viscoelastic layer on propagation behavior of shear wave." Waves in Random and Complex Media 26(4): 650-670, 2016. **(SCI, impact factor: 0.952)**.

5. **Tanupreet Kaur**, Satish Kumar Sharma, and Abhishek Kumar Singh. "Shear wave propagation in vertically heterogeneous viscoelastic layer over a micropolar elastic half-space."Mechanics of Advanced Materials and Structures (2015)

DOI: 10.1080/15376494.2015.1124948. **(SCI, impact factor:0.773)**.

6. **Tanupreet Kaur**, Satish Kumar Sharma, and Abhishek Kumar Singh. "Propagation of Love type wave in a vertically heterogeneous fibre-reinforced layer imperfectly bonded to a micropolar elastic half-space." (Communicated)

7. **Tanupreet Kaur**, Satish Kumar Sharma, and Abhishek Kumar Singh. "Propagation of shear wave at a loosely bonded corrugated interface between a fibre-reinforced layer and an isotropic half-space." (Communicated)

Table of Contents

Table of Contents **ix**

List of Figures **xii**

1 Introduction **1**

1.1 General Introduction 1

1.2 Theory of elasticity 3

1.3 Elastic waves 7

1.4 Micropolar elasticity 11

1.5 Anisotropic elastic materials 16

2 Dynamic response of normal moving load **23**

2.1 Introduction 23

2.2 Dynamic response of normal moving load on an irregular fibre-reinforced half-space 25

2.2.1 Formulation of the problem 25

2.2.2 Solution to the problem 28

2.2.3 Particular Cases 32

2.2.4 Numerical results and discussions 33

2.2.5 Conclusion 41

2.3 Dynamic response of moving load on a micropolar half-space with irregularity 42

2.3.1 Formulation of the problem 42

2.3.2 Solution of the problem 44

2.3.3 Particular cases 48

2.3.4 Numerical results and discussion 49

2.3.5 Conclusion 59

3 Effect of reinforcement, gravity and liquid loading on Rayleigh-type wave propagation 61

3.1 Introduction 61

3.2 Formulation and solution of the problem 63

3.2.1 Dynamics of inviscid liquid layer (M_1) 64

3.2.2 Dynamics of self-reinforced semi-infinite medium (M_2) 65

3.2.3 Boundary conditions 67

3.2.4 Secular equation 68

3.3 Particular cases 69

3.4 Numerical results and discussion 72

3.5 Conclusion 78

4 Shear wave propagation in vertically heterogeneous viscoelastic layer over a micropolar elastic half-space 81

4.1 Introduction 81

4.2 Formulation of the problem 82

4.2.1 Dynamics of vertically heterogeneous viscoelastic layer 83

4.2.2 Dynamics of micropolar elastic half-space 85

4.3 Boundary conditions, dispersion relation and damping equation . . . 86

4.4 Particular cases 91

4.5 Numerical results and discussion 92

4.6 Conclusion 99

5 Shear wave propagation at an imperfect interface between layer and half-space 101

5.1 Introduction 101

5.2 Influence of imperfectly bonded micropolar elastic half-space with non-homogeneous viscoelastic layer on propagation behavior of shear wave 103

5.2.1 Formulation of the problem 103

5.2.2 Boundary conditions 105

5.2.3 Particular cases 107

5.2.4 Numerical results and discussion 110

5.2.5 Conclusion 124

5.3 Propagation of Love type wave in a vertically heterogeneous fibre-reinforced layer imperfectly bonded to a micropolar elastic half-space 126

5.3.1 Formulation of the problem 126

5.3.2 Solution for heterogeneous fibre-reinforced layer 127

5.3.3 Solution for micropolar elastic half-space 128

5.3.4 Boundary Conditions 129

5.3.5 Particular Cases 131

5.3.6 Numerical results and discussion 133

5.3.7 Conclusion 139

6 Propagation of shear wave at a loosely bonded corrugated interface between a fibre-reinforced layer and an isotropic half-space 141

6.1 Introduction 141

6.2 Formulation of the problem 143

6.2.1 Dynamics of the upper heterogeneous fibre-reinforced composite layer 145

6.2.2 Dynamics of lower isotropic initially stressed half-space 146

6.3 Boundary conditions and dispersion relation 148

6.4 Particular cases 149

6.5 Numerical results and discussion 152

6.6 Conclusion 158

List of Figures

1.1 Elastic waves 9

2.1 Geometry of the problem 26
2.2 Variation of the shear stress (in fibre-reinforced medium) against depth for different irregularity depths (H/a) when $x/a = 0$. 33
2.3 Variation of the shear stress (in fibre-reinforced medium) against depth for different irregularity factor (x/a) when $H/a = 1$. 34
2.4 Variation of the shear stress (in fibre-reinforced medium) against depth for different irregularity depths in case of rectangular irregularity. 35
2.5 Variation of the shear stress (in fibre-reinforced medium) against depth for different irregularity depths in case of parabolic irregularity. 35
2.6 Variation of the shear stress (in fibre-reinforced medium) against depth for different irregularity depths in case of no irregularity. 35
2.7 Variation of the shear stress (in fibre-reinforced medium) against depth and irregularity factor when irregularity depth is $H/a = 0$. . . 36
2.8 Variation of the shear stress (in fibre-reinforced medium) against depth and irregularity factor when irregularity depth is $H/a = 0.1$. . . 36
2.9 Variation of the shear stress (in fibre-reinforced medium) against depth and irregularity factor when irregularity depth is $H/a = 1$. . . 36
2.10 Variation of the shear stress (in isotropic medium) against depth for different irregularity depths (H/a) when $x/a = 0$. 37
2.11 Variation of the shear stress (in isotropic medium) against depth for different irregularity factor ($x/1$) when $H/a = 1$. 37
2.12 Variation of the shear stress (in isotropic medium) against depth and irregularity depth in case of rectangular irregularity. 38
2.13 Variation of the shear stress against depth and irregularity depth in case of parabolic irregularity. 39
2.14 Variation of the shear stress (in isotropic medium) against depth and irregularity depth in case of no irregularity. 39

2.15 Variation of the shear stress (in isotropic medium) against depth and irregularity factor when irregularity depth is $H/a = 0$. 39
2.16 Variation of the shear stress (in isotropic medium)against depth and irregularity factor when irregularity depth is $H/a = 0.1$. 40
2.17 Variation of the shear stress (in isotropic medium)against depth and irregularity factor when irregularity depth is $H/a = 1$. 40
2.18 Variation of the shear stress against depth for different values of frictional coefficients (R). 49
2.19 Variation of the normal stress against depth for different values of frictional coefficients (R). 50
2.20 Variation of the tangential couple stress against depth for different values of frictional coefficients (R). 50
2.21 Variation of the normal stress against depth for different values of irregularity depth (H/a) when irregularity factor, $x/a = 0.5$. 50
2.22 Variation of the shear stress against depth for different values of irregularity depth (H/a) when irregularity factor, $x/a = 0.5$. 51
2.23 Variation of the tangential couple stress against depth for different values of irregularity depth (H/a) when irregularity factor, $x/a = 0.5$. 51
2.24 Variation of the normal stress against depth for different values of irregularity factor (x/a) when irregularity depth, $H/a = 1$. 51
2.25 Variation of the shear stress against depth for different values of irregularity factor (x/a) when irregularity depth, $H/a = 1$. 52
2.26 Variation of the tangential couple stress against depth for different values of irregularity factor (x/a) when irregularity depth, $H/a = 1$. . 52
2.27 Variation of the normal stress against depth for different values of coupling factor (N) when irregularity depth, $H/a = 1$ and irregularity factor, $x/a = 0.5$. 53
2.28 Variation of the shear stress against depth for different values of coupling factor (N) when irregularity depth, $H/a = 1$ and irregularity factor, $x/a = 0.5$. 53
2.29 Variation of the tangential couple stress against depth for different values of coupling factor (N) when irregularity depth, $H/a = 1$ and irregularity factor, $x/a = 0.5$. 54
2.30 Variation of the normal stress against depth and irregularity factor (x/a) when irregularity depth, $H/a = 1$. 54

2.31 Variation of the shear stress against depth and irregularity factor (x/a) when irregularity depth, $H/a = 1$. 55

2.32 Variation of the tangential couple stress against depth and irregularity factor (x/a) when irregularity depth, $H/a = 1$. 55

2.33 Variation of the normal stress against depth and irregularity depth (H/a) in case of rectangular irregularity. 55

2.34 Variation of the shear stress against depth and irregularity depth (H/a) in case of rectangular irregularity. 56

2.35 Variation of the tangential couple stress against depth and irregularity depth (H/a) in case of rectangular irregularity. 56

2.36 Variation of the normal stress against depth and irregularity depth (H/a) in case of parabolic irregularity. 56

2.37 Variation of the shear stress against depth and irregularity depth (H/a) in case of parabolic irregularity. 57

2.38 Variation of the tangential couple stress against depth and irregularity depth (H/a) in case of parabolic irregularity. 57

3.1 Geometry of the problem 63

3.2 Variation of dimensionless phase velocity (V/β_1) against dimensionless wave number (kH) for different values of gravity parameter $(G' = \rho' gH/\mu_L)$ in self-reinforced gravitating semi-infinite medium underlying an inviscid liquid layer. 73

3.3 Variation of dimensionless phase velocity (V/β_1) against dimensionless wave number (kH) for different values of gravity parameter $(G' = \rho' gH/\mu_L)$ in gravitating reinforced-free underlying an inviscid liquid layer. 73

3.4 Variation of dimensionless phase velocity (V/β_1) against gravity parameter $(G' = \rho' gH/\mu_L)$ for different values of dimensionless wave number (kH) in gravitating self-reinforced self-infinite medium underlying an inviscid liquid layer. 74

3.5 Variation of dimensionless phase velocity (V/β_1) against gravity parameter $(G' = \rho' gH/\mu_L)$ for different values of dimensionless wave number (kH) in gravitating reinforced-free self-infinite medium underlying an inviscid liquid layer. 74

3.6 Variation of dimensionless phase velocity (V/β_1) against biot's gravity parameter ($G = \rho g/k\mu_L$) in reinforced and reinforced-free gravitating self-infinite medium in the absence of an inviscid liquid layer. 75

3.7 Variation of dimensionless phase velocity (V/β_1) against dimensionless wave number (kH) and gravity parameter ($G' = \rho' gH/\mu_L$) in gravitating self-reinforced self-infinite medium underlying an inviscid liquid layer. 75

3.8 Variation of dimensionless phase velocity (V/β_1) against dimensionless wave number (kH) and gravity parameter ($G' = \rho' gH/\mu_L$) in gravitating reinforced-free self-infinite medium underlying an inviscid liquid layer. 76

4.1 Geometry of the problem 82

4.2 Variation of dimensionless phase velocity (c/β_1) against dimensionless wave number (kH') for different values of heterogeneity parameter ($\nu H'$) when half-space is comprised of micropolar elastic material (solid line curve) or elastic material without micropolarity (dashed line curve). 93

4.3 Variation of dimensionless phase velocity (c/β_1) against dimensionless wave number (kH') for different values of viscoelastic parameter ($\omega\eta_0/\mu_0$) when half-space is comprised of micropolar elastic material (solid line curve) or elastic material without micropolarity (dashed line curve). 94

4.4 Variation of dimensionless damped velocity against dimensionless wave number (kH') for different values of heterogeneity parameter ($\nu H'$) when half-space is comprised of micropolar elastic material (solid line curve) or elastic material without micropolarity (dashed line curve). . 94

4.5 Variation of dimensionless damped velocity against dimensionless wave number (kH') for different values of viscoelastic parameter ($\omega\eta_0/\mu_0$) when half-space is comprised of micropolar elastic material (solid line curve) or elastic material without micropolarity (dashed line curve). . 95

4.6 Variation of dimensionless phase velocity (c/β_1) against dimensionless wave number (kH') for different values of micropolar parameter ($\kappa H'^2/\gamma$) when a heterogeneous viscoelastic layer lies over a micropolar elastic half-space. 95

4.7 Variation of damped velocity against wave number (kH') for different values of micropolar parameter ($\kappa H'^2/\gamma$) when a heterogeneous viscoelastic layer lies over a micropolar elastic half-space. 96

5.1 Geometry of the problem 104

5.2 Variation in dimensionless phase velocity (c/β_1) against dimensionless wave number (kH') for different values of heterogeneity parameter of layer ($\nu H'$) 111

5.3 Variation in dimensionless damped velocity against dimensionless wave number (kH') for different values of heterogeneity parameter of layer ($\nu H'$) 111

5.4 Surface plot of dimensionless phase velocity (c/β_1) against dimensionless wave number (kH') and non-dimensional heterogeneity parameter ($\nu H'$). 111

5.5 Surface plot of dimensionless damped velocity against dimensionless wave number (kH') and non-dimensional heterogeneity parameter ($\nu H'$). 112

5.6 Variation in dimensionless phase velocity (c/β_1) against dimensionless wave number (kH') for different values of viscoelasticity of the layer ($\omega\eta_0/\mu_0$). 112

5.7 Variation in dimensionless damped velocity against dimensionless wave number (kH') for different values of viscoelasticity of the layer ($\omega\eta_0/\mu_0$).112

5.8 Surface plot of dimensionless phase velocity (c/β_1) against dimensionless wave number (kH') and non-dimensional viscoelasticity of the layer ($\omega\eta_0/\mu_0$). 113

5.9 Surface plot of dimensionless damped velocity against dimensionless wave number (kH') and non-dimensional viscoelasticity of the layer ($\omega\eta_0/\mu_0$). 113

5.10 Variation in dimensionless phase velocity (c/β_1) for different values of imperfectness parameter ($\Gamma = \frac{k\mu}{R}$) of complex common interface. . 113

5.11 Variation in dimensionless damped velocity against dimensionless wave number (kH') for different values of imperfectness parameter ($\Gamma = \frac{k\mu}{R}$) of complex common interface. 114

5.12 Variation in dimensionless phase velocity (c/β_1) for different values of non-dimensional flexibility imperfectness parameter ($\Gamma_1 = \frac{k\mu}{R_1}$) of complex common interface. 114

5.13 Variation in dimensionless damped velocity against dimensionless wave number (kH') for different values of non-dimensional flexibility imperfectness parameter ($\Gamma_1 = \frac{k\mu}{R_1}$) of complex common interface. 115

5.14 Variation in dimensionless phase velocity (c/β_1) against dimensionless wave number (kH') for different values of non-dimensional viscoelastic imperfectness parameter ($\Gamma_2 = \frac{k\mu}{R_2}$) of complex common interface. . . 115

5.15 Variation in dimensionless damped velocity against dimensionless wave number (kH') for different values of non-dimensional viscoelastic imperfectness parameter ($\Gamma_2 = \frac{k\mu}{R_2}$) of complex common interface. 116

5.16 Surface plot of dimensionless phase velocity (c/β_1) against dimensionless wave number (kH') and non-dimensional imperfectness parameter ($\Gamma = \frac{k\mu}{R}$) of complex common interface. 116

5.17 Surface plot of dimensionless damped velocity against dimensionless wave number (kH') and non-dimensional imperfectness parameter ($\Gamma = \frac{k\mu}{R}$) of complex common interface. 117

5.18 Surface plot of dimensionless phase velocity (c/β_1) against dimensionless wave number (kH') and non-dimensional flexibility imperfectness parameter ($\Gamma_1 = \frac{k\mu}{R_1}$) of complex common interface. 117

5.19 Surface plot of dimensionless damped velocity against dimensionless wave number (kH') and non-dimensional flexibility imperfectness parameter ($\Gamma_1 = \frac{k\mu}{R_1}$) of complex common interface. 118

5.20 Surface plot of dimensionless phase velocity (c/β_1) against dimensionless wave number (kH') and non-dimensional viscoelastic imperfectness parameter ($\Gamma_2 = \frac{k\mu}{R_2}$) of complex common interface. 118

5.21 Surface plot of dimensionless damped velocity against dimensionless wave number (kH') and non-dimensional viscoelastic imperfectness parameter ($\Gamma_2 = \frac{k\mu}{R_2}$) of complex common interface. 119

5.22 Variation in dimensionless phase velocity (c/β_1) against dimensionless wave number (kH') for different values of micropolar parameter ($\kappa H'^2/\gamma$) of micropolar elastic half-space. 119

5.23 Variation in and dimensionless damped velocity against dimensionless wave number (kH') for different values of micropolar parameter ($\kappa H'^2/\gamma$) of micropolar elastic half-space. 120

5.24 Surface plot of dimensionless phase velocity (c/β_1) against dimensionless wave number (kH') and non-dimensional micropolar parameter ($\kappa H'^2/\gamma$). 120

5.25 Surface plot of dimensionless damped velocity against dimensionless wave number (kH') and non-dimensional micropolar parameter ($\kappa H'^2/\gamma$). 121

5.26 Variation of dimensionless phase velocity (c/β_1) against dimensionless wave number (kH') for different values of heterogeneity parameter ($\nu H'$) when when $N = 0.1$, $\frac{\kappa H'^2}{\gamma} = 50$ and $\Gamma = 1$. 134

5.27 Variation of dimensionless phase velocity (c/β_1) against dimensionless wave number (kH') for different values of micropolarity parameter ($\frac{\kappa H'^2}{\gamma}$) when $\nu H' = 0.1$, $N = 0.1$ and $\Gamma = 1$. 134

5.28 Variation of dimensionless phase velocity (c/β_1) against dimensionless wave number (kH') for different values of coupling factor (N) when $\nu H' = 0.1$, $\frac{\kappa H'^2}{\gamma} = 50$ and $\Gamma = 1$. 135

5.29 Variation of dimensionless phase velocity (c/β_1) against dimensionless wave number (kH') for different values of imperfect factor ($\Gamma = \frac{k\mu}{L}$) when $\nu H' = 0.1$, $\frac{\kappa H'^2}{\gamma} = 50$ and $N = 0.1$. 135

5.30 Variation of dimensionless phase velocity (c/β_1) against dimensionless wave number (kH') for different values of flexibility parameter of imperfect common interface ($\Gamma_1 = \frac{k\mu}{L_1}$) when $\nu H' = 0.1$, $\frac{\kappa H'^2}{\gamma} = 50$, $N = 0.1$ and $\Gamma_2 = 0.5$. 135

5.31 Variation of dimensionless phase velocity (c/β_1) against dimensionless wave number (kH') for different values of viscoelastic parameter of common imperfect interface ($\Gamma_2 = \frac{k\mu}{L_2}$) when $\nu H' = 0.1$, $\frac{\kappa H'^2}{\gamma} = 50$, $N = 0.1$ and $\Gamma_2 = 5$. 136

5.32 Variation of dimensionless phase velocity (c/β_1) against dimensionless wave number (kH') for different values of reinforcement parameter a_1 when $\nu H' = 0.1$, $\frac{\kappa H'^2}{\gamma} = 50$, $N = 0.1$ and $\Gamma = 1$. 136

6.1 Geometry of the problem 144

6.2 Variation of phase velocity (c/β_1) against wave number (kH_1) for different values of heterogeneity parameter (αH_1) when $\xi = 0.2, \psi = 0.2, ab = 0.1, bH_1 = 1.4, x/H_1 = 0.04$. 153
6.3 Variation of phase velocity (c/β_1) against wave number (kH_1) for different values of horizontal initial stress (ξ) when $\alpha_1 H_1 = 1, \psi = 0.2, ab = 0.1, bH_1 = 1.4, x/H_1 = 0.04$. 153
6.4 Variation of phase velocity (c/β_1) against wave number (kH_1) for different values of bonding parameter (ψ) when $\xi = 0.2, \alpha_1 H_1 = 1, \xi = 0.2, ab = 0.1, bH_1 = 1.4, x/H_1 = 0.04$. 154
6.5 Variation of phase velocity (c/β_1) against wave number (kH_1) for different values of corrugation parameter (ab) when $\xi = 0.2, \alpha_1 H_1 = 1, \xi = 0.2, \psi = 0.2, bH_1 = 1.4, x/H_1 = 0.04$. 154
6.6 Variation of phase velocity (c/β_1) against wave number (kH_1) for different values of undulatory parameter (bH_1) when $\alpha H_1 = 1, \xi = 0.2, \psi = 0.2, ab = 0.1, x/H_1 = 0.04$. 155

Chapter 1

Introduction

1.1 General Introduction

Continuum mechanics is a part of mechanics that deals with mechanical and kinematics behaviour of fluids and solids on the macroscopic scale. It avoids the discrete nature of matter and considers the material to be continuous material, that is the distance between two neighbouring molecules is very small. The material response due to different loading conditions is studied under continuum mechanics. The subject matter of mechanics of continuous body is mainly divided into two parts: (i) derivation of fundamental equation to describe the mechanical behaviour of various materials and (ii) derivation of constitutive relations to predict and describe the behaviour of materials in different situations. The basic principle of fundamental equations is based upon the laws of physics such as the conservation of linear and angular momentum, conservation of energy, conservation of mass and the entropy inequality law. The mechanical behaviour of materials varies not only from material to material but also because of different loading conditions for the given material. This leads to formulation of many constitutive equations describing different aspects of material behaviour. Therefore, these equations act as keypoints around various

studies in the area of continuum mechanics.

Solid mechanics is branch of continuum mechanics which is concerned with the stressing, deformation and failure of solid matter under external actions. When an external load is applied to a body, it gets deformed and if after removal of external load its deformation is fully recovered then body is called elastic. Under the influence of external forces theory of elasticity presents a mathematical model that deals with determination of stress, strain and displacement distribution in an elastic solid. This mathematical model requires mathematical knowledge to understand the formulation and solution procedures. By imposing the boundary or initial conditions the formulations of mathematical model are solved using various techniques. In theory of elasticity, different methods used to find solution of mathematical model of a deformation problem are potential theory, fourier methods, complex variables, variational calculus, integral transforms, finite differences, finite elements, etc. A mathematical model of theory of elasticity that allows solutions to problems have applications in civil and mechanical engineering (rods, beams, plates), geomechanics (rocks, concrete, soil, asphalt), material engineering (crystalline solids, dislocation, materials with microstructure) and scientific fields. The extension of theory of elasticity is microcontinuum field theories which are concerned with deformation and interaction of material media in microscopic scale and short time scale. The concept of micropolar elasticity was used to model the materials with microstructure, granular media, composite materials, biological media (bones, blood) and foams. The ideal fibre-reinforced material is the simplest continuum model which incorporates the essential features of macroscopic mechanical behaviour of strong fibre-reinforced

material.

1.2 Theory of elasticity

To a certain extent all materials possess the property of elasticity i.e. the tendency of solid materials to regain its shape and size after the removal of external forces causing deformation of materials. Deformation of materials disappears only if external forces do not exceed a certain limit. Elasticity of material deals with determination of stresses, strain and displacement distribution under the influence of external forces. Theory of elasticity is the mathematical analysis of elastic behavior of a solid body. The behaviour of construction materials (various sorts of aluminium, steel, concrete) is well described by the classical theory of elasticity provided the stresses do not exceed the elastic limit and no stress concentration occurs. In Classical theory of elasticity the material is considered as a continuum in mathematical sense.

The first attempt about the description of solids was made by Galileo Galilei, called the father of science. In sixteenth and seventeenth centuries, he was the first mathematician, astronomer, physicist and philosopher who worked on fracture and strength of beams and mainly cantilever beams. However, he treated the behaviour of solids as inelastic, not depending on any law connecting the forces and displacements produced with them, or capable of any physical hypothesis furnishing such a law, yet many investigators followed the direction given by his enquiries. The resistance of a beam was determined by him, one end of beam is built into a wall, when the tendency to break it increases from its own or an applied weight; and he concluded that the beam tends to turn about an axis perpendicular to its length,

and in the plane of the wall. In particular, Galileo's problem is known as the determination of this axis. It was Robert Hooke who gave law of proportionality between the forces and displacements after the appearance of Galileo's Discourses [55]. In 1678, Hooke gave the relation between stress and deformation, called constitutive relation for a solid which is also known as the Hooke's law. This law says that the body deformation is directly proportional to the load applied to it. The base of mathematical theory of elasticity is established by this law. Up to a certain limit solid bodies obey Hooke's law, known as the elastic limit, which is the maximum deformation of a body that a body will undergo without being permanently deformed. If a body exceeds the elastic limit then the body is known as a plastic body. At or near the elastic limits brittle materials like cast iron or glass break. Mostly, at short time, low temperatures and small enough loads, many materials are elastic. With increase in these quantities, plastic behavior of material is observed unless the material is fracture and brittle.

Moreover, in the limit of small strain, which is sufficiently accurate for most applications in seismic wave propagation, the stress-strain relationship is linear and described by the generalized Hooke's law:

$$\tau_{ij} = c_{ijkl} e_{kl}, \tag{1.1}$$

where τ_{ij} is the stress tensor, c_{ijkl} is the fourth order stiffness tensor and e_{kl} is the strain tensor defined as

$$e_{kl} = \frac{1}{2}\left(\frac{\partial u_k}{\partial x_l} + \frac{\partial u_l}{\partial x_k}\right), \tag{1.2}$$

$\boldsymbol{u} = (u_1, u_2, u_3)$ is the displacement vector.

c_{ijkl} have 81 components. If the elastic constants c_{ijkl} are independent of position i.e. the elastic constants are same for all points of the medium, then the medium is said to be elastically homogeneous. Further, if the elastic constants c_{ijkl} are function of position i.e. the elastic constants of the medium varies from point to point, then the medium is called elastically non homogeneous or inhomogeneous. These elastic constants reduce to 36 by considering symmetry of strain tensor and stress tensor. But using the balance of angular momentum, Cauchy had shown that the stress and strain tensors each have six independent components only. Further, Green introduced the strain-energy density function and had shown that only 21 number of independent elastic constants in general anisotropic media were necessary. The equation of motion for general anisotropic, linearly elastic material follows from the second Newton's law applied to a volume ΔV within a continuum [9] is

$$c_{ijkl}\frac{\partial^2 u_k}{\partial x_j \partial x_l} + f_i = \rho\frac{\partial^2 u_i}{\partial t^2}, \tag{1.3}$$

where ρ is the density of the material, $f_i = (f_1, f_2, f_3)$ is the external or body force per unit volume, $x_i (i = 1, 2, 3)$ are the cartesian coordinates and t is the time.

Further, if we take elastic symmetry with respect to two different planes we are left with 9 elastic constants. Now, assuming two different types of rotations for transversely isotropic and isotropic materials, the number of elastic constants of material reduces to 2. The historical details of elasticity may be found in the texts by Love [81] and Sokolnikoff [128]. Hence, the number of independent elastic constants reduces considerably; for a perfectly isotropic material there are only two elastic constants usually expressed as λ and μ. These elastic constants are known

as Lamé's constants in isotropic case, and it can be shown that

$$c_{ijkl} = \lambda\delta_{ij}\delta_{kl} + 2\mu\delta_{ik}\delta_{jl},\ \tau_{ij} = \lambda\delta_{ij}e_{kk} + 2\mu e_{ij}, \tag{1.4}$$

where

$\delta_{ij}=\begin{cases} 1, & i = j \\ 0, & i \neq j \end{cases}$, is the Kronecker delta and

$e_{kk} = \triangle = e_{11} + e_{22} + e_{33}$, is the dilatation which defines the change of volume per unit volume.

The governing equation in terms of displacement for isotropic medium in the absence of body force is given by [60]

$$(\lambda + \mu)u_{j,ji} + \mu u_{i,jj} = \rho\ddot{u}_i. \tag{1.5}$$

In vector form equation (1.5) can be written as

$$(\lambda + \mu)\nabla\nabla.\boldsymbol{u} + \mu\nabla^2\boldsymbol{u} = \rho\ddot{\boldsymbol{u}}. \tag{1.6}$$

Decomposing displacement vector by introducing the scalar and vector potential ϕ and ψ such that

$$\boldsymbol{u} = \nabla\phi + \nabla \times \boldsymbol{\psi},\ \ \bigtriangledown .\boldsymbol{\psi} = 0. \tag{1.7}$$

The resolution of a vector field into the gradient of a scalar and the curl of a zero divergence vector was proposed by Helmholtz. The condition $\bigtriangledown.\boldsymbol{\psi} = 0$ provide the necessary additional condition to uniquely determine the displacement components of $\boldsymbol{u}$ and is sufficient condition for the elastodynamic displacement $\boldsymbol{u}$ to be of the form $\boldsymbol{u} = \bigtriangledown\phi + \bigtriangledown \times \boldsymbol{\psi}$.

Using equation (1.7) in equation (1.6), we have

$$\bigtriangledown\{(\lambda + 2\mu)\bigtriangledown^2\phi - \rho\ddot{\phi}\} + \bigtriangledown \times \{\mu\bigtriangledown^2\boldsymbol{\psi} - \rho\ddot{\boldsymbol{\psi}}\} = 0. \tag{1.8}$$

Equation (1.8) yields two equations

$$\bigtriangledown^2\phi = \frac{1}{c_p^2}\ddot{\phi}, \tag{1.9}$$

and

$$\bigtriangledown^2\boldsymbol{\psi} = \frac{1}{c_s^2}\ddot{\boldsymbol{\psi}}, \tag{1.10}$$

where

$c_p^2 = \dfrac{\lambda + 2\mu}{\rho}$, $c_s^2 = \dfrac{\mu}{\rho}$.

Equation (1.9) describes a dilatational wave travelling with a velocity c_p in the interior of an elastic body. These waves are known as volumetric, compressional, irrotational, pressure or primary waves (P-waves). Equation (1.10) represents a rotational wave involving no volume change and travelling with speed c_s and is also known as equivoluminal, shear, distortional, transverse and secondary waves (S-waves).

1.3 Elastic waves

Earthquakes are one of the most major problems that cause great loss to mankind, killing thousands each year. Since past decade, earthquakes have been of great concern to people due to devasting damage capabilities and capacity of destroying a community in a matter of seconds without any warning. Each incident radiates seismic waves which travel in every part of Earth and different ground motions are produced by many earthquakes per day, even if too weak to be noticed, are easily detected with modern instruments anywhere on the globe. Seismology is the study of earthquake and phenomenon associated with earthquake or the study of elastic waves propagating in the Earth. The term seismology is derived from two Greek

words 'seismos' which means shaking and 'logos' which means treatise. Thus, the science of earthquakes or the science of shaking Earth is known as seismology. As a separate part of natural science, seismology and geophysics were established at the end of nineteenth and beginning of twentieth centuries. The primary aim of scientist is to learn about Earth's deep interior. Seismology is good way to illustrate effects of earthquake on Earth's interior.

Elastic waves are the motions in the medium which are transmitted by the energy communicated into the Earth by the disturbance source at some point. It is a disturbance that propagates through, or on the surface of a medium. Elastic wave generated by an explosion, a volcano or earthquake and traveling through the Earth or along surface of a medium are also known as seismic waves. A seismic wave transmits energy from one point to another within the earth. The velocity of wave propagation depends upon the density and elasticity of the material. There are two types of seismic waves: (i) body waves and (ii) surface waves.

Body waves: Those seismic waves which travel through the Earth's interior are known as body waves. There are two types of body waves: P (primary) waves and S (secondary) waves. P waves are longitudinal in nature, the particle vibrates in the same or opposite direction of wave propagation and is associated with volume change. These waves are fastest waves and travel at speed from about 6 km/sec in surface rock to 10.4 km/sec near the Earth's core (some 2900 km below the surface). The P waves travel in curved paths that are concave upward due to increase in depth.

S waves, secondary waves or shear waves are shear or transverse in nature, i.e. motion of particle is perpendicular to the direction of wave propagation. These waves produce a rolling effect along the surface without any change in volume. Velocity of

S wave is about 60% of the P wave velocity of the material. These waves are further classified into two types.

(a) Horizontally polarized shear wave (SH): Shear waves in which the motion of particle is normal to the direction of wave propagation and is at right angle to the plane of wave propagation.

(b) Vertically polarized shear wave (SV): Shear waves in which the motion of particle is normal to the direction of propagation and stays in the plane of wave propagation.

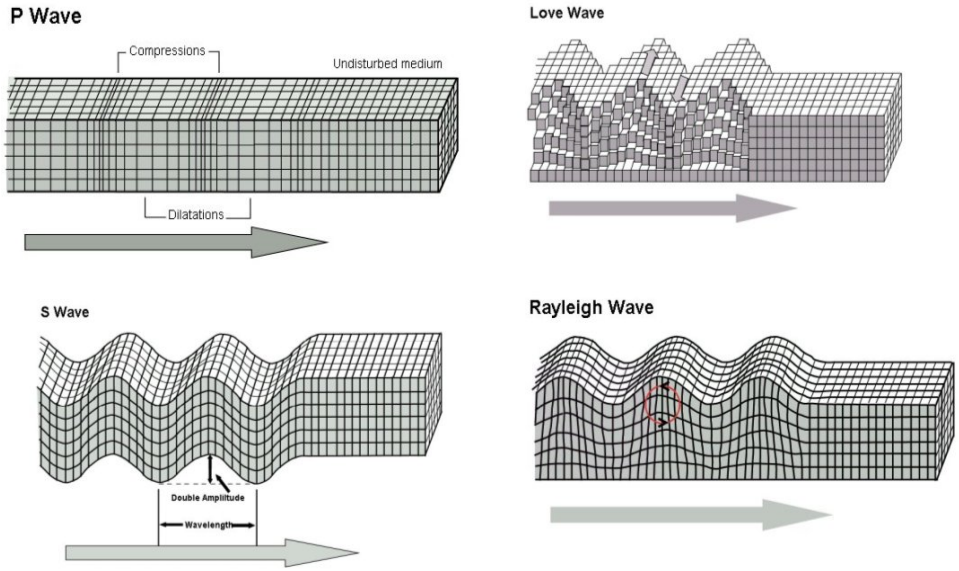

Figure 1.1: Elastic waves (Ref: www.google/images.com)

Surface waves: Seismic waves that propagate along the boundary between two half-spaces or layer over half-space are known as surface waves. These are the most destructive types of seismic waves. Further, surface waves are classified into two types of waves, known as Love wave and Rayleigh wave, by the types of motion they transmit.

Love waves: British seismologist Love [81], found a significant surface wave. In Love waves, the motion of particle is transverse to direction of wave propagation

and occur in the horizontal plane only. Love wave is the resulting wave of interference of many shear waves trapped near the surface. The velocity of Love wave depends on the wavelength, thickness of the upper layer and the elastic properties of the two materials of the stratified layers. Love waves can travel in a layer lying over an elastic half space, provided the phase speed of the wave lies between the phase speed of shear wave in the layer and that of in the half space. Love waves cannot develop in a homogeneous half-space.

Rayleigh surface waves: In 1885, British physicist Rayleigh [102] showed the motion of plane waves in an elastic half-space and predicted the existence of surface waves, named Rayleigh waves. The motion of particle in these types of waves is always in a vertical plane and moves in an elliptical path, which is retrograde to the direction of wave propagation.These waves are due to combination of longitudinal wave and transverse wave vibrations. These waves are also known as ground roll, as these travel as ripples with motions which is similar to the waves on the surface of water. The velocity of rayleigh wave is approximately 0.9 times the velocity of Love wave. The simplest model in which Rayleigh wave can propagate is a homogeneous isotropic half-space.

In case of an elastic solid half-space lying under a single solid layer, the first comprehensive treatment of dispersion of Rayleigh and Love waves was given by Love [82]. Biot [15, 16, 17, 18] was the first who study the propagation of elastic waves in a fluid saturated, statically isotropic, porous solid. Biot's theory was used by various investigators to study the propagation of surface waves such as Rayleigh and Love waves. Achenbach [4] observed that the elastic properties of the medium are affected by the propagation of elastic surface waves. Various authors Bose [19],

Burridge and Vargas [22] have contributed their work in this field. Literature of wave propagation and their related phenomena is given in some noteable books by Ewing et al. [52], Brekhovskikh [20], Achenbach [4], Graff [60], Udias [134], Aki and Richards [9] and several other books.

1.4 Micropolar elasticity

Classical theory of elasticity describes the behaviour of materials like steel, aluminium, concrete, coal etc. which are considered as continuum in mathematical sense. This theory neglects the atomic, molecular structure of the body and body is considered as three-dimensional Euclidean space, whose points being regarded as material particles of the body. The density is a single scalar quantity which describe the continuous distribution of particles, in the three-dimensional Euclidean space. In this theory, the displacement vector describes the deformation of the body and the principal force vector, known as stress vector uniquely determine the transmission of loadings through a surface element lying inside the body. Thus, the description of deformation of the body is obtained in terms of symmetric stress and strain tensors. However, this theory is insufficient to explain the behaviour of materials exhibiting microstructure like asphalts, fibrous, polymers, cellular solids, granular media, biological media (bones, blood) and crystals. In particular, this theory doesn't explain some discrepancies that occur in the case of elastic vibration of high frequency and small wave length. When magnitude of order of the wavelength is same as the average dimension of the microelements, the intrinsic motion of the microelements of a volume element with respect to the center of mass of the volume element, can affect the response remarkably. The influence of microstructure has great impact

in the case of multimolecular bodies and vibrations of granular, where new types of waves appear, not encountered in classical theory of elasticity. Therefore, it was desired to develop size dependent consistent continuum mechanics that can analyze the behaviour of material at microscale and explain the behaviour at macroscale.

The shortcomings of the classical theory of elasticity were first removed by Voigt [137] by taking the assumption that interaction between two particles of a body through an area element lying within the material is not only transmitted by force vector but also by a couple (moment) vector. This assumption gave rise to couple stresses in elasticity. However, Cosserat and Cosserat [38] developed the complete theory of asymmetric elasticity. They take the assumption that the body consists of interconnected particles in the form of small rigid bodies and deformation of the medium is described not only through the displacement vector but also by independent rotation vector. The orientation of triad of direction vector attached to every particle of material is specified by the rotation vector. A particle can undergo a microrotation without undergoing a macro displacement. An infinitesimal surface element transmits a force and a couple vector which gives rise to non-symmetric stress and couple stress tensor. The first is associated to non-symmetric tensor and the second is associated to a non-symmetric curvature tensor known as gradient of rotation tensor. The idea of Cosserat brothers provided a good continuum modelization for molecular lattices, in which a group of particles (atoms, molecules) bounded by important cohesive forces forms a rigid system subjected to rotational motion. Further, classical theory of elasticity was generalised by Eringen [46] by taking into account that the directors are rigid and there are three rotational degrees of freedom in addition to the three classical displacement degrees of freedom.

Several other Cosserat-type theories were developed independently using Cosserats theory, e.g., Gunther [63], Grioli [61], Aero and Kuvshinskii [8], Rajagopal [100], Eringen [44], Mindlin and Tiersten [87], Toupin [133], Koiter [74], Palmov [96], Nowacki [93] and many others. In all these theories, the kinematic variable corresponding to rotation of a point is taken into account, but not as an independent variable like in Cosserats theory. Of course, all these theories were identical to Cosserats theory, however they were called by different names such as Koiter's theory was known as 'Couple stress theory', Toupin's theory was known as 'Cosserat theory with constrained motion', Eringen's theory was known as 'Indeterminate couple stress theory', Nowacki's theory was known as 'Cosserat pseudo-continuum theory' etc. For 'micro-elasticity', a non-linear theory was originated by Eringen [45], Eringen and Suhubi [51], which considers intrinsic motions of the microelements. This theory is basically the generalization of 'Indeterminate couple stress theory' and 'Cosserat theory' in the sense that in this theory the skew-symmetric part of the stress tensor, the symmetric part of the couple stress tensor and the spin inertia are fully covered. Eringen himself applied his theory to liquid crystals ([50], [47], and [49]) and to suspensions with rigid anisometric particles, especially fiber suspensions [48].

Fatemi et al. [54] studied the generalization of continuum mechanics theories reporting the effects of microstructure related scale on the macroscopic mechanical properties of bone. Yang and Lakes [141] found the existence of couple stress by measuring the size effect on apparent stiffness of bone in quasi-static torsion. Moreover, they obtained the characteristic length in couple stress theory. Yang and Lakes [142] found the size effects in quasistatic bending of compact bone. These

effects were consistent with micropolar theory. Park and Lakes [97] showed that in wet bones, strain distribution follows the prediction of Cosserat elasticity whereas; strain distribution in dry bones is very close to that in classical elasticity. Khoshgofter et al. [72] used micropolar continuum theory and composite material rules to investigate brain biomechanics. It was shown by Anderson and Lakes [12] that the classical theory of elasticity does not always describe behaviour of cellular materials and proved that Rohacell polymethacrylimide foam behaves as a Cosserat elastic material. Pabst [95] found the application of micropolar theory to two classes of materials, one is with periodic microstructure and the other is with random microstructure. He also gave non-linear and linear constitutive equations (material models) for anisotropic and isotropic solids, as well as anisotropic and isotropic fluids, respectively. He also explained the physical significance of parameters of the material parameters and discussed the reduction of number of material parameters due to symmetry. Iesan, while studying problem on Earth science [66] proposed that micropolar model is more realistic as compared to classical elastic model. An asymptotic method was proposed to investigate the free vibration of a micropolar continuum layer by Achenbach [3]. The microrotations, displacements and the frequencies were sought as power series of the dimensionless wave number in this method.

Due to the presence of a compressional wave source inside the upper solid substratum the propagation of two-dimensional waves in a micropolar solid-solid semi-space was studied by Ghosh et al. [58]. Sharma and Pathania [115] studied the propagation of generalized thermoelastic Lamb waves in plate with layers of inviscid liquid. Sharma et al. [114] studied the propagation of Rayleigh surface waves

in microstretch thermoelastic solid lying under inviscid fluid loadings with varying temperature. Sahu [106] proposed the mathematical model of rotating beam in presence of resisting media and other parameter changes on the fundamental frequency of bending vibrations. A modified theoretical frequency equation for bending vibrations of an exponentially tapered beam under rotation has been determined by Sahu [107]. The problem of free convection of a chemically reacting micropolar fluid with mass transfer in the presence of a uniformly applied transverse magnetic field and variable suction has been studied by Prakash et al. [99]. Kumar et al. [77] have studied generalised thermoelastic waves in microstretch plates loaded with fluid of varying temperature. The propagation of Lamb waves in a homogeneous isotropic thermoelastic micropolar solid with two temperatures bordered with layers or half-spaces of inviscid liquid subjected to stress free boundary conditions was studied by Sharma et al. [118]. Altenbach et al. [11] have highlighted the three dimensional Cosserat type model and its ability to describe complex media like micro-inhomogeneous materials, polycrystalline and cellular solids, foams, lattices, masonries, particle assemblies, magnetic rheological fluids, liquid crystals, etc.

The equation of motion for micropolar elastic half-space in the absence of body force may be written as [46]:

$$(\lambda+\mu)\nabla(\nabla.\vec{u})+(\mu+\kappa)\nabla^2\vec{u}+\kappa(\nabla\times\vec{\phi})=\rho\frac{\partial^2\vec{u}}{\partial t^2}, \tag{1.11}$$

$$(\alpha+\beta+\gamma)\nabla(\nabla.\vec{\phi})-\gamma\nabla\times(\nabla\times\vec{\phi})+\kappa(\nabla\times\vec{u})-2\kappa\vec{\phi}=\rho j\frac{\partial^2\vec{\phi}}{\partial t^2}, \tag{1.12}$$

with the constitutive relations

$$\sigma_{in}=\lambda u_{l,l}\delta_{in}+\mu(u_{i,n}+u_{n,i})+\kappa(u_{n,i}-\varepsilon_{inl}\phi_l), \tag{1.13}$$

$$m_{in}=\alpha\phi_{l,l}\delta_{in}+\beta\phi_{i,n}+\gamma\phi_{n,i}, (i,n,l=1,2,3). \tag{1.14}$$

where $\vec{u} = (u_2, v_2, w_2)$ is the displacement vector, $\vec{\phi} = (\phi_1, \phi_2, \phi_3)$ is microrotation vector, λ, μ are Lamé parameters and $\gamma, \kappa, \alpha, \beta$ are micropolar material constants, ρ is the density. σ_{in} and m_{in} are the stress tensor and couple stress tensor respectively, δ_{in} is the Kronecker delta, ε_{inl} is permutation tensor and j is the micro-inertia.

1.5 Anisotropic elastic materials

It is widely known that the Earth's materials are neither perfectly elastic nor perfectly isotropic. Anisotropic material are those materials whose elastic properties are not same in all direction at a point of the body. Due to the effects of physical properties of an anisotropic materials, it is becoming an important subject in seismology. Two types of anisotropy have been observed. The first type of anisotropy has symmetry with principal axis in vertical direction and is due to principally to stratifications or horizontal alignments of structural or mineralogical nature. Anisotropy due to preferential alignments of crystal, cracks or heterogeneities along a particular azimuth (azimuthal anisotropy) is second kind of anisotropy.

Fibre-reinforced material

The elastic behaviour of many fibre-reinforced composite materials is strongly anisotropic. These material are family of composite materials and their characteristic property is that components of fibre-reinforced material act together as a single anisotropic unit as long as they remain in an elastic condition (i.e., the two components are bound together so that there is no relative displacement between them). The study of the mechanical behaviour of fibre-reinforced composites has been developed along two distinct approaches: macrocontinuum approach and the

micro or discrete approach. In the macrocontinuum approach a continuous and homogeneous system having overall material properties of the macrostructure is used to replace nonhomogeneous fibre composite. In the second approach, the actual geometrical and physical characteristic properties of constituent material are taken into consideration. The idea of continuous theory in the fibre reinforced material is developed by Adkins and Rivlin [7], Adkins [6], Spencer ([129], [130]) and Maugin [84] on the theory of large deformations of elastic materials reinforced by inextensible cords. Concrete or alumina is an example of fibre-reinforced material. By reinforcing a matrix material of the same fibre the fibre-reinforced material can be modified to a self-reinforced material under certain temperature and pressure. It is well known that Earth crust contains some hard and soft rocks that may exhibit property of reinforcement. Therefore, the study of wave propagation in reinforced media plays a very important role in geophysics and civil engineering. These studies give information about rock's structure as well as elastic properties of material. The idea of introducing a continuous reinforcement at every point of an elastic solid was introduced by Belfield et al. [14]. Later, this model was applied to the rotation of a tube by Verma and Rana [136] by illustrating its utility in strengthening the lateral surface of the tube.

The problem of reflection, transmission and propagation of magnetoelastic shear waves in a self-reinforced elastic medium was studied by Chattopadhyay and Choudhury [24]. The magnetoelastic shear wave propagation in an infinite self-reinforced plate was discussed by Chattopadhyay and Choudhury [25]. Stress produced by a pulse of shearing force moving over the boundary of a fibre-reinforced medium was investigated by Chattopadhyay and Venkateswarlu [32]. Hashin and

Rosen [65] gave the elastic moduli for the fibre-reinforced material. The influence of anisotropy on the Love waves in a self-reinforced layer lying over an elastic non-homogeneous half space has been studied by Pradhan et al. [98]. A problem of reflection and transmission of plane SH-wave through a perfectly conducting self-reinforced elastic layer interposed between two vertically inhomogeneous viscoelastic solid half-spaces has been studied by Chaudhary et al. [34]. The response of plane SH-wave was discussed by Chaudhary et al. [33] in elastic slab interposed between two different self-reinforced elastic solids. The propagation of horizontally polarised shear waves in an internal irregular magnetoelastic self-reinforced stratum which is sandwiched between two semi-infinite magnetoelastic was discussed by Chattopadhyay et al. [29]. Chattopadhyay et al. [27] discussed the propagation of magnetoelastic shear waves in an irregular self-reinforced layer. Chattopadhyay et al. [31] have shown dispersion of SH waves in an irregular non homogeneous self-reinforced crustal layer over a semi-infinite self-reinforced medium.

The constitutive equation for a fibre-reinforced linearly elastic medium with preferred direction [14] is

$$\tau_{ij} = \lambda' e_{kk}\delta_{ij} + 2\mu_T e_{ij} + \alpha'(a_k a_m e_{km}\delta_{ij} + e_{kk}a_i a_j) + 2(\mu_L - \mu_T)(a_i a_k e_{kj} + a_j a_k e_{ki}) + \beta' a_k a_m e_{km} a_i a_j;\ (i,j,k,m = 1,2,3), \tag{1.15}$$

where τ_{ij} are stress components, $e_{ij} = \dfrac{u_{i,j} + u_{j,i}}{2}$ are infinitesimal strain components, δ_{ij} is the Kronecker delta and a_i are the components of $\vec{a}$, all referred to rectangular cartesian co-ordinates x_i, $\vec{a} = (a_1, a_2, a_3)$ is the preferred directions of reinforcement such that $a_1^2 + a_2^2 + a_3^2 = 1$. The vector may be function of position. Indices take the values 1, 2, 3 and summation convention is employed. The coefficients $\lambda', \mu_T, \alpha', \beta'$

and μ_L are elastic constants with dimension of stress. μ_T can be identified as the shear modulus in transverse shear across the preferred direction, and μ_L as the shear modulus in longitudinal shear in the preferred direction. α' and β' are specific stress components to take into account different layers for concrete part of the composite material.

The equations of motion for small elastic disturbance in fibre-reinforced half-space in the absence of body forces are given as

$$\tau_{ij,j} = \rho' \ddot{u}_i, (i, j = 1, 2, 3) \tag{1.16}$$

where ρ' is the density of the medium.

Viscoelastic material:

Since the behaviour of Earth is not perfectly elastic body. Due to this fact, Earth which is composed of silicate and iron-alloy materials, under the application of small-magnitude transient forces responds nearly elastically but under the application of long-duration forces over the wide range of pressure and temperature conditions existing within the planet responds viscously. Materials that exhibit both elastic and viscous properties under deformation are known as viscoelastic materials. Anelastic solids are subset of viscoelastic materials. Wide variety of materials, including synthetic polymers, ceramics, human tissue, coal tar, salt sediments etc describe the viscoelastic phenomena. Relationship between stress and strain of viscoelastic material depends on time. For linearly elastic material the stress-strain curve is straight line with slope proportional to the elastic modulus. But for linearly viscoelastic material plot of stress-strain is curved because during constant strain rate deformation of both strain and time increase together. The study of viscoelastic

material is of great importance because viscoelastic behaviour has a great effect on the performance of material. The asthenosphere which forms the transition zone between the low dense crust and higher density mantle is viscous in nature and most of the dynamic earth processes responsible for the earthquake takes place in this zone. Therefore, different type of physical phenomena may occur.

The propagation of SH-waves in viscoelastic material has been studied by various authors. At an interface between viscoelastic material the problem of reflection and transmission of oblique plane waves was studied by Cooper [37]. The plane waves transmission through linear viscoelastic layered media was studied by Shaw and Bugl [120]. The reflected and transmitted waves due to an elastic plane sinusoidal P or SV wave impinging on the plane interface between an elastic and a linearly viscoelastic medium were found analytically for any type of viscoelastic behaviour by Schoenberg [109]. Kaushik and Chopra [71] studied the phenomena of reflection and transmission of plane SH wave through a self-reinforced elastic layer sandwiched between two homogeneous viscoelastic solid half-spaces. Gogna and Chander [59] represented the problem of reflection and transmission of SH-waves at an interface between anisotropic inhomogeneous elastic and viscoelastic half-spaces. Romeo [103] discussed SH-wave in interfacial viscoelastic medium. Kanai [68] studied the effect of viscosity of surface layer on the earthquake movements. The propagation of SH-waves in viscoelastic media with and without heterogeneity was studied by Cerveny [23]. Wang et al. [138] studied the wave propagation in an inhomogeneous transversely isotropic material obeying the generalized power law model. The problem of steady, mixed convective, laminar flow of two incompressible, electrically conducting and heat absorbing immiscible fluids in a vertical porous channel

filled with viscoelastic fluid in one region and viscous fluid in the other region was analysed by Sivaraj et al. [126]. Roy [104] studied the propagation of SH-wave in laterally heterogeneous medium. SH-wave propagation in viscoelastic heterogenous layer over half-space with self-weight has been studied by Sahu et al. [108].

Chapter 2

Dynamic response of normal moving load

2.1 Introduction

The moving load problem over a surface of an elastic medium is a subject of considerable investigation to civil engineers, seismologist and applied mathematicians due to its impact in determining the strength of a structure. The waves produced due to moving vehicles, impact and other types of dynamical loads on a surface fall in this category. The physical problem of a fracture due to moving load is a dynamic problem in which consequences of stress conditions are considered as slip and the material strength in the focal region. In view of this, the earthquake mechanism is described by a shear fracture caused in the focal region due to the drop in stress. At a point of the fault, fracture initiates when the stress propagating with certain velocity exceeds a critical value and stops when conditions disrupt it to propagate further. The failure will be occurred when the stress produced in the medium is more than the strength of the medium. So, determination of stresses produced due

The contents of this chapter are published in following journals:
1. The contents of section (2.2) are published in *Journal of Vibration and Control, 22(1): 77-88, 2016, (SCI, Impact factor-1.643).*
2. The contents of section (2.3) are published in *Applied Mathematical Modelling, 40 (5-6): 3535-3549, 2016, (SCI, Impact factor-2.291).*

to moving load is an interesting problem to study. In the engineering discipline, the investigation of stress is an essential part that includes various methods to analyse the stresses in structures and materials subjected to loads or forces. In design of all sizes structures such as rocket bodies, aircrafts, space shuttles etc. the determination of stress is main task for electrical, mechanical, aerospace and electronics engineers. Drawing on this knowledge, it can be said that the analysis of stress can be employed to determine the strength, durability and endurance of the structure so that different types of materials available in the nature can be efficiently used in technological and dynamics applications.

In an elastic half-space, Cole and Huth [36] discussed the moving load problem and find out the steady state solution of this problem. Sneddon [127] discussed the problem of normal line load discussed by Cole and Huth [36] somewhat with different method for solution. Stresses produced in a transversely isotropic elastic half-space due to a moving load has been determined by Mukherjee [88]. The moving load problem on a plate resting over a layered half-space has been discussed by Miles [86] and Sackman [105]. Some remarkable work related to the moving load problem on a elastic half-space has been done by Achenbach et al. [5], Chonan [35], Ungar [135], Olsson [94], Lee and Ng [79], Alkeseyeva [10] etc. In the symmetry plane of a monoclinic half-space the dynamic response of a normal moving load was studied by Chattopadhyay and Saha [30]. The effect of moving load in the micropolar solid media was discussed by Ghosh [57]. In micropolar theory of elasticity Kumar and Gogna [76] and Kumar and Deswal [75] discussed the steady state response of moving loads.

All the Earth media are not regular; there exist irregularities of different sizes

and shapes on the earth curst. So, it becomes essential to consider the problem of moving load involving irregularity in the medium. Mukhopadhyay [89] discussed the normal moving load problem over a transversely isotropic layer which is lying on a rigid foundation, Selim [110] investigated the static deformation of a medium which is irregular and initially stressed. To solve the problem of static deformation he used the eigen value approach. The stresses produced due to normal moving load on a rough irregular isotropic half-space was studied by Chattopadhyay et al. [28]. Many problems dealing with irregularity have been studied by Chattopadhyay et al. [26, 27, 31]. Singh and Singh [123] studied the normal and shear stresses produced due to a normal moving load in a rough heterogeneous monoclinic half-space with irregularity.

This chapter aims to study the stress produced in an irregular fibre-reinforced half-space due to a normal moving load on a free surface. Section 2.2 of this chapter deals with the stresses produced in an irregular fiber-reinforced half-space due to a normal moving load on a free surface and in section 2.3, the stresses produced in an irregular micropolar half-space due to a normal moving load on a free surface are discussed. The stresses produced in both sections have been obtained in a closed form.

2.2 Dynamic response of normal moving load on an irregular fibre-reinforced half-space

2.2.1 Formulation of the problem

Following Chattopadhyay et al. [28], we considered an irregular homogenous fibre-reinforced half-space which is subjected to a normal line load F independent of y

and moving with a constant velocity c in the direction of positive x-axis. Here, y-axis vertically downwards and the x-axis along the surface of the half-space. We assume the irregularity in the form of a parabola with the span $2a$ and maximum depth H. The origin is placed at the middle point of the span of the irregularity as shown in Fig. (2.1).

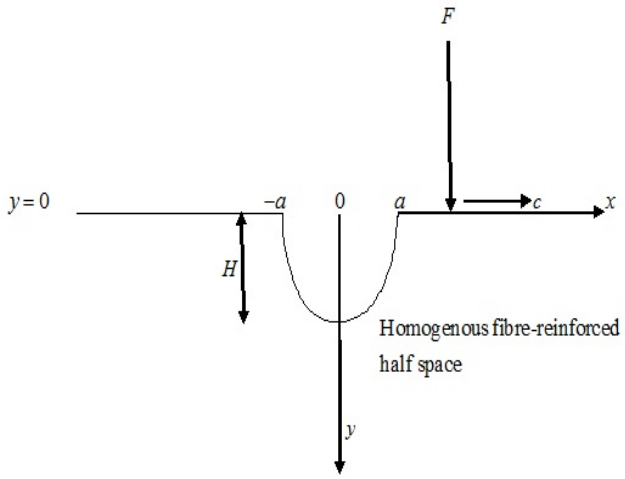

Figure 2.1: Geometry of the problem

The equation of upper interface containing irregularity is (Chattopadhyay et al. [28])

$$y = \varepsilon h(x), \tag{2.1}$$

where

$$h(x)=\begin{cases} 0, & |x| \geq a \\ \frac{2(a^2-x^2)}{a}, & |x| < a \end{cases}$$

and $\varepsilon = \frac{H}{2a} << 1$, is a small positive number, H is the maximum depth of the irregularity below the interface and $2a$ is the span of the irregularity.

The constitutive equation for a fibre-reinforced linearly elastic medium with preferred direction $\vec{a}$ is given by equation (1.15) in Chapter-1.

If $\vec{a}$ is chosen so that its components are $(1, 0, 0)$, i.e. the preferred direction is

everywhere along $x-$axis, then equation (1.15) gives

$$\begin{aligned}
\tau_{11} &= (\lambda' + 2\alpha' + 4\mu_L - 2\mu_T + \beta')e_{11} + (\lambda' + \alpha')e_{22} + (\lambda' + \alpha')e_{33},\\
\tau_{22} &= (\lambda' + \alpha')e_{11} + (\lambda' + 2\mu_T)e_{22} + \lambda' e_{33},\\
\tau_{33} &= (\lambda' + \alpha')e_{11} + \lambda' e_{22} + (\lambda' + 2\mu_T)e_{33},\\
\tau_{23} &= 2\mu_T e_{23},\\
\tau_{13} &= 2\mu_L e_{13},\\
\tau_{12} &= 2\mu_L e_{12}.
\end{aligned} \tag{2.2}$$

We assume

$$u = u(x, y, t), v = v(x, y, t) \text{ and } w = 0. \tag{2.3}$$

In the absence of body forces, the equations of motion for a small elastic disturbance in fibre-reinforced half-space are given through (1.16) in Chapter-1.

Using (2.2) and (2.3), the equation of motion (1.16) becomes

$$(\lambda' + 2\alpha' + 4\mu_L - 2\mu_T + \beta')\frac{\partial^2 u}{\partial x^2} + (\alpha' + \lambda' + \mu_L)\frac{\partial^2 v}{\partial x \partial y} + \mu_L \frac{\partial^2 u}{\partial y^2} = \rho' \frac{\partial^2 u}{\partial t^2}, \tag{2.4}$$

$$\mu_L \frac{\partial^2 v}{\partial x^2} + (\alpha' + \lambda' + \mu_L)\frac{\partial^2 u}{\partial x \partial y} + (\lambda' + 2\mu_T)\frac{\partial^2 v}{\partial y^2} = \rho' \frac{\partial^2 v}{\partial t^2}. \tag{2.5}$$

As pulse of shearing force F is moving with a uniform velocity c along the free surface in the positive direction of x-axis (shown in Fig. 2.1), therefore, the boundary conditions of the problem at $y = \varepsilon h(x)$ may be written as

$$\begin{aligned}
\tau_{12} &= -F\delta(x - ct),\\
\tau_{22} &= 0,
\end{aligned} \tag{2.6}$$

where τ_{12} and τ_{22} are shearing and normal stresses.

Using equation (2.2), boundary condition (2.6) gives

$$\begin{aligned}
\mu_L \left(\frac{\partial u}{\partial y} + \frac{\partial v}{\partial x}\right) &= -F\delta(x - ct),\\
(\lambda' + \alpha')\frac{\partial u}{\partial x} + (\lambda' + 2\mu_T)\frac{\partial v}{\partial y} &= 0,
\end{aligned} \tag{2.7}$$

where $\delta(x)$ stands for Dirac delta function of the argument x and

$$\delta(x-ct) = \frac{1}{\pi}\int_0^\infty \cos(k(x-ct))dk. \tag{2.8}$$

2.2.2 Solution to the problem

The solution of equations of motion (2.4) and (2.5) may be assumed as (Chattopadhyay et al. [28])

$$\begin{aligned} u &= \int_0^\infty Ae^{-kqy}\cos(k(x-ct))dk, \\ v &= \int_0^\infty Be^{-kqy}\sin(k(x-ct))dk, \end{aligned} \tag{2.9}$$

where q is a parameter independent of k.

Using equation (2.9) in equations (2.4) and (2.5), we get

$$A[(\lambda'+2\alpha'+4\mu_L-2\mu_T+\beta') - \mu_L q^2 - \rho' c^2] + B(\lambda'+\mu_L+\alpha')q = 0, \tag{2.10}$$

and

$$A(\lambda'+\mu_L+\alpha')q + B[(\lambda'+2\mu_T)q^2 - \mu_L + \rho' c^2] = 0, \tag{2.11}$$

Equations (2.10) and (2.11) are consistent if

$$\begin{aligned} &q^4 + \left[\frac{\rho' c^2-\mu_L}{\lambda'+2\mu_T} + \frac{\rho' c^2-(\lambda'+2\alpha'+4\mu_L-2\mu_T+\beta')}{\mu_L} + \frac{(\lambda'+\mu_L+\alpha')^2}{\mu_L(\lambda'+2\mu_T)}\right] q^2 \\ &+ \frac{(\rho' c^2-\mu_L)(\rho' c^2-(\lambda'+2\alpha+4\mu_L-2\mu_T+\beta'))}{\mu_L(\lambda'+2\mu_T)} = 0. \end{aligned} \tag{2.12}$$

Let q_1^2 and q_2^2 be the two roots of equation (2.12), $q_1$and q_2 are both positive. So for real q_1 and q_2, the term $\rho' c^2-(\lambda'+2\alpha'+4\mu_L-2\mu_T+\beta')$ should be positive. Hence, c must be greater than both

$$\sqrt{\frac{\mu_L}{\rho'}} \text{ and } \sqrt{\frac{\lambda'+\alpha'+4\mu_L-2\mu_T+\beta'}{\rho'}},$$

the coefficient of q^2 and the constant term in equation (2.12) become positive.

Therefore,

$$q_i = \frac{-A' \pm \sqrt{A'^2 - 4C'}}{2},\ (i = 1, 2) \tag{2.13}$$

where

$$A' = \left[\frac{\rho' c^2 - \mu_L}{\lambda' + 2\mu_T} + \frac{\rho' c^2 - (\lambda' + 2\alpha' + 4\mu_L - 2\mu_T + \beta')}{\mu_L} + \frac{(\lambda' + \mu_L + \alpha')^2}{\mu_L(\lambda' + 2\mu_T)}\right],$$
$$C' = \frac{(\rho' c^2 - \mu_L)[\rho' c^2 - (\lambda' + 2\alpha' + 4\mu_L - 2\mu_T + \beta')]}{\mu_L(\lambda' + 2\mu_T)}.$$

In view of equations (2.10), (2.11) and (2.13), equation (2.9) gives the expressions for u and v as

$$u = \int_0^\infty (A_1 e^{-kq_1 y} + A_2 e^{kq_2 y}) \cos(k(x - ct))dk, \tag{2.14}$$

and

$$v = \int_0^\infty (A_1\alpha_1 e^{-kq_1 y} + A_2\beta_1 e^{kq_2 y}) \sin(k(x - ct))dk, \tag{2.15}$$

where

$$\alpha_1 = \frac{\mu_L q_1^2 + \rho' c^2 - (\lambda' + 2\alpha' + 4\mu_L - 2\mu_T + \beta')}{(\lambda' + \mu_T + \alpha')q_1},$$
$$\beta_1 = \frac{\mu_L q_2^2 + \rho' c^2 - (\lambda' + 2\alpha' + 4\mu_L - 2\mu_T + \beta')}{(\lambda' + \mu_T + \alpha')q_2}.$$

Since the boundary is not uniform, the terms A_1 and A_2 in equations (2.14) and (2.15) are functions of ε. Expanding these terms in ascending powers of ε and retaining the terms up to the first order of ε (as ε is very small), we get

$$A_1 \cong A_{10} + A_{11}\varepsilon, A_2 \cong A_{20} + A_{21}\varepsilon, e^{\pm\nu\varepsilon h} = 1 \pm \nu\varepsilon h. \tag{2.16}$$

Using (2.16) in (2.14) and (2.15) and applying in condition (2.7), we get

$$[(\lambda' + \alpha') + \alpha_1 q_1(\lambda' + 2\mu_T)]A_{10} + [(\lambda' + \alpha') + \beta_1 q_2(\lambda' + 2\mu_T)]A_{20} = 0, \tag{2.17}$$

$$[(\lambda' + \alpha') + \alpha_1 q_1(\lambda' + 2\mu_T)]A_{11} + [(\lambda' + \alpha') + \beta_1 q_2(\lambda' + 2\mu_T)]A_{21} + [-kq_1 h(\lambda' + \alpha') - kq_1^2\alpha_1 h(\lambda' + 2\mu_T)]A_{10} + [-kq_2 h(\lambda' + \alpha') - kq_2^2\beta_1 h(\lambda' + 2\mu_T)]A_{20} = 0, \tag{2.18}$$

$$(\alpha_1 - q_1)A_{10} + (\beta_1 - q_2)A_{20} = \frac{-F}{\pi k \mu_L}, \tag{2.19}$$

$$(\alpha_1 - q_1)A_{11} + (\beta_1 - q_2)A_{21} + (kq_1^2 h - \alpha_1 q_1 kh)A_{10} + (kq_2^2 h - \beta_1 q_2 kh)A_{20} = 0. \tag{2.20}$$

Now solving the above equations, we obtain

$$A_{10} = \frac{(N + \beta_1 q_2 M)D}{k},\ A_{20} = -\frac{(N + \alpha_1 q_1 M)D}{k},$$

$$A_{11} = [D_1(\beta_1 - q_2) - D_2(N + \beta_1 q_2 M)]\frac{\pi \mu_L D}{F},$$

$$A_{21} = [D_2(N + \alpha_1 q_1 M) - D_1(\alpha_1 - q_1)]\frac{\pi \mu_L D}{F},$$

where

$$N = \lambda' + \alpha',\ M = \lambda' + 2\mu_T,\ D = \frac{-F}{\pi \mu_L[(N + q_1\alpha_1 M)(q_2 - \beta_1) - (q_1 - \alpha_1)(N + q_2\beta_1 M)]},$$

$$D_1 = (N + \beta_1 q_2 M)(N + q_1\alpha_1 M)(q_1 h - q_2 h)D,$$

$$D_2 = [(N + \alpha_1 q_1 M)(q_2 - \beta_1)q_2 h - q_1 h(N + \beta_1 q_2 M)(q_1 - \alpha_1)]D.$$

With the help of obtained values of $A_{10}, A_{11}, A_{20}, A_{21}$, equations (2.14) and (2.15) reduces to

$$u = \int_0^\infty D\left[\left[\frac{N + \beta_1 q_2 M}{k} + \varepsilon[D_1(\beta_1 - q_2) - D_2(N + \beta_1 q_2 M)]\frac{\pi \mu_L}{F}\right] e^{-kq_1 y} - \left[\frac{N + \alpha_1 q_1 M}{k} + \varepsilon\frac{[-D_2(N + \alpha_1 q_1 M) + D_1(\alpha_1 - q_1)]\pi \mu_L}{F}\right] e^{-kq_2 y}\right] \cos(k(x - ct))dk, \tag{2.21}$$

$$v = \int_0^\infty D\left[\left[\frac{N + \beta_1 q_2 M}{k} + \varepsilon[D_1(\beta_1 - q_2) - D_2(N + \beta_1 q_2 M)]\frac{\pi \mu_L}{F}\right] \alpha_1 e^{-kq_1 y} - \left[\frac{N + \alpha_1 q_1 M}{k} + \varepsilon\frac{[-D_2(N + \alpha_1 q_1 M) + D_1(\alpha_1 - q_1)]\pi \mu_L}{F}\right] \beta_1 e^{-kq_2 y}\right] \sin(k(x - ct))dk, \tag{2.22}$$

Since q_1, q_2, α_1 and β_1 do not depend on k, hence substituting the values of u and v from equations (2.21) and (2.22) in equation (2.2), and performing integration, we obtain the expressions for non-vanishing stresses as

$$\tau_{11} = \left[\frac{S_1}{\xi_1} + \frac{S_3}{\xi_2} + 2\varepsilon\left(\frac{S_2 q_1 y}{\xi_1^2} + \frac{S_4 q_2 y}{\xi_2^2}\right)\right](x - ct), \tag{2.23}$$

$$\tau_{22} = \left[\frac{S_5}{\xi_1} + \frac{S_7}{\xi_2} + 2\varepsilon\left(\frac{S_6 q_1 y}{\xi_1^2} + \frac{S_8 q_2 y}{\xi_2^2}\right)\right](x - ct), \tag{2.24}$$

$$\tau_{12} = \mu_L \left[\frac{S_9 q_1 y}{\xi_1} + \frac{S_{11} q_2 y}{\xi_2} + \varepsilon \left(\frac{S_{10} \xi_3}{\xi_1^2} + \frac{S_{12} \xi_4}{\xi_2^2} \right) \right], \tag{2.25}$$

where

$$\begin{aligned}
&S_1 = -D(N + \beta_1 q_2 M)((\lambda' + 2\alpha' + 4\mu_L - 2\mu_T + \beta') + \alpha_1 q_1 N),\\
&S_2 = -A_{11}[(\lambda' + 2\alpha' + 4\mu_L - 2\mu_T + \beta') - \alpha_1 q_1 N],\\
&S_3 = D(N + \alpha_1 q_1 M)((\lambda' + 2\alpha' + 4\mu_L - 2\mu_T + \beta') + \beta_1 q_2 N),\\
&S_4 = -A_{21}[(\lambda' + 2\alpha' + 4\mu_L - 2\mu_T + \beta') - \beta_1 q_2 N],\\
&S_5 = -D(N + \beta_1 q_2 M)(N + \alpha_1 q_1 M), S_6 = -A_{11}(N + \alpha_1 q_1 M),\\
&S_7 = -D(N + \alpha_1 q_1 M)(N + \beta_1 q_2 M), S_8 = -A_{21}(N + \beta_1 q_2 M),\\
&S_9 = D(N + \beta_1 q_2 M)(\alpha_1 - q_1), S_{10} = A_{11}(\alpha_1 - q_1),\\
&S_{11} = D(N + \alpha_1 q_1 M)(q_2 - \beta_1), S_{12} = A_{21}(\beta_1 - q_2),\\
&\xi_1 = q_1^2 y^2 + (x - ct)^2, \xi_2 = q_2^2 y^2 + (x - ct)^2,\\
&\xi_3 = q_1^2 y^2 - (x - ct)^2, \xi_4 = q_2^2 y^2 - (x - ct)^2.
\end{aligned} \tag{2.26}$$

From equations (2.23), (2.24) and (2.25), it is clear that the whole stress system is moving with uniform velocity c in the x-direction. The expression for the shearing stress shows that in any plane parallel to the boundary, the shearing stress attains maximum value at $x - ct$, i.e., at the point directly below the point of application of the shearing force on the boundary. It is clear from (2.23) and (2.24) that the normal stresses are zero at the point directly below the point of application of the shearing force on the boundary. In further discussion of this section we deal with the shearing stress which attains maximum value at $x - ct$.

2.2.3 Particular Cases

2.2.3.1 Case 1

When $\varepsilon = 0$ then the expression of shear stress (2.25) reduces to

$$\tau_{12} = \mu_L \left(\frac{S_9}{q_1 y} + \frac{S_{11}}{q_2 y} \right), \tag{2.27}$$

where S_9 and S_{11} are given in equation (2.26).

Equation (2.27) is the expression for shear stress produced due to normal moving load on a regular fibre-reinforced half-space.

2.2.3.2 Case 2

When $\mu_L = \mu_T = \mu'$ and $\alpha' = \beta' = 0$, then the expression for shear stress (2.25) reduces to

$$\tau_{12} = \mu \left[\left(\frac{S'_9}{q_1 y} + \frac{S'_{11}}{q_2 y} \right) + \varepsilon \left(\frac{S'_{10}}{q_1^2 y^2} + \frac{S'_{12}}{q_2^2 y^2} \right) \right], \tag{2.28}$$

where

$$D' = \frac{-F}{\pi\mu'[(\lambda' + q'_1\alpha'_1(\lambda' + 2\mu'))(q'_2 - \beta'_1) - (q'_1 - \alpha'_1)(\lambda' + q'_2\beta'_1(\lambda' + 2\mu'))]},$$

$$\alpha'_1 = \frac{\mu' q'^2_1 + \rho' c^2 - (\lambda' + \mu')}{(\lambda' + \mu')q'_1},\ \beta_1 = \frac{\mu' q'^2_2 + \rho' c^2 - (\lambda' + \mu')}{(\lambda' + \mu')q'_2},$$

$$P' = \frac{\rho' c^2 - \mu'}{\lambda' + 2\mu'} + \frac{\rho' c^2 - (\lambda' + 2\mu')}{\mu'} + \frac{(\lambda' + \mu')^2}{\mu'(\lambda' + 2\mu')^2},\ Q' = \frac{(\rho' c^2 - \mu')(\rho' c^2 - (\lambda' + 2\mu')}{\mu'(\lambda' + 2\mu')},$$

$$q'_i = \frac{-P' \pm \sqrt{P'^2 - 4Q'}}{2},\ (i = 1, 2),$$

$$A'_{11} = [D'_1(\beta'_1 - q'_2) - D'_2(\lambda' + \beta'_1 q'_2(\lambda' + 2\mu'))]\frac{\pi\mu' D'}{F},$$

$$A'_{21} = [D'_2(\lambda' + \alpha'_1 q'_1(\lambda' + 2\mu')) - D'_1(\alpha'_1 - q'_1)]\frac{\pi\mu' D'}{F},$$

$$S'_9 = D'[\lambda' + \beta'_1 q'_2(\lambda' + 2\mu')](\alpha'_1 - q'_1),\ S'_{10} = A'_{11}(\alpha'_1 - q'_1),$$

$$S'_{11} = D'[\lambda' + \alpha'_1 q'_1(\lambda' + 2\mu')](q'_2 - \beta'_1),\ S'_{12} = A'_{21}(\beta'_1 - q'_2).$$

Equation (2.28) is the expression for shear stress produced due to normal moving load on an irregular isotropic half-space.

2.2.3.3 Case 3

When $\mu_L = \mu_T = \mu'$, $\alpha' = \beta' = 0$ and $\varepsilon = 0$, then the expression for shear stress (2.25) reduces to

$$\tau_{12} = \mu \left(\frac{S'_9}{q_1 y} + \frac{S'_{11}}{q_2 y} \right), \tag{2.29}$$

which is the expression for shear stress produced due to normal moving load on a regular isotropic half-space.

2.2.4 Numerical results and discussions

For numerical computation of shear stress in an irregular homogenous fibre-reinforced half-space which is subjected to a normal line load F moving with a constant velocity in the positive direction of x-axis, we consider the following data [83]:

$\mu_L = 5.66 \times 10^9 Nm^{-2}$, $\mu_T = 2.46 \times 10^9 Nm^{-2}$, $\lambda' = 5.65 \times 10^9 Nm^{-2}$,

$\alpha' = -1.28 \times 10^9 Nm^{-2}$, $\beta' = 220.90 \times 10^9 Nm^{-2}$, $\rho' = 7800 kgm^{-3}$,

and $x = ct$ unless stated otherwise.

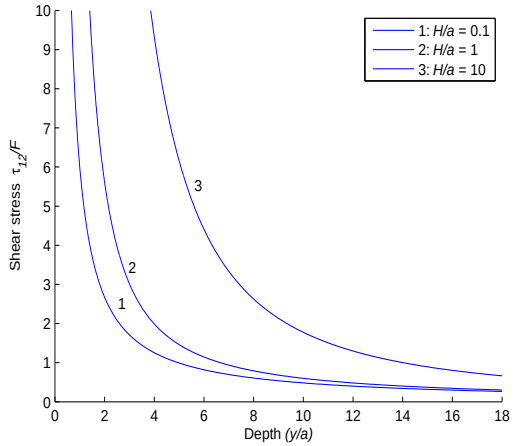

Figure 2.2: Variation of the shear stress (in fibre-reinforced medium) against depth for different irregularity depths (H/a) when $x/a = 0$.

The effects of depth of irregularity and irregularity factor on non-dimensional shear

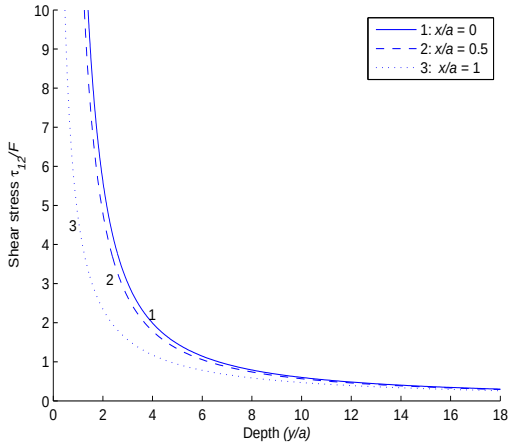

Figure 2.3: Variation of the shear stress (in fibre-reinforced medium) against depth for different irregularity factor (x/a) when $H/a = 1$.

stress in an irregular fibre-reinforced medium are shown in Figs. (2.2) and (2.3) respectively. It is evident from both the figures that non-dimensional shear stress decreases with an increase in depth. Specifically, Fig. (2.2) reveals that shear stress increases with an increase in the depth of irregularity whereas Fig. (2.3) suggests that shear stress decreases with an increase in irregularity factor. In Fig. (2.3) the solid line curve represents the case of rectangular irregularity, the dashed curve corresponds to the case of parabolic irregularity and the dotted curve refers to the case with no irregularity. It is observed that shear stress is more in the case of rectangular irregularity than in parabolic irregularity of same depth.

Variation of shear stress against depth and irregularity of depth in the case of rectangular irregularity, parabolic irregularity and no irregularity has been shown by surface plot in Figs. (2.4), (2.5) and (2.6) respectively. Also, the variation of shear stress against depth and irregularity factor for different values of irregularity depth has been shown by surface plot in Figs. (2.7), (2.8) and (2.9).

For numerical computation of shear stress in an irregular homogenous isotropic

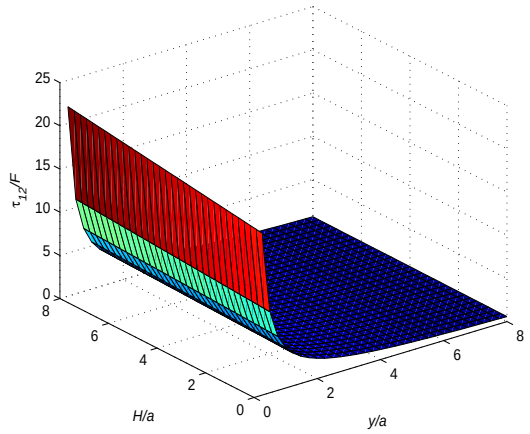

Figure 2.4: Variation of the shear stress (in fibre-reinforced medium) against depth for different irregularity depths in case of rectangular irregularity.

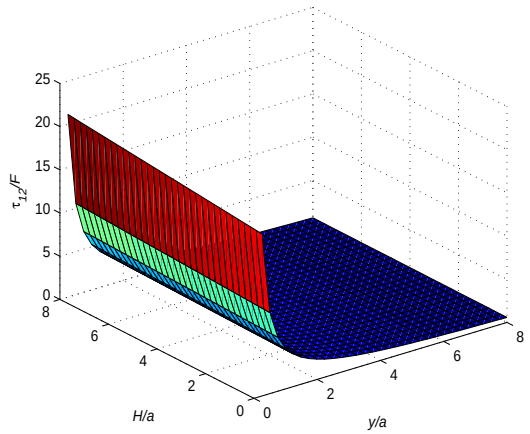

Figure 2.5: Variation of the shear stress (in fibre-reinforced medium) against depth for different irregularity depths in case of parabolic irregularity.

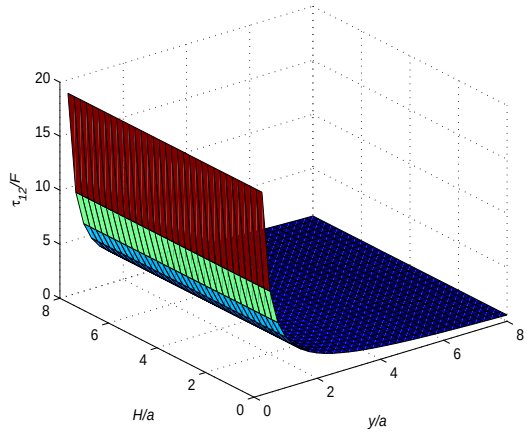

Figure 2.6: Variation of the shear stress (in fibre-reinforced medium) against depth for different irregularity depths in case of no irregularity.

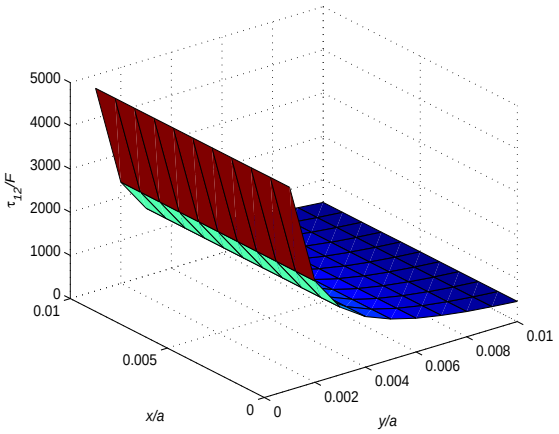

Figure 2.7: Variation of the shear stress (in fibre-reinforced medium) against depth and irregularity factor when irregularity depth is $H/a = 0$.

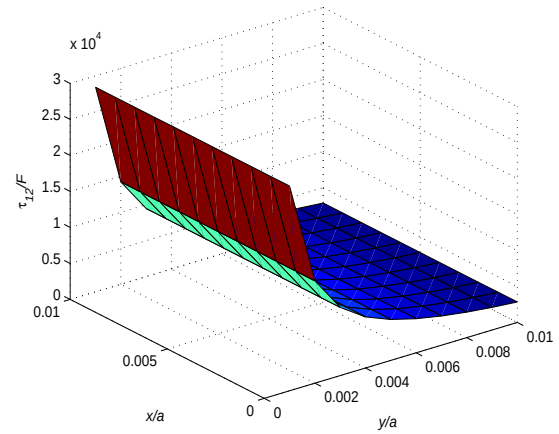

Figure 2.8: Variation of the shear stress (in fibre-reinforced medium) against depth and irregularity factor when irregularity depth is $H/a = 0.1$.

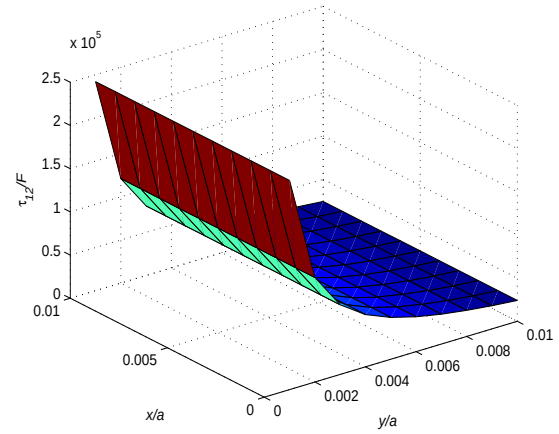

Figure 2.9: Variation of the shear stress (in fibre-reinforced medium) against depth and irregularity factor when irregularity depth is $H/a = 1$.

half-space which is subjected to a normal line load F moving with a constant velocity in the positive direction of x-axis, we consider the following data [62]:

$\mu' = 1.987 \times 10^{10} N/m^2$, $\lambda' = 2.510 \times 10^{10} N/m^2$, $\rho' = 4705 kg/m^3$.

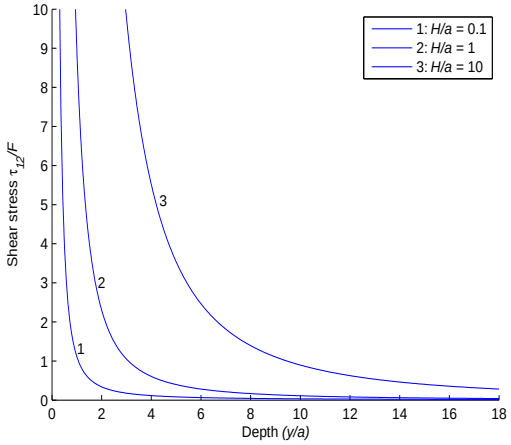

Figure 2.10: Variation of the shear stress (in isotropic medium) against depth for different irregularity depths (H/a) when $x/a = 0$.

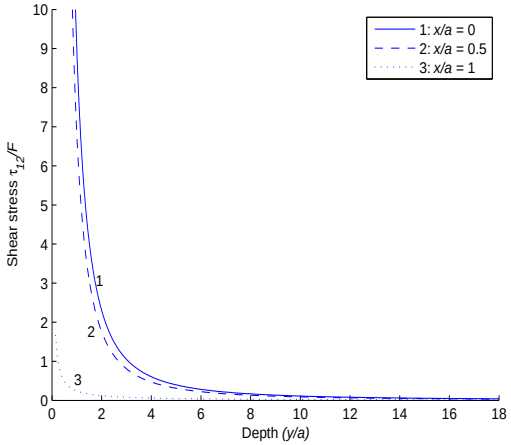

Figure 2.11: Variation of the shear stress (in isotropic medium) against depth for different irregularity factor $(x/1)$ when $H/a = 1$.

Figs. (2.10) and (2.11), show the effect of the depth of irregularity and the irregularity factor on non-dimensional shear stress in an irregular isotropic medium respectively. It is observed from both the figures that non-dimensional shear stress decreases with an increase in depth as in fibre-reinforced medium. But comparative study of shear stress in both isotropic and fibre-reinforced mediums suggest that shear stress is more in fibre-reinforced mediums as compared to isotropic cases. Fig. (2.10) gives the variation of shear stress for different values of depth of irregularity whereas Fig. (2.11) gives the variation of shear stress for different values of irregularity factor. The solid line curve (1), the dashed curve (2) and the dotted curve (3) in Fig. (2.11) correspond to the case of rectangular irregularity, parabolic irregularity and no irregularity respectively. On comparing the curves, we find that rectangular irregularity has more effect on shear stress than parabolic irregularity.

Figs. (2.12), (2.13) and (2.14) give the variation of shear stress against depth

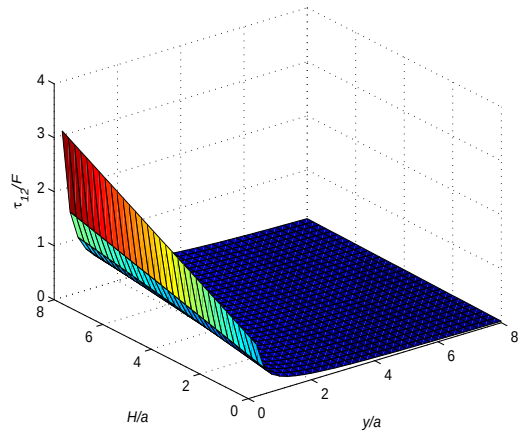

Figure 2.12: Variation of the shear stress (in isotropic medium) against depth and irregularity depth in case of rectangular irregularity.

and irregularity depth in the case of rectangular irregularity, parabolic irregularity and no irregularity respectively for an isotropic medium. The surface plot in Figs.

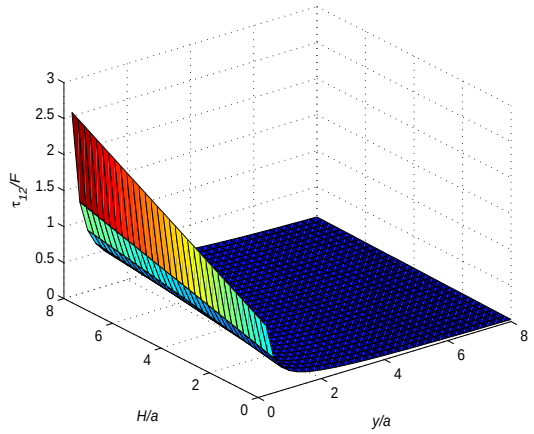

Figure 2.13: Variation of the shear stress against depth and irregularity depth in case of parabolic irregularity.

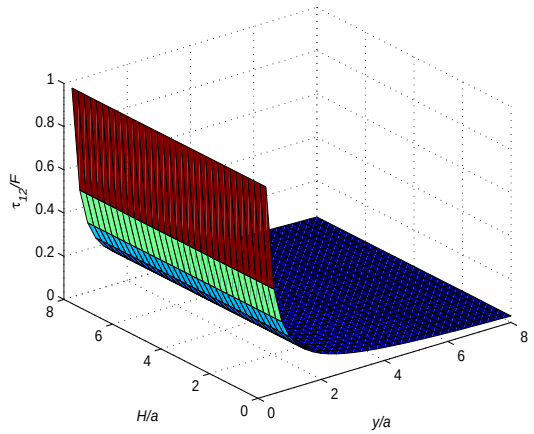

Figure 2.14: Variation of the shear stress (in isotropic medium) against depth and irregularity depth in case of no irregularity.

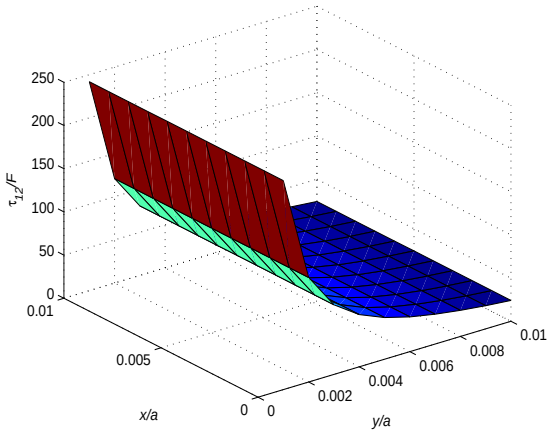

Figure 2.15: Variation of the shear stress (in isotropic medium) against depth and irregularity factor when irregularity depth is $H/a = 0$.

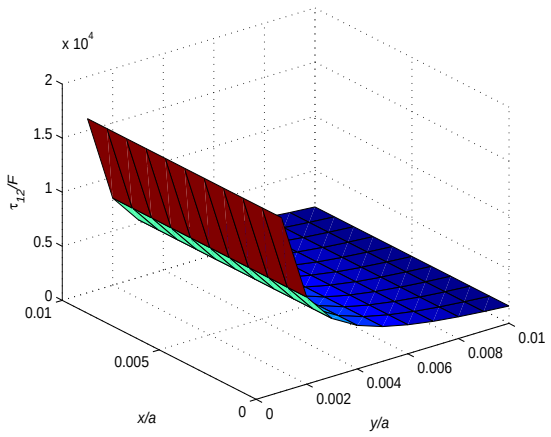

Figure 2.16: Variation of the shear stress (in isotropic medium)against depth and irregularity factor when irregularity depth is $H/a = 0.1$.

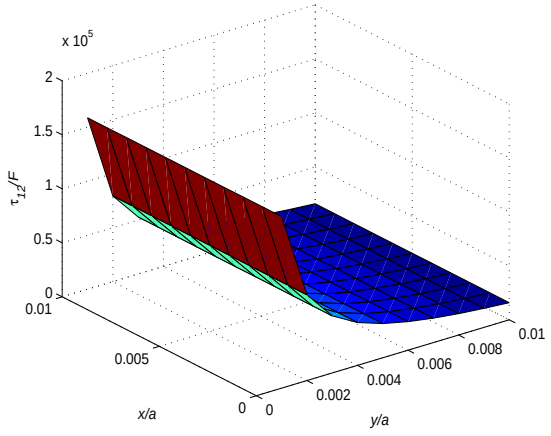

Figure 2.17: Variation of the shear stress (in isotropic medium)against depth and irregularity factor when irregularity depth is $H/a = 1$.

(2.15), (2.16) and (2.17) are the variation of shear stress against depth and irregularity factor for different values of irregularity depth in the isotropic case. Thus it can be concluded that variation of shear stress against different parameters follows the same pattern in both fibre-reinforced medium and isotropic medium, but shear stress is found more in the fibre-reinforced case compared to the isotropic case.

2.2.5 Conclusion

The stress produced in an irregular fibre-reinforced half-space due to a normal moving load on a free surface has been investigated. The study has been done for three different types of irregularity, namely parabolic, rectangular and no irregularity. The effects of irregularity depth, irregularity factor and depth of half-space on shear stress have been discussed. Also, a comparative study has been made for isotropic and fibre-reinforced medium. The following outcomes can be highlighted as an outcome of the study:

- Depth has a substantial effect on the shear stress, i.e. shear stress decreases with an increase in the depth.
- The shear stress increases with an increase in the maximum depth of irregularity.
- The effect of irregularity factor on shear stress is significant. Specifically, as irregularity prevails in the medium, shear stress increases. Moreover, the rectangular irregularity has a more favorable effect on the shear stress than the parabolic irregularity of the same depth and span.
- The comparative study of fibre-reinforced and isotropic medium suggests that

depth, irregularity factor and maximum depth of irregularity have the same effect on shear stress, but shear stress is more in the case of fibre-reinforced medium compared with isotropic medium.

2.3 Dynamic response of moving load on a micropolar half-space with irregularity

Owing to its ability to explain the size effects in the small length scale by considering additional degrees of freedom, micropolar theory is preferred to describe the media with complex microstructure like soil, composite materials, granular and powered like materials, masonries, bones and liquid crystals etc. A theoretical model is presented to study the response of moving load on a micropolar half-space with irregularity. The expressions of normal stress, shear stress and tangential couple stress have been obtained in closed form. The effects of friction, microstructure and irregularity in the medium have been studied by introducing frictional coefficient (R), coupling factor (N) and irregularity factor (x/a). The effects of varying depth of half-space and irregularity on stresses have been discussed. The comparative study is made for different cases of irregularity viz. rectangular, parabolic and no irregularity.

2.3.1 Formulation of the problem

We consider a normal moving load F on a micropolar half-space with parabolic irregularity which is independent of y and moving with a constant velocity V in the direction of positive x-axis. The x-axis is chosen in the direction of moving load and y-axis vertically downwards. The origin is placed at the middle point of span of the

irregularity as shown in Fig. (2.1).

The equation of upper interface containing irregularity is given by (2.1).

The basic governing equations of motion and constitutive relations in micropolar elastic half-space in absence of body force are given by equations (1.11), (1.12), (1.13) and (1.14) in Chapter-1.

For two-dimensional problem, we assume

$\overrightarrow{u} = (u, v, 0)$ and $\overrightarrow{\phi} = (0, 0, \phi)$.

Thus, the equations of motion (1.11) and (1.12) can be written as

$$(\lambda + 2\mu + \kappa)\frac{\partial^2 u}{\partial x^2} + (\mu + \kappa)\frac{\partial^2 u}{\partial y^2} + (\lambda + \mu)\frac{\partial^2 v}{\partial x \partial y} + \kappa\frac{\partial \phi}{\partial y} = \rho\frac{\partial^2 u}{\partial t^2}, \tag{2.30}$$

$$(\lambda + 2\mu + \kappa)\frac{\partial^2 v}{\partial y^2} + (\mu + \kappa)\frac{\partial^2 v}{\partial x^2} + (\lambda + \mu)\frac{\partial^2 u}{\partial x \partial y} - \kappa\frac{\partial \phi}{\partial x} = \rho\frac{\partial^2 v}{\partial t^2}, \tag{2.31}$$

$$\gamma(\frac{\partial^2 \phi}{\partial x^2} + \frac{\partial^2 \phi}{\partial y^2}) + \kappa(\frac{\partial v}{\partial x} - \frac{\partial u}{\partial y}) - 2\kappa\phi = \rho j\frac{\partial^2 \phi}{\partial t^2}. \tag{2.32}$$

The micropolar theory of elasticity offers more advantage over classical elasticity in the prediction of stresses in materials with microstructure. Fatemi et al. [54] defined the characteristic length and coupling factor (N) for these types of materials as

$$\gamma = 4l^2\mu, \kappa = 2N^2\mu/(1 - N^2),$$

where $0 \leq N < 1$. Here $N = 0$ corresponds to a classical elastic materials and $N = 1$ refers to famous coupled stress theory.

The boundary conditions at $y = \varepsilon h(x)$ may be written as:

$$\sigma_{22} = -F\delta(x - Vt), \sigma_{21} = -FR\delta(x - Vt), m_{13} = 0, \tag{2.33}$$

where m_{13} is tangential couple stress, σ_{22} and σ_{21} are normal and shearing stresses.

2.3.2 Solution of the problem

The solution of equations of motion (2.30), (2.31) and (2.32) may be assumed as

$$u = \int_0^\infty [Ae^{-\omega qy}\cos(\omega(x-Vt)) + Be^{-\omega qy}\sin(\omega(x-Vt))]d\omega, \tag{2.34}$$

$$v = \int_0^\infty [Ce^{-\omega qy}\cos(\omega(x-Vt)) + D'e^{-\omega qy}\sin(\omega(x-Vt))]d\omega, \tag{2.35}$$

$$\phi = \int_0^\infty \omega[Ee^{-\omega qy}\cos(\omega(x-Vt)) + Fe^{-\omega qy}\sin(\omega(x-Vt))]d\omega, \tag{2.36}$$

where ω is the wave number and q is independent of ω.

Using equations (2.34), (2.35) and (2.36) in equations of motion (2.30), (2.31) and (2.32), we have

$$\alpha_1 A - \alpha_2 D' - \kappa qE = 0, \tag{2.37}$$

$$\alpha_1 B + \alpha_2 C - \kappa qF = 0, \tag{2.38}$$

$$\alpha_2 A + \alpha_3 D' + \kappa E = 0, \tag{2.39}$$

$$-\alpha_2 B + \alpha_3 C - \kappa F = 0, \tag{2.40}$$

$$\gamma(-E + Eq^2) = -\rho j V^2 E, \tag{2.41}$$

$$\gamma(-F + Fq^2) = -\rho j V^2 F, \tag{2.42}$$

$$2E = Aq + D', \tag{2.43}$$

$$2F = Bq - C, \tag{2.44}$$

where

$\alpha_1 = (\mu+\kappa)q^2 - \lambda - 2\mu - \kappa + \rho V^2$, $\alpha_2 = (\lambda+\mu)q$, $\alpha_3 = (\lambda+2\mu+\kappa)q^2 - \mu - \kappa + \rho V^2$.

Solving above equations, we get

$D' = mA, C = -mB$ and $V^2 = \alpha_4(1-q^2)$,

where $\alpha_4 = \dfrac{\gamma}{\rho j}$.

Using these relations and above equations, we get

$$q^2 = \frac{-R \pm \sqrt{R^2 - 4QS}}{2Q}, \tag{2.45}$$

and

$$m_1 = \frac{2\alpha_1 - \kappa q_1^2}{2\alpha_2 + \kappa q_1}, m_2 = -\frac{2\alpha_2 + \kappa q_2}{2\alpha_3 + \kappa}, \tag{2.46}$$

where

$Q = 2(2\mu + \kappa)(\lambda + 2\mu + \kappa) + 4\rho^2\alpha_4^2 - 2\rho\alpha_4(6\mu + 3\kappa + 2\lambda)$,

$R = -(2\mu + \kappa)^2 - 4(\lambda + 2\mu + \kappa)^2 + (2\lambda + 2\mu + \kappa)^2 + 2\rho\alpha_4(6\mu + 3\kappa + 2\lambda) - 8\rho^2\alpha_4^2 -$

$2\rho\alpha_4(-2\lambda - 6\mu - 3\kappa)$, $S = (2\lambda + 4\mu + 2\kappa)(2\mu + \kappa) + 4\rho^2\alpha_4^2 + 2\rho\alpha_4(-2\lambda - 6\mu - 3\kappa)$,

q_1 and q_2 are two different roots of q, both are numerically same but opposite in sign.

Solution of equations of motion (2.30), (2.31) and (2.32) can be written as

$$u = \int_0^\infty [A_1 e^{-\omega q_1 y}\cos(\omega(x - Vt)) + A_2 e^{-\omega q_2 y}\cos(\omega(x - Vt)) + B_1 e^{-\omega q_1 y}\sin(\omega(x - Vt))$$

$$+ B_2 e^{-\omega q_2 y}\sin(\omega(x - Vt))]d\omega, \tag{2.47}$$

$$v = \int_0^\infty [-B_1 m_1 e^{-\omega q_1 y}\cos(\omega(x - Vt)) - B_2 m_2 e^{-\omega q_2 y}\cos(\omega(x - Vt)) + A_1 m_1 e^{-\omega q_1 y}$$

$$\sin(\omega(x - Vt)) + A_2 m_2 e^{-\omega q_2 y}\sin(\omega(x - Vt))]d\omega, \tag{2.48}$$

$$\phi = \int_0^\infty \omega[(m_1 + q_1)A_1 e^{-\omega q y}\cos(\omega(x - Vt)) + (m_2 + q_2)A_2 e^{-\omega q y}\cos(\omega(x - Vt)) + (m_1 + q_1)$$

$$B_1 e^{-\omega q_1 y}\sin(\omega(x - Vt)) + (m_2 + q_2)B_2 e^{-\omega q_2 y}\sin(\omega(x - Vt))]d\omega. \tag{2.49}$$

Using approximation (2.16) in (2.47), (2.48) and (2.49) and applying boundary conditions (2.33), we get

$$\xi_1 B_{10} + \xi_2 B_{20} = -\frac{F}{\pi\omega}, \tag{2.50}$$

$$\xi_1 A_{10} + \xi_2 A_{20} = 0, \tag{2.51}$$

$$-\xi_1 \omega q_1 h B_{10} - \xi_2 \omega q_2 h B_{20} + \xi_1 B_{11} + \xi_2 B_{21} = 0, \tag{2.52}$$

$$\xi_1 \omega q_1 h A_{10} + \xi_2 \omega q_2 h A_{20} - \xi_1 A_{11} - \xi_2 A_{21} = 0, \tag{2.53}$$

$$\xi_3 B_{10} + \xi_4 B_{20} = 0, \tag{2.54}$$

$$\xi_3 A_{10} + \xi_4 A_{20} = -\frac{FR}{\pi\omega}, \tag{2.55}$$

$$-\xi_3 \omega q_1 h B_{10} - \xi_4 \omega q_2 h B_{20} + \xi_3 B_{11} + \xi_4 B_{21} = 0, \tag{2.56}$$

$$-\xi_3 \omega q_1 h A_{10} - \xi_4 \omega q_2 h A_{20} + \xi_3 A_{11} + \xi_4 A_{21} = 0, \tag{2.57}$$

$$\lambda(m_1 + q_1) B_{10} + \lambda(m_2 + q_2) B_{20} = 0, \tag{2.58}$$

$$\lambda(m_1 + q_1) A_{10} + \lambda(m_2 + q_2) A_{20} = 0, \tag{2.59}$$

$$\lambda(m_1 + q_1)(-\omega q_1 h B_{10} + B_{11}) + \lambda(m_2 + q_2)(-\omega q_2 h B_{20} + B_{21}) = 0, \tag{2.60}$$

$$\lambda(m_1 + q_1)(-\omega q_1 h A_{10} + A_{11}) + \lambda(m_2 + q_2)(-\omega q_2 h A_{20} + A_{21}) = 0. \tag{2.61}$$

Solving above equations, we get

$$A_{10} = \frac{FR\xi_2}{\pi\omega D}, A_{20} = -\frac{FR\xi_1}{\pi\omega D}, B_{10} = -\frac{F\xi_4}{\pi\omega D}, B_{20} = \frac{F\xi_3}{\pi\omega D},$$

$$A_{11} = \frac{FRh\xi_{11}}{\pi}, A_{21} = -\frac{FRh\xi_{12}}{\pi}, B_{11} = \frac{Fh\xi_9}{\pi}, B_{21} = \frac{Fh\xi_{10}}{\pi}, \tag{2.62}$$

where

$\xi_1 = 2\lambda + 2m_1 q_1(\lambda + 2\mu + \kappa)$, $\xi_2 = 2\lambda + 2m_2 q_2(\lambda + 2\mu + \kappa)$, $\xi_3 = (\mu + \kappa)m_1 - \mu q_1$,
$\xi_4 = (\mu + \kappa)m_2 - \mu q_2$, $D = \xi_1\xi_4 - \xi_2\xi_3$, $\xi_5 = \dfrac{-\xi_3\xi_2 q_2 + \xi_1\xi_4 q_1}{D}$, $\xi_6 = \dfrac{\xi_3\xi_4(q_1 - q_2)}{D}$,
$\xi_7 = \dfrac{\xi_1\xi_2(q_1 - q_2)}{D}$, $\xi_8 = \dfrac{-\xi_3\xi_2 q_1 + \xi_4\xi_1 q_1}{D}$, $\xi_9 = \dfrac{\xi_2\xi_6 - \xi_4\xi_5}{D}$,
$\xi_{10} = \dfrac{\xi_5\xi_3 - \xi_1\xi_6}{D}$, $\xi_{11} = \dfrac{\xi_2\xi_8 + \xi_4\xi_7}{D}$, $\xi_{12} = \dfrac{\xi_3\xi_7 + \xi_1\xi_8}{D}$.

With the help of obtained values displacement components given in equations (2.47), (2.48) and (2.49) can be written as

$$u = \frac{F}{\pi}\int_0^\infty \left(\frac{R\xi_2}{\omega D} + \varepsilon h R\xi_{11}\right) e^{-\omega q_1 y}\cos(\omega(x-Vt)) - \left(\frac{R\xi_1}{\omega D} + \varepsilon h R\xi_{12}\right) e^{-\omega q_2 y}\cos(\omega(x-Vt))$$
$$+ \left(-\frac{\xi_4}{\omega D} + \varepsilon h\xi_9\right) e^{-\omega q_1 y}\sin(\omega(x-Vt)) + \left(\frac{\xi_3}{\omega D} + \varepsilon h\xi_{10}\right) e^{-\omega q_2 y}\sin(\omega(x-Vt))d\omega, \tag{2.63}$$

$$v = \frac{F}{\pi}\int_0^\infty -\left(-\frac{\xi_4}{\omega D} + \varepsilon h\xi_9\right) m_1 e^{-\omega q_1 y}\cos(\omega(x-Vt)) - \left(\frac{\xi_3}{\pi D} + \varepsilon h\xi_{10}\right) m_2 e^{-\omega q_2 y}\cos(\omega(x-Vt))$$
$$+ \left(\frac{R\xi_2}{\omega D} + \varepsilon h R\xi_{11}\right) m_1 e^{-\omega q_1 y}\sin(\omega(x-Vt)) - \left(\frac{R\xi_1}{\omega D} + \varepsilon h R\xi_{12}\right) m_2 e^{-\omega q_2 y}\sin(\omega(x-Vt))d\omega, \tag{2.64}$$

$$\phi = \frac{F}{\pi}\int_0^\infty \left((m_1+q_1)\left(\frac{\xi_2}{\omega D} + \varepsilon h\xi_{11}\right) e^{-\omega q_1 y} - (m_2+q_2)\left(\frac{\xi_1}{\omega D} + \varepsilon h\xi_{12}\right) e^{-\omega q_2 y}\right) R\omega\cos\omega(x-Vt)$$
$$+ \left((m_1+q_1)\left(-\frac{\xi_4}{\omega D} + \varepsilon h\xi_9\right) e^{-\omega q_1 y}) + (m_2+q_2)\left(\frac{\xi_3}{\omega D} + \varepsilon h\xi_{10}\right) e^{-\omega q_2 y}\right)\omega\sin(\omega(x-Vt)))d\omega. \tag{2.65}$$

Since q_1, q_2, m_1 and m_2 do not depend on ω. Hence substituting the values of u, v and ϕ from equations (2.63), (2.64) and (2.65) in expressions of stresses and performing integration, we obtain the expressions for non-vanishing stresses as

$$\frac{\sigma_{22}}{F} = \frac{1}{\pi}\left(S_1 + (x-Vt)S_2 + \varepsilon h\left(S_3 + (x-Vt)S_4\right)\right), \tag{2.66}$$

$$\frac{\sigma_{21}}{F} = \frac{1}{\pi}\left(S_5 + (x-Vt)S_6 + \varepsilon h\left(S_7 + (x-Vt)S_8\right)\right), \tag{2.67}$$

$$\frac{m_{13}}{F} = \frac{\lambda}{\pi}\left(S_9 + S_{10}(x-Vt) + \varepsilon h(S_{11} + S_{12}(x-Vt))\right), \tag{2.68}$$

where

$$S_1 = -\frac{\xi_4\xi_1 q_1 y}{D\phi_1} + \frac{\xi_3\xi_2 q_2 y}{D\phi_2},\ S_2 = -\frac{R\xi_1\xi_2}{D\phi_1} + \frac{R\xi_1\xi_2}{D\phi_2},\ S_3 = \frac{\xi_1\xi_9\phi_3}{\phi_1^2} + \frac{\xi_2\xi_{10}\phi_4}{\phi_2^2},$$
$$S_4 = -\frac{2R\xi_1\xi_{11}q_1 y}{\phi_1^2} + \frac{2R\xi_2\xi_{12}q_2 y}{\phi_2^2},\ S_5 = \frac{R\xi_2\xi_3 q_1 y}{D\phi_1} - \frac{R\xi_1\xi_4 q_2 y}{D\phi_2},\ S_6 = -\frac{\xi_3\xi_4}{D\phi_1} + \frac{\xi_3\xi_4}{D\phi_2},$$
$$S_7 = \frac{R\xi_3\xi_{11}\phi_3}{\phi_1^2} - \frac{R\xi_4\xi_{12}}{\phi_2^2},\ S_8 = \frac{2q_1 y\xi_3\xi_9}{\phi_1^2} + \frac{2q_2 y\xi_4\xi_{10}}{\phi_2^2},$$

$S_9 = -(m_1+q_1)\dfrac{\xi_4\phi_3}{D\phi_1^2}+(m_2+q_2)\dfrac{\xi_3\phi_4}{D\phi_2^2}$, $S_{10} = -(m_1+q_1)\dfrac{2R\xi_2 q_1 y}{D\phi_1^2}+(m_2+q_2)\dfrac{2R\xi_1 q_2 y}{D\phi_2^2}$,

$S_{11} = (m_1+q_1)\dfrac{2\xi_9(-q_1^3y^3+3q_1y(x-Vt)^2)}{\phi_1^3}+(m_2+q_2)\dfrac{2\xi_{10}(-q_2^3y^3+3q_2y(x-Vt)^2)}{\phi_2^3}$,

$S_{12} = -(m_1+q_1)\dfrac{2R\xi_{11}(-3q_1^2y^2+(x-Vt)^2)}{\phi_1^3}+(m_2+q_2)\dfrac{2R\xi_{12}(-3q_2^2y^2+(x-Vt)^2)}{\phi_2^3}$,

$\phi_1 = q_1^2y^2+(x-Vt)^2$, $\phi_2 = q_2^2y^2+(x-Vt)^2$,

$\phi_3 = q_1^2y^2-(x-Vt)^2$, $\phi_4 = q_2^2y^2-(x-Vt)^2$.

From equations (2.66), (2.67) and (2.68), it is clear that the whole stress system is moving with uniform velocity V in the x-direction. The expression of stresses show that in any plane lying below the free boundary surface and parallel to the xz-plane, the stresses attain maximum value at $x = Vt$, i.e., at the point directly below the point of application of the moving load with velocity V at time t. In further discussion we shall deal with the stresses at $x = Vt$.

2.3.3 Particular cases

2.3.3.1 Case 1

When $\varepsilon = 0$ then the expressions for stresses reduce to

$$\frac{\sigma_{22}}{F} = \frac{1}{\pi}S_1,$$
$$\frac{\sigma_{21}}{F} = \frac{1}{\pi}S_5,$$
$$\frac{m_{13}}{F} = \frac{\lambda}{\pi}S_9,$$

which are the expressions for stresses produced due to normal moving load on a regular micropolar half-space.

2.3.3.2 Case 2

The expressions for stresses produced due to normal moving load on irregular and regular elastic isotropic half-space can be obtained as the particular by taking

(i) $\kappa = 0$ and (ii) $\kappa = 0$ and $\varepsilon = 0$, respectively.

2.3.4 Numerical results and discussion

Following Gauthier [56] the relevant physical constants for aluminum-epoxy composite as micropolar elastic solid are

$\rho = 2.19 \times 10^3\ Kg/m^3, \lambda = 7.59 \times 10^{10}\ N/m^2, \mu = 1.89 \times 10^{10}\ N/m^2,$

$\kappa = 0.0149 \times 10^{10}\ N/m^2, \gamma = 0.268 \times 10^6\ N, j = 0.196 \times 10^4\ m^2,$

$\alpha = 0.01 \times 10^6\ N,\ \beta = 0.015 \times 10^6\ N.$

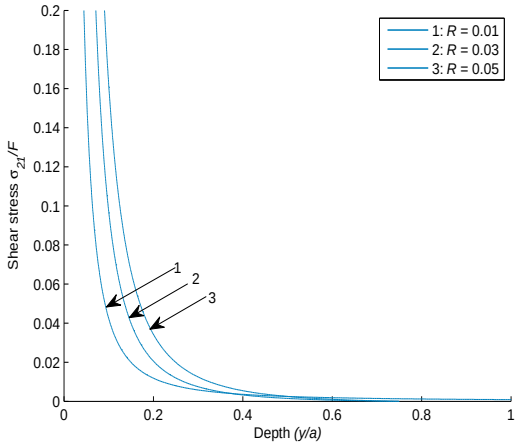

Figure 2.18: Variation of the shear stress against depth for different values of frictional coefficients (R).

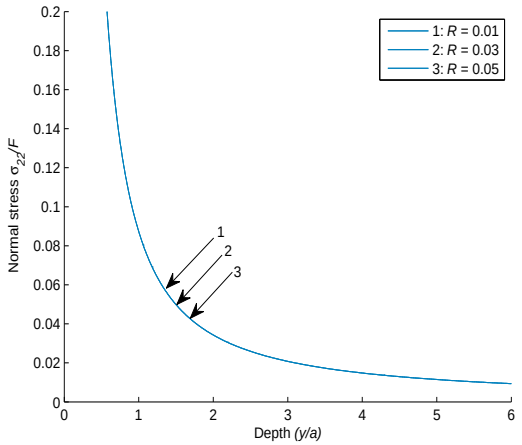

Figure 2.19: Variation of the normal stress against depth for different values of frictional coefficients (R).

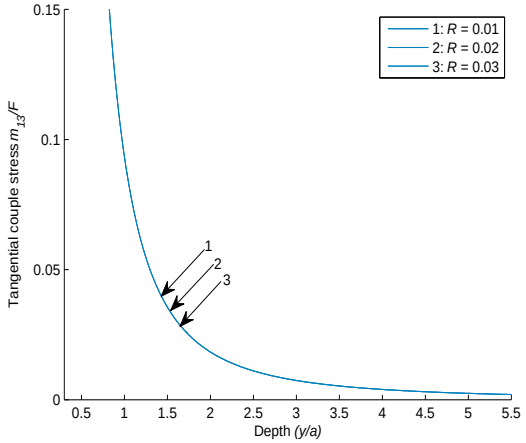

Figure 2.20: Variation of the tangential couple stress against depth for different values of frictional coefficients (R).

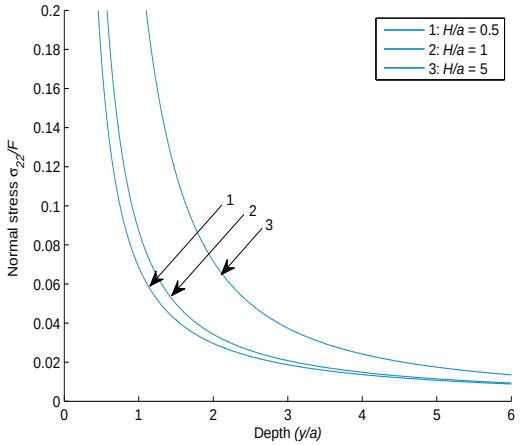

Figure 2.21: Variation of the normal stress against depth for different values of irregularity depth (H/a) when irregularity factor, $x/a = 0.5$.

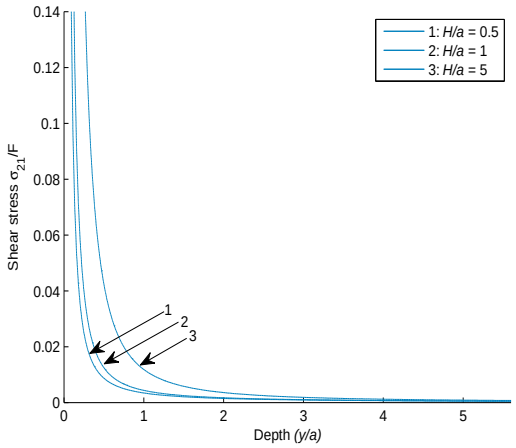

Figure 2.22: Variation of the shear stress against depth for different values of irregularity depth (H/a) when irregularity factor, $x/a = 0.5$.

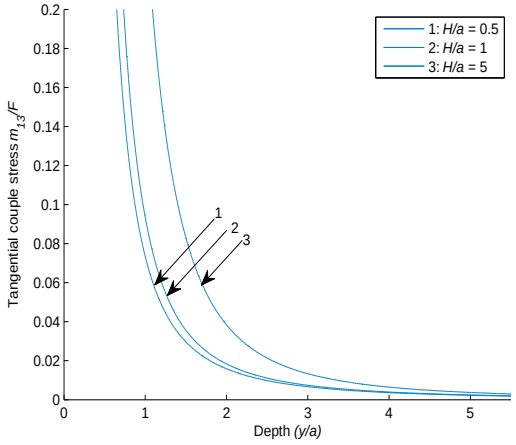

Figure 2.23: Variation of the tangential couple stress against depth for different values of irregularity depth (H/a) when irregularity factor, $x/a = 0.5$.

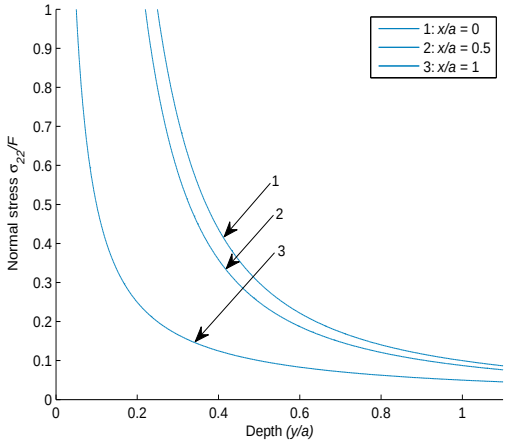

Figure 2.24: Variation of the normal stress against depth for different values of irregularity factor (x/a) when irregularity depth, $H/a = 1$.

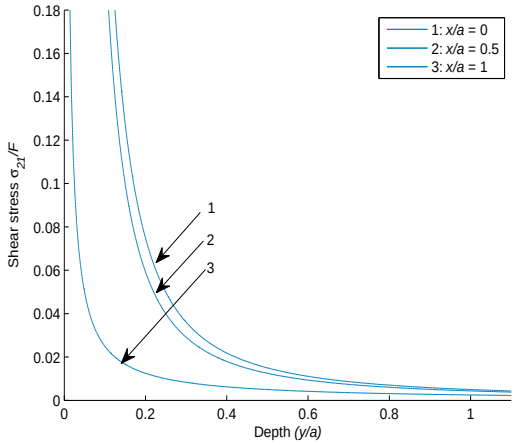

Figure 2.25: Variation of the shear stress against depth for different values of irregularity factor (x/a) when irregularity depth, $H/a = 1$.

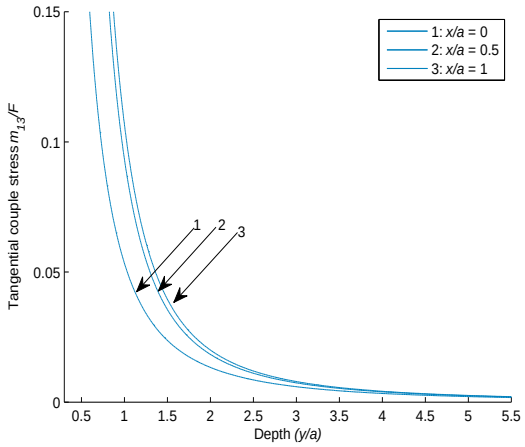

Figure 2.26: Variation of the tangential couple stress against depth for different values of irregularity factor (x/a) when irregularity depth, $H/a = 1$.

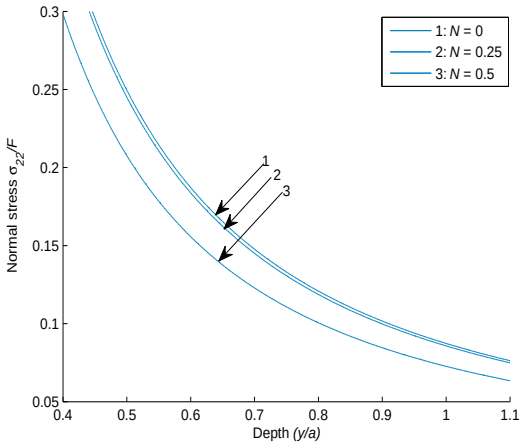

Figure 2.27: Variation of the normal stress against depth for different values of coupling factor (N) when irregularity depth, $H/a = 1$ and irregularity factor, $x/a = 0.5$.

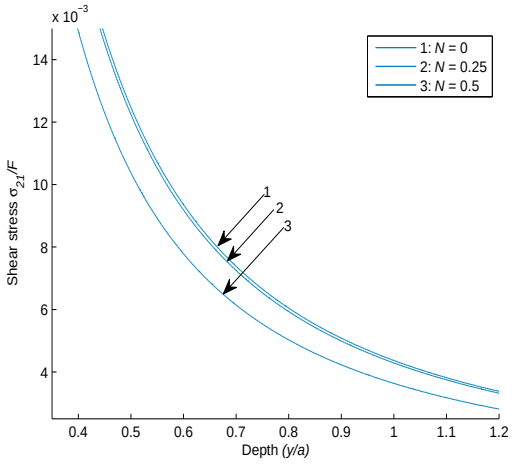

Figure 2.28: Variation of the shear stress against depth for different values of coupling factor (N) when irregularity depth, $H/a = 1$ and irregularity factor, $x/a = 0.5$.

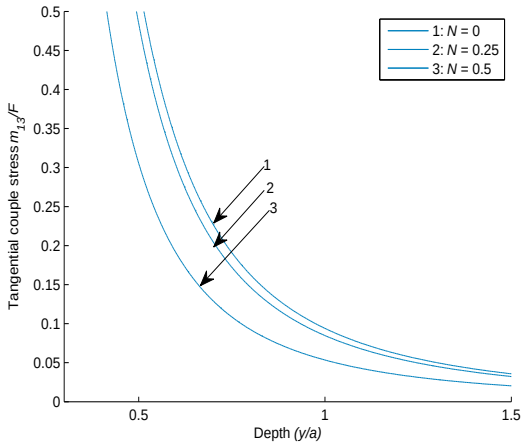

Figure 2.29: Variation of the tangential couple stress against depth for different values of coupling factor (N) when irregularity depth, $H/a = 1$ and irregularity factor, $x/a = 0.5$.

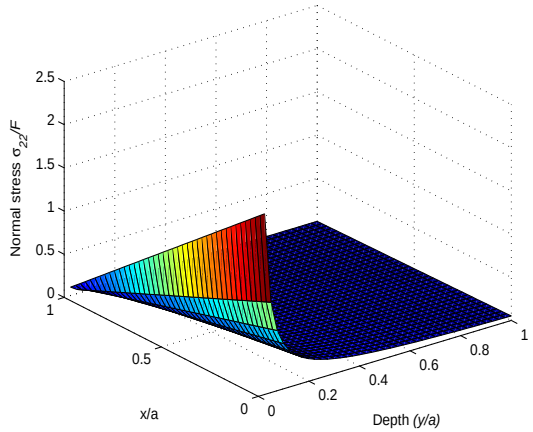

Figure 2.30: Variation of the normal stress against depth and irregularity factor (x/a) when irregularity depth, $H/a = 1$.

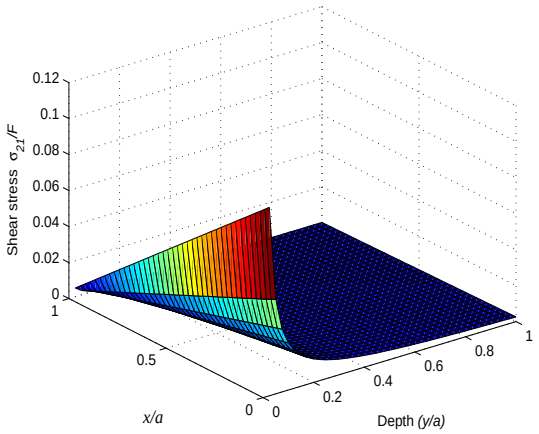

Figure 2.31: Variation of the shear stress against depth and irregularity factor (x/a) when irregularity depth, $H/a = 1$.

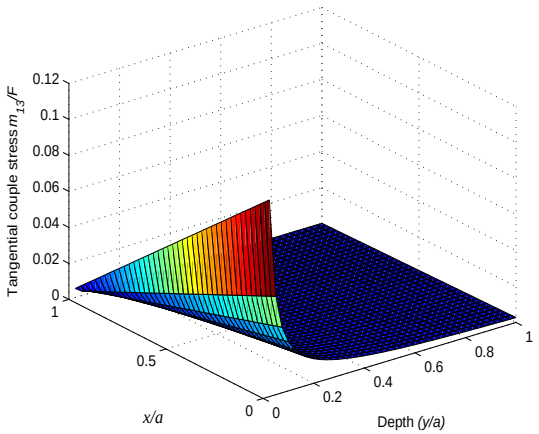

Figure 2.32: Variation of the tangential couple stress against depth and irregularity factor (x/a) when irregularity depth, $H/a = 1$.

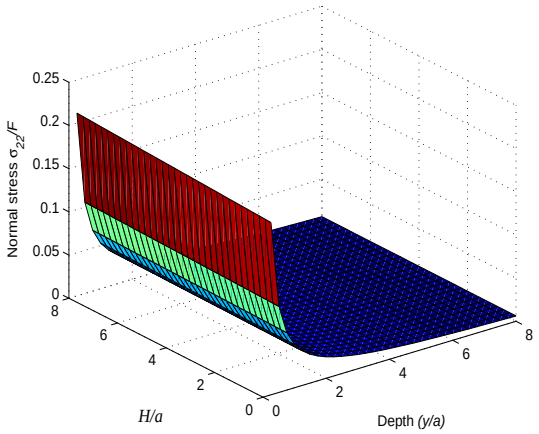

Figure 2.33: Variation of the normal stress against depth and irregularity depth (H/a) in case of rectangular irregularity.

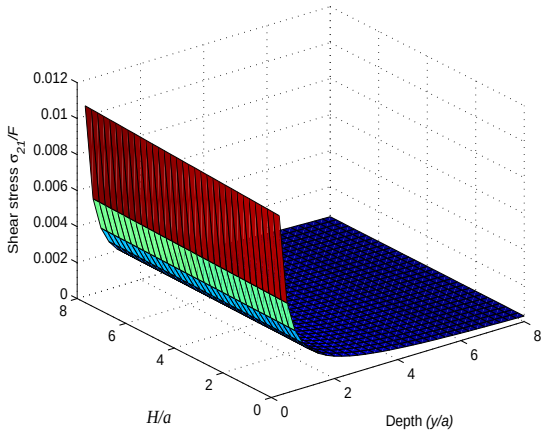

Figure 2.34: Variation of the shear stress against depth and irregularity depth (H/a) in case of rectangular irregularity.

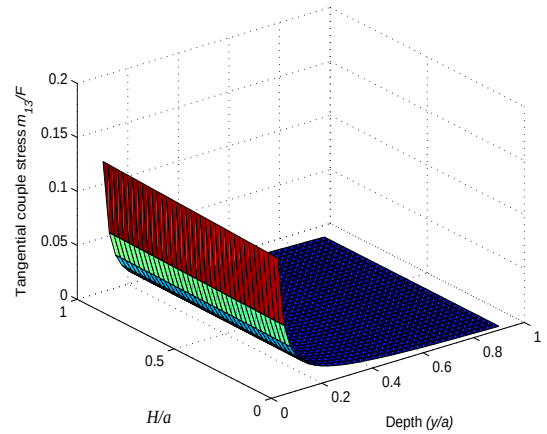

Figure 2.35: Variation of the tangential couple stress against depth and irregularity depth (H/a) in case of rectangular irregularity.

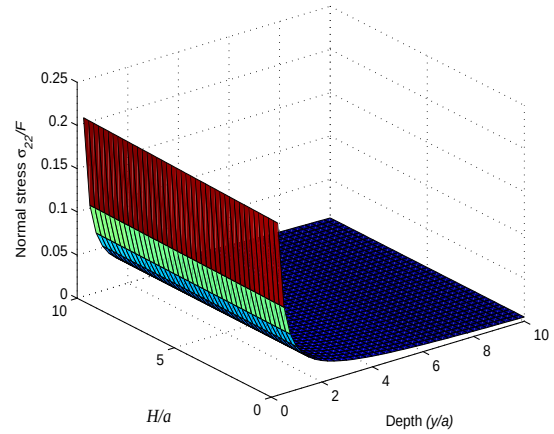

Figure 2.36: Variation of the normal stress against depth and irregularity depth (H/a) in case of parabolic irregularity.

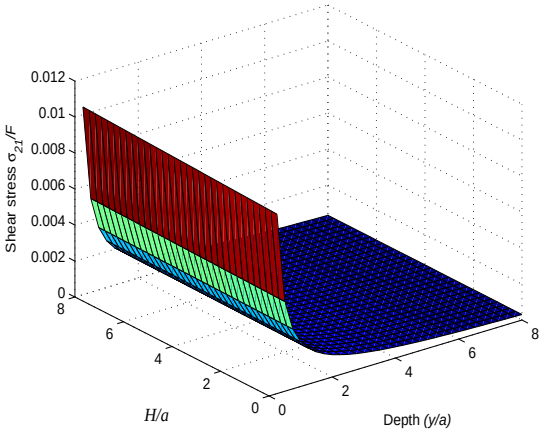

Figure 2.37: Variation of the shear stress against depth and irregularity depth (H/a) in case of parabolic irregularity.

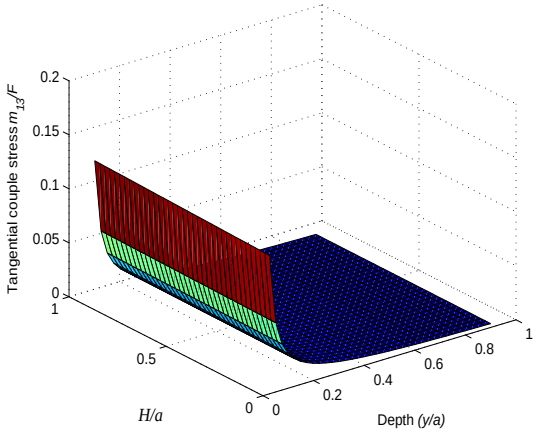

Figure 2.38: Variation of the tangential couple stress against depth and irregularity depth (H/a) in case of parabolic irregularity.

In Figs. (2.18), (2.19) and (2.20), the non-dimensional shear stress, normal stress and tangential couple stress have been studied with respect to depth (y/a) for different values of frictional coefficient (R) in irregularity free zone (i.e. $|x| \geq a$). It can be observed from these figures that all the stresses decrease with increase in depth. It is also observed from these figures that the frictional coefficient affects shear stress predominately which increases with increase in frictional coefficient. However, normal stress and tangential couple stress are observed to be independent of frictional coefficient.

To study the effect of irregularity on normal, shear and tangential couple stresses, we have considered a parabolic shape of irregularity. Figs. (2.21), (2.22) and (2.23) show that the stresses decrease with increase in depth in irregularity zone (i.e. $|x| \leq a$) which is quite similar to the phenomenon observed in irregularity free zone. It is evident from these figures that the maximum irregularity depth (H/a) has a significant effect on normal, shear and tangential couple stresses. It is clearly observed from these figures that the maximum depth of irregularity favors all the stresses i.e. stresses increase with increase in maximum depth of irregularity. A close inspection of the curves reveals that for a particular value of irregularity depth, there is abrupt decrement in stresses when $(y/a) < (H/a)$ whereas when $(y/a) > (H/a)$, then stresses gradually approach to zero in asymptotic manner. More precisely, the impact of maximum depth of irregularity on stresses developed at point directly below to the point of application of the moving load on the free surface of the medium is significant and it decreases with increase in depth.

The variations of stresses for different types of irregularity have been shown in

Figs. (2.24), (2.25) and (2.26). Curve 1 in these figures represents the case of rectangular irregularity, curve 2 corresponds to the case of parabolic irregularity and curve 3 represents the case of no irregularity. It is observed in these figures that stresses are more in case of rectangular irregularity than the case of parabolic irregularity. More precisely, as the irregularity prevails in the medium stress increases.

In order to study the effect of characteristic length study has been made for different values of coupling factor in Figs. (2.27), (2.28) and (2.29). It is observed that as the value of coupling factor increases the magnitude of stresses decrease. So the characteristic length is also affecting the stresses.

Variation of stresses against depth and irregularity factor have been plotted through surface plots in Figs. (2.30), (2.31) and (2.32). Surface plots in Figs. (2.33), (2.34) and (2.35) give the variation of stresses against depth and irregularity depth in case of rectangular irregularity whereas Figs. (2.36), (2.37) and (2.38) depict the variation in case of parabolic irregularity.

2.3.5 Conclusion

In this section, the stresses developed in an irregular micropolar half-space due to a normal moving load at a rough free surface have been investigated. Significant effects of depth, frictional coefficient, coupling factor, maximum irregularity depth and irregularity factor on stresses in a micropolar half-space have been observed. Three different cases of irregularity have been discussed (i) rectangular irregularity, (ii) parabolic irregularity and (iii) no irregularity. Closed form of expressions for the normal stress, shear stress and tangential couple stress have been obtained. The following points can be highlighted as an outcome of the study:

- The frictional coefficient of the rough surface has notable effect on the shear stress. The shear stress obtained at different depths below the surface is increasing with increasing value of the frictional coefficient, while the normal and tangential couple stresses are not affected by the frictional coefficient.

- Microstructure also plays an important role in the variation of stresses. Profiles are modified for different values of coupling factor. It is found that all the three stresses decrease as the value of coupling factor increases.

- The irregularity factor has significant effect on stresses. Specifically, as irregularity prevails in the medium stresses increase. Moreover, the rectangular irregularity has more favorable effect on the stresses than the parabolic irregularity of same depth and span.

- Maximum depth of irregularity has remarkable effect on stresses. All the three stresses increase with increase in the maximum depth of irregularity.

- For a particular depth of irregularity, it is observed that the stresses decrease abruptly with depth when depth is lesser than the maximum depth of the considered irregularity, whereas stresses asymptotically approach to zero when depth is higher than the maximum depth of the considered irregularity.

- Depth has a substantial effect on the stresses. Stresses are more near the surface and magnitude decay as we go deep in the half-space i.e. stresses decrease with increase in the depth.

Chapter 3

Effect of reinforcement, gravity and liquid loading on Rayleigh-type wave propagation

3.1 Introduction

As it is well known that Earth is gravitating medium, therefore gravity has a remarkable effect on the propagation of the seismic waves and plays a vital role in study of the static and dynamic problems of the Earth. The effect of gravity and its variation might be small at times but it should not be ignored in order to accommodate the actual situation of the problem. The impact of gravity on the propagation of wave in an elastic solid medium was studied by Bromwich [21], in this problem he considered the force of gravity to be a type of body force. The work done by Bromwich was extended by Love [81] who explored the effect of gravity on superficial waves and showed that the gravity field affects the velocity of Rayleigh wave. Biot [18] investigated the effect of gravity on Rayleigh waves, by considering that the force of gravity produces a initial stress of a hydrostatic nature and the medium was considered to be incompressible. Various problems of variation and elastic waves under the effect

The contents of this chapter are published in *Meccanica, 51 (10), 24492458, 2016, (SCI, Impact factor-1.828).*

of gravity field have been studied by De and Sengupta [42, 41, 43]. The influence of gravity on the propagation of waves was studied by Sengupta and Acharya [111] in a thermoelastic layer. Datta [40] studied the effect of gravity on the wave propagation of Rayleigh wave in a homogeneous, isotropic elastic solid medium. Das et al. [39] studied the wave propagation of surface wave in a non-homogeneous elastic solid medium under the influence of the gravity. Under influence of gravity and intital stress the propagation of Rayleigh waves in an orthotropic thermoelastic medium was investigated by Abd-Alla and Ahmed [1]. In a non-homogeneous orthotropic elastic medium the propagation of wave under the influence of gravity was discussed by Abd-Alla and Ahmed [2].

The problem of fluid loading in different geometries dealing with the propagation of Rayleigh waves and Lamb waves was studied by various authors. Some notable work by Wu and Zhu [140], Sharma and Pathania [116] and Sharma and Kumar [113, 119] can be cited. Also, the study of reflection and transmission of a three-dimensional plane qP-wave in a layered fluid medium lying between two different triclinic half-spaces was carried out by Chattopadhyay et al. [31]. It is observed that the dynamic characteristic of the structure are influenced under the fluid loading.

In this chapter, we deduce the secular relation for the propagation of Rayleigh-type surface wave in self-reinforced half-space under the influence of gravity and liquid loading. The effects of reinforcement, gravity, liquid loading and wave number on the phase velocity of Rayleigh-type surface wave have been identified. Numerical computation and graphical demonstration are preformed to highlight the important peculiarities of the problem.

3.2 Formulation and solution of the problem

Following the fluid-solid model as adopted by Wu and Zhu [140], Sharma and Pathania [116] and Sharma and Kumar [113, 119], we considered a self-reinforced elastic semi-infinite medium (M_2) under the influence of gravity and bounded by an inviscid liquid layer (M_1) of finite thickness H which is free of stress. Here, the coordinate system is taken in such a way that x-axis is in direction of wave propagation, z-axis is pointing vertically downward and origin is lying on the xy-plane which is common interface of layer and half-space has shown in Fig. (3.1).

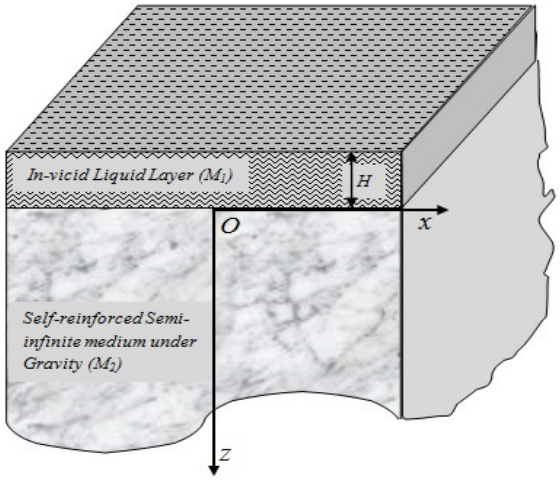

Figure 3.1: Geometry of the problem

As Rayleigh-type wave is a surface wave, therefore, disturbance is largely confined to the neighbourhood of the boundary surface and at any instant, all the particles in any line parallel to y-axis have equal displacement and all partial derivatives with respect to y are zero. Further, let us assume that (u_l, v_l, w_l) and (u_f, v_f, w_f) denote displacement in layer and semi-infinite medium respectively, and any point (x, y, z) at any time t.

For the propagation of Rayleigh-type surface wave propagating in x-direction,

we have

$$u_l = u_l(x,z,t),\ u_f = u_f(x,z,t),\ w_l = w_l(x,z,t),\ w_f = w_f(x,z,t),\ v_l = 0,\ v_f = 0 \text{ and } \frac{\partial}{\partial y} \equiv 0. \tag{3.1}$$

3.2.1 Dynamics of inviscid liquid layer (M_1)

The equation of motion for the inviscid liquid layer (M_1) is given as [52]

$$\lambda_l \bigtriangledown (\bigtriangledown . \vec{u}) = \rho_l \frac{\partial^2 \vec{u}}{\partial t^2}, \tag{3.2}$$

where λ_l, ρ_l are the elastic constants and the density of the inviscid liquid layer respectively.

The stress displacement relations in an inviscid liquid layer are given by

$$\tau_{ij}^{(l)} = \lambda_l u_{r,r} \delta_{ij}, (i,j,r = 1,2,3). \tag{3.3}$$

where l in superscript and subscript stand for the quantity associated to inviscid liquid layer.

According to equation (3.1), we have $\vec{u} = (u_l, 0, w_l)$.

In order to solve equation (3.2), we introduce displacement potential function ϕ_l , defined by

$$u_l = \frac{\partial \phi_l}{\partial x} \text{ and } w_l = \frac{\partial \phi_l}{\partial z}. \tag{3.4}$$

With the help of equation (3.4), the equation of motion for the propagation of Rayleigh-type surface wave in an inviscid liquid layer in terms of displacement potential function ϕ_l can be written as

$$\frac{\partial^2 \phi_l}{\partial x^2} + \frac{\partial^2 \phi_l}{\partial z^2} = \frac{1}{\alpha_l^2} \frac{\partial^2 \phi_l}{\partial t^2}, \tag{3.5}$$

where $\alpha_l = \sqrt{\lambda_l/\rho_l}$, is the dilatational wave velocity in liquid.

We may assume the solution of equation (3.5) as

$$\phi_l = \bar{\phi}_l(z)e^{ik(x-Vt)}, \tag{3.6}$$

where V is the phase velocity and k is the wave number.

Using the solution (3.6) in equation (3.5) and solving the resulting differential equation, we get

$$\phi_l = (A_1 e^{Tkz} + A_2 e^{-Tkz})e^{ik(x-Vt)}, \tag{3.7}$$

where

$T = [1 - (V^2/\alpha_1^2)]^{1/2}$.

Substituing equation (3.7) in equation (3.4), the displacement components of inviscid liquid layer are given by

$$u_l = ik(A_1 e^{Tkz} + A_2 e^{-Tkz})e^{ik(x-Vt)}, \tag{3.8}$$

and

$$w_l = kT(A_1 e^{Tkz} - A_2 e^{-Tkz})e^{ik(x-Vt)}. \tag{3.9}$$

3.2.2 Dynamics of self-reinforced semi-infinite medium (M_2)

The dynamical equations of motion for a three-dimensional elastic solid medium under the influence of gravity are given by

$$\frac{\partial \tau_{xx}^{(f)}}{\partial x} + \frac{\partial \tau_{xy}^{(f)}}{\partial y} + \frac{\partial \tau_{xz}^{(f)}}{\partial z} + \rho' g \frac{\partial w_f}{\partial x} = \rho' \frac{\partial u_f}{\partial t^2}, \tag{3.10}$$

$$\frac{\partial \tau_{yx}^{(f)}}{\partial x} + \frac{\partial \tau_{yy}^{(f)}}{\partial y} + \frac{\partial \tau_{yz}^{(f)}}{\partial z} + \rho' g \frac{\partial w_f}{\partial y} = \rho' \frac{\partial v_f}{\partial t^2}, \tag{3.11}$$

$$\frac{\partial \tau_{zx}^{(f)}}{\partial x} + \frac{\partial \tau_{zy}^{(f)}}{\partial y} + \frac{\partial \tau_{zz}^{(f)}}{\partial z} + \rho' g \frac{\partial w_f}{\partial z} = \rho' \frac{\partial w_f}{\partial t^2}, \tag{3.12}$$

where f in superscript and subscript stands for the quantity associated to self-reinforced semi-infinite medium; ρ' is the density of the material medium (self-reinforced); g is the acceleration due to gravity; $\tau_{ij}^{(f)} = \tau_{ji}^{(f)}, (i, j = 1, 2, 3)$ are the stress components and $\frac{\partial w_f}{\partial z} = -\left(\frac{\partial u_f}{\partial x} + \frac{\partial v_f}{\partial y}\right)$.

The constitutive equation for a self-reinforced linearly elastic medium with preferred direction $\vec{a}$ is given through equation (1.15) in Chapter-1.

Using equations (3.1) and (2.2) in equations (3.10), (3.11) and (3.12), the equations of motion for self-reinforced semi-infinite medium under influence of gravity become

$$P_1 \frac{\partial^2 u_f}{\partial x^2} + P_2 \frac{\partial^2 w_f}{\partial x \partial z} + u_l \frac{\partial^2 u_f}{\partial z^2} + \rho' g \frac{\partial w_f}{\partial x} = \rho' \frac{\partial^2 u_f}{\partial t^2}, \tag{3.13}$$

$$u_L \frac{\partial^2 w_f}{\partial x^2} + P_2 \frac{\partial^2 u_f}{\partial x \partial z} + P_3 \frac{\partial^2 w_f}{\partial z^2} + \rho' g \frac{\partial w_f}{\partial z} = \rho' \frac{\partial^2 w_f}{\partial t^2}, \tag{3.14}$$

where

$P_1 = (\lambda' + 2\alpha' + 4\mu_L - 2\mu_T + \beta')$, $P_2 = (\alpha' + \lambda' + \mu_L)$, $P_3 = (\lambda' + 2\mu_T)$.

We may assume the solution of equations (3.13) and (3.14) as

$$\begin{aligned} u_f &= Be^{-skz + ik(x - Vt)}, \\ w_f &= Ce^{-skz + ik(x - Vt)}, \end{aligned} \tag{3.15}$$

where s is parameter independent of k.

Using equation (3.15) in equations (3.13) and (3.14), we get

$$(s^2 \mu_L + \rho' V^2 - P_1)B + \left(\frac{\rho' g}{k} - sP_2\right) iC = 0, \tag{3.16}$$

$$\left(-\frac{\rho' g}{k} - sP_2\right) iB + (s^2 P_3 + \rho' V^2 - \mu_L)C = 0. \tag{3.17}$$

For non-trivial solution of equations (3.16) and (3.17), we get

$$\mu_L P_3 s^4 + M_1 s^2 + N_1 = 0,$$

$$s_j^2 = \frac{-M_1 \pm \sqrt{M_1^2 - 4N_1(P_3/\mu_L)}}{2(P_3/\mu_L)},\ (j = 1, 2) \tag{3.18}$$

where

$M_1 = \left(\frac{V^2}{\beta_1^2} - 1\right) + \frac{P_3}{\mu_L}\left(\frac{V^2}{\beta_1^2} - \frac{P_1}{\mu_L}\right) - \frac{P_2^2}{\mu_L^2}$, $N_1 = \left(\frac{V^2}{\beta_1^2} - \frac{P_1}{\mu_L}\right)\left(\frac{V^2}{\beta_1^2} - 1\right) + G$,
$\beta_1^2 = \frac{\mu_L}{\rho}$, $G = \frac{\rho' g}{\mu_L k}$.

Equations (3.15) and (3.16) yield

$$\frac{w_f}{u_f} = \frac{s_j^2 + (V^2/\beta_1^2) - (P_1/\mu_L)}{i(s_j(P_2/\mu_L) - G)} = \eta_j\ (j = 1, 2). \tag{3.19}$$

Using equations (3.18) and (3.19) in (3.15), we get

$$u_f = (B_1 e^{-s_1 kz} + B_2 e^{-s_2 kz}) e^{ik(x - Vt)}, \tag{3.20}$$

$$w_f = (\eta_1 B_1 e^{-s_1 kz} + \eta_2 B_2 e^{-s_2 kz}) e^{ik(x - Vt)}. \tag{3.21}$$

3.2.3 Boundary conditions

The boundary conditions for the problem are defined as

(i) The upper surface is stress free i.e.

$$\tau_{zz}^{(l)} = 0,\ \text{at } z = -H. \tag{3.22}$$

(ii) The magnitude of normal component of the stress tensor of the solid (semi-infinite medium) should be equal to pressure of the liquid i.e.

$$\tau_{zz}^{(f)} = \tau_{zz}^{(l)},\ \text{at } z = 0. \tag{3.23}$$

(iii) The normal component of displacement of solid (semi-infinite medium) should be equal to that of liquid i.e.

$$w_f = w_l,\ \text{at } z = 0. \tag{3.24}$$

(iv) The tangential component of the stress tensor solid (semi-infinite medium) should be zero i.e.

$$\tau_x^{(f)} = 0, \text{ at } z = 0. \tag{3.25}$$

3.2.4 Secular equation

Using equations (3.8), (3.9), (3.20) and (3.21) in boundary conditions (3.22), (3.23), (3.24) and (3.25), we get the following equations:

$$A_2 = -A_1 e^{-2TkH}, \tag{3.26}$$

$$\xi_1 A_1 + \xi_2 B_1 + \xi_3 B_2 = 0, \tag{3.27}$$

$$\xi_4 B_1 + \xi_5 B_2 = 0, \tag{3.28}$$

$$-kTA_1(1 + e^{-2TkH}) + \eta_1 B_1 + \eta_2 B_2 = 0, \tag{3.29}$$

where

$\xi_1 = \lambda_l(1 - T^2)(1 - e^{-2TkH})$, $\xi_2 = i(\lambda' + \alpha') - \eta_1 s_1(\lambda' + 2\mu_T)$,

$\xi_3 = i(\lambda' + \alpha') - \eta_2 s_2(\lambda' + 2\mu_T)$, $\xi_4 = (\eta_1 i - s_1)\mu_L$, $\xi_5 = (\eta_2 i - s_2)\mu_L$.

Eliminating A_1, A_2, B_1 and B_2 from equations (3.26), (3.27), (3.28) and (3.29), we get

$$T(1 + e^{-2TkH})(\xi_2\xi_5 - \xi_3\xi_4) + \xi_1(\eta_1\xi_5 - \eta_2\xi_4) = 0, \tag{3.30}$$

which is the secular equation for propagation of Rayleigh-type surface wave in a self-reinforced semi-infinite medium with gravity underlying an inviscid liquid layer.

3.3 Particular cases

3.3.1 Case 1

When $G = 0$, the secular equation (3.30) reduces to

$$T(1 + e^{-2TkH})(\xi'_2\xi'_5 - \xi'_3\xi'_4) + \xi'_1(\eta'_1\xi'_5 - \eta'_2\xi'_4) = 0, \tag{3.31}$$

where

$N'_1 = (\rho'V^2 - P_1)(\rho'V^2 - \mu_L)$, $s_j^2 = \dfrac{-M_1 \pm \sqrt{M_1^2 - 4N'_1(P_3/\mu_L)}}{2(P_3/\mu_L)}$, $(j = 1, 2)$

$\eta'_j = \dfrac{s_j'^2\mu_L + \rho'V^2 - P_1}{i(s'_jP_2}$, $\xi'_1 = \lambda_l(1-T^2)(1-e^{-2TkH})$, $\xi'_2 = i(\lambda'+\alpha') - \eta'_2s'_2(\lambda'+2\mu_T)$,

$\xi'_3 = i(\lambda' + \alpha') - \eta'_1s'_1(\lambda' + 2\mu_T)$, $\xi'_4 = (\eta'_1 i - s'_1)\mu_L$, $\xi'_5 = (\eta'_2 i - s'_2)\mu_L$.

Equation (3.31) represents the secular equation for the propagation of Rayleigh-type surface wave in a self-reinforced semi-infinite medium without gravity bounded by an inviscid liquid layer.

3.3.2 Case 2

When $H = 0$, the secular equation (3.30) leads to

$$\xi_2\xi_5 - \xi_3\xi_4 = 0. \tag{3.32}$$

Equation (3.32) establishes the secular equation for the propagation of Rayleigh-type surface wave in a self-reinforced semi-infinite medium under the effect of gravity in the absence of inviscid liquid layer (liquid loading).

3.3.3 Case 3

When $H = 0$ and $G = 0$, the secular equation (3.30) gives

$$\xi'_2\xi'_5 - \xi'_3\xi'_4 = 0. \tag{3.33}$$

Equation (3.33) denotes the secular equation for the propagation of Rayleigh-type surface wave in a self-reinforced semi-infinite medium without gravity in the absence of liquid loading.

3.3.4 Case 4

When $\mu_L = \mu_T = \mu'$, $\alpha' = 0$ and $\beta' = 0$, the secular equation (3.30) reduces to

$$T(1 + e^{-2TkH})(\chi_2\chi_5 - \chi_3\chi_4) + \chi_1(\eta_3\chi_5 - \eta_4\chi_4) = 0, \tag{3.34}$$

where

$P_1' = \lambda' + 2\mu'$, $P_2' = \lambda' + \mu'$, $M_1' = \left(\frac{V^2}{\beta_1'^2} - 1\right) + \frac{P_1'}{\mu'}\left(\frac{V^2}{\beta_1'^2} - \frac{P_1'}{\mu'}\right) - \frac{P_2'^2}{\mu'^2}$,

$N_1' = \left(\frac{V^2}{\beta_1'^2} - \frac{P_1'}{\mu'}\right)\left(\frac{V^2}{\beta_1'^2} - 1\right) + G'$, $\beta_1'^2 = \frac{\mu'}{\rho'}$, $G' = \frac{\rho' g}{\mu' k}$,

$s_j^2 = \frac{-M_1' \pm \sqrt{M_1'^2 - 4N_1'(P_1'/\mu')}}{2(P_1'/\mu')}$, $\eta_j = \frac{s_j'^2 + (V^2/\beta_1'^2) - (P_1'/\mu')}{i(s_j'(P_2'/\mu') - G')}$, $(j = 3, 4)$,

$\chi_1 = \lambda_l(1 - T^2)(1 - e^{-2TkH})$, $\chi_2 = i(\lambda' + \alpha') - \eta_3 s_3(\lambda' + 2\mu')$,

$\chi_3 = i(\lambda' + \alpha') - \eta_4 s_4(\lambda' + 2\mu)$, $\chi_4 = (\eta_3 i - s_3)\mu$ $\chi_5 = (\eta_4 i - s_4)\mu$.

Equation (3.34) represents the secular equation for the propagation of Rayleigh-type surface wave in reinforced-free semi-infinite medium under the influence of gravity and bounded by an inviscid liquid layer.

3.3.5 Case 5

When $\mu_L = \mu_T = \mu'$, $\alpha' = 0$, $\beta' = 0$ and $G = 0$ the secular equation (3.30) reduces to

$$T(1 + e^{-2TkH})(\chi_2'\chi_5' - \chi_3'\chi_4') + \chi_1'(\eta_3'\chi_5' - \eta_4'\chi_4') = 0, \tag{3.35}$$

where

$$N_2' = \left(\frac{V^2}{\beta_1'^2} - \frac{P_1'}{\mu'}\right)\left(\frac{V^2}{\beta_1'^2} - 1\right),$$

$s_j'^2 = \frac{-M_1' \pm \sqrt{M_1'^2 - 4N_2'(P_1'/\mu')}}{2(P_1'/\mu')}$, $\eta_j' = \frac{s_j'^2 + (V^2/\beta_1'^2) - (P_1'/\mu')}{i(s_j'(P_2'/\mu'))}$, $(j = 3, 4)$,

$\chi_1' = \lambda_l(1 - T^2)(1 - e^{-2TkH})$, $\chi_2' = i(\lambda' + \alpha') - \eta_3' s_3'(\lambda' + 2\mu')$,

$\chi_3' = i(\lambda' + \alpha') - \eta_4' s_4'(\lambda' + 2\mu')$, $\chi_4' = (\eta_3' i - s_3')\mu'$, $\chi_5' = (\eta_4' i - s_4')\mu'$.

Equation (3.35) establishes the secular equation for the propagation of Rayleigh-type surface wave in a reinforced-free semi-infinite medium without gravity and bounded by an inviscid liquid layer.

3.3.6 Case 6

When $\mu_L = \mu_T = \mu'$, $\alpha' = 0$, $\beta' = 0$ and $H = 0$ the secular equation (3.30) reduces to

$$\chi_2\chi_5 - \chi_3\chi_4 = 0. \tag{3.36}$$

Equation (3.36) denotes the secular equation for the propagation of Rayleigh-type surface wave in a reinforced-free semi-infinite medium under the influence of gravity in the absence of liquid loading.

3.3.7 Case 7

When $\mu_L = \mu_T = \mu'$, $\alpha' = 0$, $\beta' = 0$, $G = 0$ and $H = 0$ the secular equation (3.30) reduces to

$$\chi_2'\chi_5' - \chi_3'\chi_4' = 0. \tag{3.37}$$

Equation (3.37) is the secular equation for the propagation of Rayleigh-type surface wave in a reinforced-free semi-infinite medium without gravity and in absence liquid loading.

3.4 Numerical results and discussion

To perform numerical computation and to unravel the effect of reinforcement, gravity, liquid loading and wave number on phase velocity of Rayleigh-type surface wave propagating in self-reinforced semi-infinite medium with gravity underlying an inviscid liquid layer, we use secular equation (3.30). Following data is taken into account for numerical study and graphical illustration.

(i) For inviscid liquid layer, M_1 [77]:

$\alpha_l = 1.5 \times 10^3 ms^{-1}$, $\rho_l = 1000 kgm^{-3}$.

(ii) For self-reinforced semi-infinite medium, M_2 [83]:

$\mu_L = 5.66 \times 10^9 Nm^{-2}$, $\mu_T = 2.46 \times 10^9 Nm^{-2}$, $\lambda' = 5.65 \times 10^9 Nm^{-2}$,

$\alpha' = -1.28 \times 10^9 Nm^{-2}$ $\beta' = 220.90 \times 10^9 Nm^{-2}$ $\rho' = 2660 kgm^{-3}$.

For the sake of study of the case of reinforced-free semi-infinite medium with gravity underlying an inviscid liquid layer, we consider the following data [62]:

$\mu_L = \mu_T = \mu = 1.987 \times 10^9 Nm^{-2}$, $\lambda = 2.510 \times 10^9 Nm^{-2}$, $\rho = 4705 kgm^{-3}$, $\alpha = 0$, $\beta = 0$.

Due to variations in the Earth properties, the velocity of Rayleigh-type surface wave is varying with the wave number and this phenomenon is referred as dispersion. It is observed that at long wavelengths (at short wave number) phase velocity is very large and in the short wavelength region effect of wavelength on the phase velocity is very small. Same type of phenomenon was observed by Lord Rayleigh [102] while dealing with the elastic half-space. The effects of reinforcement, gravity, liquid loading and wave number on the phase velocity of Rayleigh-type surface wave propagating in a gravitating self-reinforced semi-infinite medium underlying

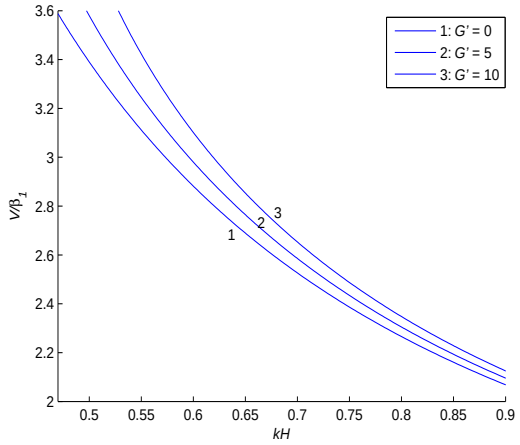

Figure 3.2: Variation of dimensionless phase velocity (V/β_1) against dimensionless wave number (kH) for different values of gravity parameter ($G' = \rho' gH/\mu_L$) in self-reinforced gravitating semi-infinite medium underlying an inviscid liquid layer.

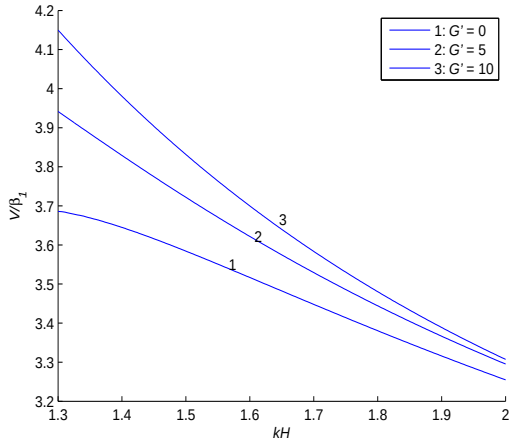

Figure 3.3: Variation of dimensionless phase velocity (V/β_1) against dimensionless wave number (kH) for different values of gravity parameter ($G' = \rho' gH/\mu_L$) in gravitating reinforced-free underlying an inviscid liquid layer.

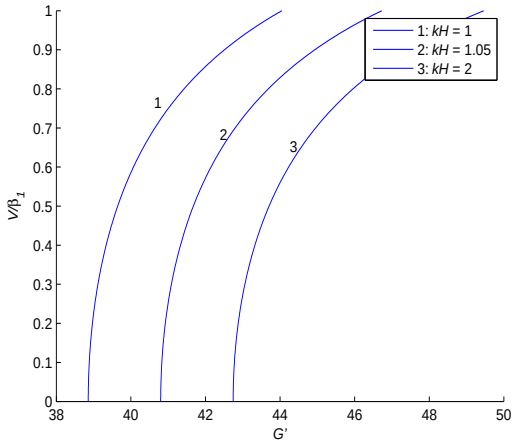

Figure 3.4: Variation of dimensionless phase velocity (V/β_1) against gravity parameter ($G' = \rho' gH/\mu_L$) for different values of dimensionless wave number (kH) in gravitating self-reinforced self-infinite medium underlying an inviscid liquid layer.

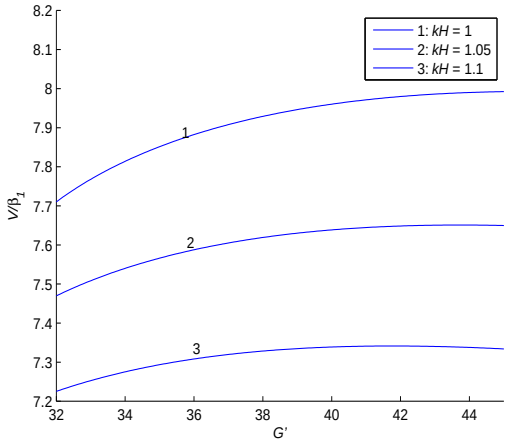

Figure 3.5: Variation of dimensionless phase velocity (V/β_1) against gravity parameter ($G' = \rho' gH/\mu_L$) for different values of dimensionless wave number (kH) in gravitating reinforced-free self-infinite medium underlying an inviscid liquid layer.

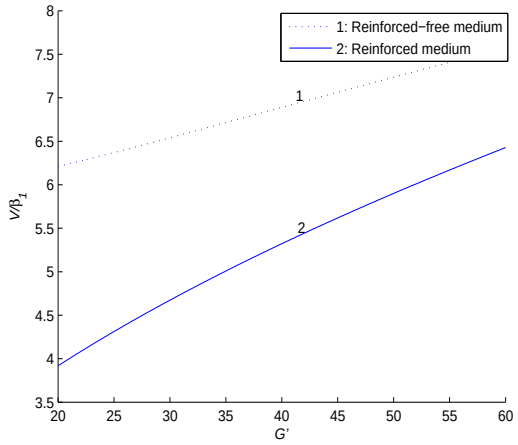

Figure 3.6: Variation of dimensionless phase velocity (V/β_1) against biot's gravity parameter ($G = \rho g/k\mu_L$) in reinforced and reinforced-free gravitating self-infinite medium in the absence of an inviscid liquid layer.

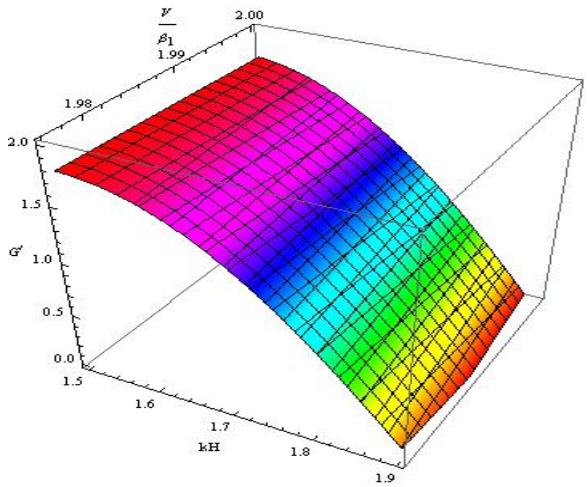

Figure 3.7: Variation of dimensionless phase velocity (V/β_1) against dimensionless wave number (kH) and gravity parameter ($G' = \rho' gH/\mu_L$) in gravitating self-reinforced self-infinite medium underlying an inviscid liquid layer.

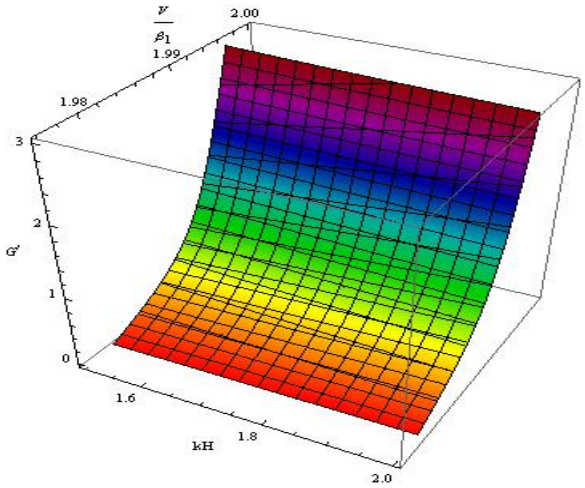

Figure 3.8: Variation of dimensionless phase velocity (V/β_1) against dimensionless wave number (kH) and gravity parameter ($G' = \rho' gH/\mu_L$) in gravitating reinforced-free self-infinite medium underlying an inviscid liquid layer.

an inviscid liquid layer are depicted through Figs. (3.2) to (3.8).

Curves in Figs. (3.2) and (3.3) are the dispersion curves showing variations of phase velocity against wave number. It is observed in these two figures that phase velocity of Rayleigh-type surface wave decreases with an increase in wave number. In particular, Fig. (3.2) delineates the influence of gravity parameter on the phase velocity of Rayleigh-type surface wave when semi-infinite medium is self-reinforced whereas Fig. (3.3) depicts the effect of gravity parameter on the phase velocity of Rayleigh-type surface wave when semi-infinite medium is reinforced-free. It can be adduced from these figures that with an increase in gravity parameter, phase velocity of Rayleigh-type surface wave increases in both the cases of self-reinforced gravitating semi-infinite medium and reinforced-free gravitating semi-infinite medium. The comparative study of these two figures indicates that phase velocity is more in the case of reinforced-free semi-infinite medium underlying an inviscid liquid layer as compared to self-reinforced semi-infinite medium underlying an inviscid liquid layer. It is worthy to note that curve 1 in Figs. (3.2) and (3.3) corresponds to the case

when an inviscid liquid layer lies above a self-reinforced semi-infinite medium without gravity and reinforced-free semi-infinite medium without gravity respectively.

Figs. (3.4) and (3.5) are the plots of phase velocity of Rayleigh-type surface wave against gravity parameter for different values of non-dimensional wave number. It is evident from these figures that phase velocity increases with increase in gravity parameter in both reinforced and reinforced-free cases for particular wave number or frequency.

The effect of absence of liquid loading on phase velocity of Rayleigh-type surface wave is elucidated in Fig. (3.6). In this figure, curves 1 and 2 represent the case when there is no liquid loading in gravitating reinforced-free and self-reinforced semi-infinite medium respectively. Meticulous examination of this figure establishes that phase velocity of Rayleigh-type surface wave is found to be more in the case when it propagates in gravitating reinforced-free semi-infinite medium in absence of an inviscid liquid layer as compared to the case when it propagates self-reinforced semi-infinite medium in absence of an inviscid liquid layer.

Surface plots in Figs. (3.7) and (3.8) furnish the combine effect of wave number and gravity parameter on the phase velocity of Rayleigh-type surface wave. More precisely, Fig. (3.7) represents the variation of non-dimensional phase velocity against non-dimensional wave number and gravity parameter in the case when Rayleigh-type surface wave propagates in a gravitating self-reinforced semi-infinite medium underlying an inviscid liquid layer. Fig. (3.8) depicts the variation of non-dimensional phase velocity against non-dimensional wave number and gravity parameter in the case when Rayleigh-type surface wave propagates in a gravitating reinforced-free semi-infinite medium underlying an inviscid liquid layer. Subtle

observation of these two figures concludes that as reinforcement prevails in the semi-infinite medium, phase velocity of Rayleigh-type surface wave decreases.

3.5 Conclusion

In this chapter, propagation of Rayleigh-type surface wave in gravitating self-reinforced semi-infinite medium underlying an inviscid liquid layer has been studied. Secular equation has been established in closed form and the effects of reinforcement, gravity and liquid loading on the phase velocity of Rayleigh-type surface wave have been observed and depicted graphically. Following points can be outlined as an outcome of the study:

- Wave number has substantial effect on phase velocity of Rayleigh-type surface wave. In both the cases of gravitating self-reinforced semi-infinite medium underlying an inviscid liquid layer and gravitating reinforced-free semi-infinite medium underlying an inviscid liquid layer, phase velocity decreases with an increase in wave number.

- Gravity parameter has significant effect on phase velocity of Rayleigh-type surface wave. Gravity parameter favors the phase velocity of Rayleigh-type surface wave in both gravitating self-reinforced semi-infinite medium underlying an inviscid liquid layer and gravitating reinforced-free semi-infinite medium underlying an inviscid liquid layer.

- In absence of an inviscid liquid layer, phase velocity of Rayleigh-type surface wave is found to be more in the case of gravitating reinforced-free semi-infinite medium as compared to the case of gravitating self-reinforced semi-infinite

medium.

- The comparative study of self-reinforced case and reinforced-free case suggests that phase velocity of Rayleigh-type wave is more in latter case as compared to former case.

Chapter 4

Shear wave propagation in vertically heterogeneous viscoelastic layer over a micropolar elastic half-space

4.1 Introduction

This chapter deals with the propagation of SH-wave in vertically heterogeneous viscoelastic layer lying over micropolar elastic half-space. Dispersion and damping equations are obtained analytically in closed form. Phase and damped velocities are computed numerically and depicted by means of graphs to exhibit the substantial effects of heterogeneity, viscoelasticity (internal friction) and micropolar parameter. As a special case of the problem, it is found that deduced dispersion relation is in well agreement to the classical-Love wave equation and damping equation vanishes identically for isotropic case. Influence of micropolarity present in the medium of half-space is highlighted through comparative study.

The contents of this chapter are published in *Mechanics of Advanced Materials and Structures (Taylor & Francis) (SCI Journal, Impact factor: 0.773) DOI: 10.1080/15376494.2015.1124948.*

4.2 Formulation of the problem

Sahu et al. [108] studied the propagation of SH-wave in viscoelastic heterogeneous layer over half-space with self -weight. Following the same approach here, we considered a viscoelastic layer of width H' (with vertical heterogeneity in exponential form) lying over a micropolar elastic half-space. The rectangular Cartesian coordinate system is considered such that x–axis is along the direction of propagation of SH-wave and the z–axis is positive vertically downward, as shown in Fig. (4.1). Let

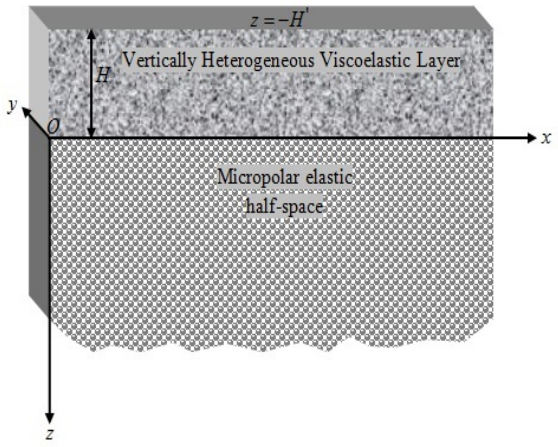

Figure 4.1: Geometry of the problem

us assume (u_1, v_1, w_1) and (u_2, v_2, w_2) as the displacement component caused due to propagation of SH-wave in upper layer and lower half-space respectively. Now, for the propagation of SH-wave in the $x-$direction and causing displacement only in $y-$direction, we shall assume that

$$u_i = 0,\ v_i = v_i(x, z, t),\ w_i = 0;\ (i = 1, 2). \tag{4.1}$$

4.2.1 Dynamics of vertically heterogeneous viscoelastic layer

The non-vanishing equation of motion for the propagation of SH-wave in heterogenous viscoelastic layer in the absence of body force [101] is given in view of equation (4.1) as

$$\frac{\partial}{\partial x}p_{xy} + \frac{\partial}{\partial z}p_{yz} = \rho_1 \frac{\partial^2 v_1}{\partial t^2}, \tag{4.2}$$

where

$$p_{xy} = \left(\mu_1 + \eta_1 \frac{\partial}{\partial t}\right) \frac{\partial v_1}{\partial x} \text{ and } p_{yz} = \left(\mu_1 + \eta_1 \frac{\partial}{\partial t}\right) \frac{\partial v_1}{\partial z}, \tag{4.3}$$

with μ_1, η_1 and ρ_1 as modulus of rigidity, internal friction and density respectively of viscoelastic layer.

Since, the interior of the earth have sharp increasing trend of elastic constants (density) with increase in depth which can be modelled by using exponential function [85]. Owing to this fact, we have considered the exponential form of heterogeneity in the viscoelastic layer as

$$\mu_1 = \mu_0 e^{\nu z}, \eta_1 = \eta_0 e^{\nu z} \text{ and } \rho_1 = \rho_0 e^{\nu z}, \tag{4.4}$$

where μ_0, η_0 and ρ_0 are modulus of rigidity, internal friction and density respectively of the viscoelastic layer at the common interface of layer and half-space. ν is a heterogeneity parameter having dimension inverse of length.

Using equation (4.4) and (4.3) in equation (4.2), we get the dynamical equation of motion for propagation of SH-wave in heterogeneous viscoelastic layer as

$$\left(\mu_1 + \eta_1 \frac{\partial}{\partial t}\right) \frac{\partial^2 v_1}{\partial x^2} + \frac{\partial}{\partial z}\left[\left(\mu_1 + \eta_1 \frac{\partial}{\partial t}\right) \frac{\partial v_1}{\partial z}\right] = \rho_1 \frac{\partial^2 v_1}{\partial t^2}. \tag{4.5}$$

We may assume the solution of (4.5) as

$$v_1 = V_1(z) e^{i(kx - \omega t)}, \tag{4.6}$$

where k is wave number and $\omega(= kc)$ is circular frequency.

Using equations (4.4) and (4.6) in equation (4.5), we get

$$\frac{d^2V_1}{dz^2} + \frac{1}{\bar{\mu_1}}\frac{d\bar{\mu_1}}{dz}\frac{dV_1}{dz} + \left(\frac{\omega^2\rho_1}{\bar{\mu_1}} - k^2\right)V_1 = 0, \tag{4.7}$$

where

$$\bar{\mu_1} = \mu_1 - i\eta_1\omega.$$

Under the substitution

$$V_1(z) = \frac{Y_1(z)}{\sqrt{\bar{\mu_1}}}, \tag{4.8}$$

Equation (4.7) leads to

$$\frac{d^2Y_1}{dz^2} + m^2Y_1 = 0, \tag{4.9}$$

where

$m = T_3 + iT_4$, $T_1 = -\frac{\nu^2}{4} + \frac{k^2c^2}{\beta_1^2\left(1 - \frac{\omega^2\eta_0^2}{\mu_0^2}\right)} - k^2$, $T_2 = \frac{k^2c^2\omega\eta_0}{\beta_1^2\mu_0\left(1 + \frac{\omega^2\eta_0^2}{\mu_0^2}\right)}$,

$T_3^2 = \frac{\sqrt{T_1^2 + T_2^2} + T_1}{2}$, $T_4^2 = \frac{\sqrt{T_1^2 + T_2^2} - T_1}{2}$, $\beta_1^2 = \frac{\mu_0}{\rho_0}$.

The solution of equation (4.9) is given as

$$Y_1 = A\cos(mz) + B\sin(mz), \tag{4.10}$$

where A and B are arbitrary constants.

Hence, using (4.1) and (4.8) in equation (4.6) the displacement in heterogeneous viscoelastic layer due to the propagation of SH-wave is given by

$$v_1 = \frac{1}{\sqrt{\bar{\mu_0}}}e^{-\frac{\nu z}{2}}(A\cos(mz) + B\sin(mz))e^{i(kx-\omega t)}, \tag{4.11}$$

where

$\bar{\mu_0} = \mu_0 - i\omega\eta_0$.

4.2.2 Dynamics of micropolar elastic half-space

The equations of motion and the constitutive relations for micropolar elastic half-space in the absence of body force are given through (1.11), (1.12), (1.13) and (1.14) in Chapter-1.

Let us introduce potential functions ψ and φ as

$$\phi_1 = \frac{\partial \psi}{\partial x} + \frac{\partial \varphi}{\partial z} \text{ and } \phi_3 = \frac{\partial \psi}{\partial z} - \frac{\partial \varphi}{\partial x}. \tag{4.12}$$

Using equations (4.1) and (4.12), the system of equation of motion (1.11), (1.12), (1.13) and (1.14) reduces to

$$\nabla^2 v_2 + c_1 \nabla^2 \varphi = \frac{1}{c_2^2} \frac{\partial^2 v_2}{\partial t^2}, \tag{4.13}$$

$$\nabla^2 \psi - 2\frac{c_5^2}{c_3^2 + c_4^2}\psi = \frac{1}{c_3^2 + c_4^2} \frac{\partial^2 \psi}{\partial t^2}, \tag{4.14}$$

$$\nabla^2 \varphi - 2\frac{c_5^2}{c_3^2}\varphi - \frac{c_5^2}{c_3^2} v_2 = \frac{1}{c_3^2} \frac{\partial^2 \varphi}{\partial t^2}, \tag{4.15}$$

where

$c_1 = \dfrac{\kappa}{\mu + \kappa}$, $c_2 = \sqrt{\dfrac{\mu + \kappa}{\rho}}$, $c_3 = \sqrt{\dfrac{\gamma}{\rho j}}$, $c_4 = \sqrt{\dfrac{\alpha + \beta}{\rho j}}$, $c_5 = \sqrt{\dfrac{\kappa}{\rho j}}$.

We assume solution of the form

$$(\psi, \varphi, v_2)(x, z, t) = (\psi, \varphi, v_2)(z) e^{i(kx - \omega t)}. \tag{4.16}$$

With the help of equation (4.16), equations (4.13), (4.14) and (4.15) result in

$$\frac{d^2 \psi}{dz^2} + r^2 \psi = 0, \tag{4.17}$$

$$[D'^4 + PD'^2 + Q](\varphi, v_2) = 0, \tag{4.18}$$

Equation (4.18) can be rewritten as

$$(D'^2 + p^2)(D'^2 + q^2)(\varphi, v_2) = 0, \tag{4.19}$$

where $D' \equiv \dfrac{d}{dz}$,

$p^2, q^2 = \dfrac{-P \pm \sqrt{P^2 - 4Q}}{2}$,

$P = -\dfrac{c_5^2}{c_3^2}(-c_1 + 2) + \omega^2 \left(\dfrac{1}{c_3^2} + \dfrac{1}{c_2^2}\right) - 2k^2$,

$Q = \left(\dfrac{\omega^2}{c_2^2} - k^2\right)\left(\dfrac{\omega^2}{c_3^2} - \dfrac{2c_5^2}{c_3^2} - k^2\right) - k^2\dfrac{c_1 c_5^2}{c_3^2}$,

$r^2 = \left(\dfrac{\omega^2}{c_3^2 + c_4^2} - \dfrac{2c_5^2}{c_3^2 + c_4^2} - k^2\right)$.

For small value of κ, we may obtain p, q and r as

$p = \sqrt{\dfrac{k^2 c^2 j\mu}{\gamma\beta_2^2} - \dfrac{2c_5^2}{c_3^2}}, q = \sqrt{\dfrac{k^2 c^2 \mu}{\beta_2^2(\mu + \kappa)}}$ and $r = \sqrt{\dfrac{k^2 c^2 j\mu}{\beta_2^2(\alpha + \beta + \gamma)} - \dfrac{c_5^2}{c_3^2 + c_4^2}}$,

where

$\beta_2^2 = \dfrac{\mu}{\rho}$.

The solutions of equations (4.17) and (4.19) are obtained as

$$v_2 = (Fe^{-ipz}s_1 + He^{-iqz}s_2)e^{i(kx-\omega t)},$$

$$\phi_1 = (De^{-irz}ik - ipFe^{-ipz} - iqHe^{-iqz})e^{i(kx-\omega t)}, \tag{4.20}$$

$$\phi_3 = [-irDe^{-irz} - ik(Fe^{-ipz} + He^{-iqz})]e^{i(kx-\omega t)},$$

where

D, F, H are the arbitrary constants,

$s_1 = \left(-p^2 + \dfrac{\omega^2}{c_3^2} - \dfrac{2c_5^2}{c_3^2} - k^2\right)\dfrac{c_3^2}{c_5^2}$,

and

$s_2 = \left(-q^2 + \dfrac{\omega^2}{c_3^2} - \dfrac{2c_5^2}{c_3^2} - k^2\right)\dfrac{c_3^2}{c_5^2}$.

4.3 Boundary conditions, dispersion relation and damping equation

For the propagation of SH-wave in vertically heterogeneous viscoelastic layer lying over and in welded contact of a micropolar elastic half-space, the following boundary

conditions are to be satisfied

(i) The upper most surface of heterogeneous viscoelastic layer is stress free, i.e.

$$p_{yz} = 0 \text{ at } z = -H'. \tag{4.21}$$

(ii) Displacements are continuous at the common interface of layer and half-space, i.e.

$$v_1 = v_2 \text{ at } z = 0. \tag{4.22}$$

(iii) Stresses are continuous at the common interface of layer and half-space, i.e.

$$p_{yz} = \sigma_{yz} \text{ at } z = 0. \tag{4.23}$$

Using equations (4.11) and (4.20) in the boundary conditions (4.21), (4.22) and (4.23), we get

$$A(2m\sin(mH') - \nu\cos(mH')) + B(2m\cos(mH') + \nu\sin(mH')) = 0, \tag{4.24}$$

$$A = \sqrt{\bar{\mu}_0}(Fs_1 + Hs_2), \tag{4.25}$$

$$\sqrt{\bar{\mu}_0}(-\frac{\nu A}{2} + Bm) = i\kappa kD - is_3F - is_4H, \tag{4.26}$$

where $s_3 = p(\mu s_1 + \kappa)$ and $s_4 = q(\kappa + \mu s_2)$.

In the present problem, we have a common interface between viscoelastic layered medium and micropolar elastic semi-infinite medium. Since the considered viscoelastic layered medium doesn't exhibit micropolar property, therefore, at a common interface couple stress must vanish. This condition may be mathematically expressed as:

$$m_{zz} = 0 \text{ at } z = 0, \tag{4.27}$$

$$m_{zx} = 0 \text{ at } z = 0. \tag{4.28}$$

Using equations (4.11) and (4.20) in the boundary condition (4.27) and (4.28), we get

$$s_5 D + s_6 F + s_7 H = 0, \tag{4.29}$$

$$s_8 D + s_9 F + s_{10} H = 0, \tag{4.30}$$

Three conditions mentioned in (4.21), (4.22) and (4.23) together with two conditions provided in (4.27) and (4.28) constitute five boundary conditions (Set-I) for the present problem.

Elimination of arbitrary constants A, B, D, F and H from equations (4.24), (4.25), (4.26), (4.29) and (4.30) leads to

$$\tan(mH') = \frac{\nu s_{14} + 2m}{\nu + 2m s_{14}}, \tag{4.31}$$

where

$s_5 = -\alpha k^2 - r^2(\alpha + \beta + \gamma),\ s_6 = \alpha pk - kp(\alpha + \beta + \gamma),\ s_7 = \alpha qk - kp(\alpha + \beta + \gamma),$

$s_8 = rk\beta + kr\gamma,\ s_9 = \beta k^2 - p^2\gamma,\ s_{10} = k^2\beta - \gamma q^2,$

$s_{11} = s_6 s_{10} - s_9 s_7,\ s_{12} = s_5 s_9 - s_8 s_6,\ s_{13} = s_5 s_{10} - s_8 s_7,$

$$s_{14} = \frac{m\bar{\mu_0}(s_1 s_{11} - s_2 s_{12})}{i(\kappa k s_{11} s_3 s_{13} + s_4 s_{12}) + \frac{\nu}{2}\bar{\mu_0}(s_1 s_{11} - s_2 s_{12})}.$$

Now, comparing real and imaginary parts on both sides of equation (4.31), we get

$$\tan(T_3 H') = \frac{\xi_9 + \xi_{11}\tanh(T_4 H)}{\xi_{12} + \xi_{10}\tanh(T_4 H)}, \tag{4.32}$$

and

$$\tan(T_3 H') = \frac{\xi_{10} - \xi_{11}\tanh(T_4 H)}{\xi_{12} + \xi_9\tanh(T_4 H)}, \tag{4.33}$$

where

$s_5 = -\alpha k^2 - r^2(\alpha + \beta + \gamma),\ s_6 = \alpha pk - kp(\alpha + \beta + \gamma),\ s_7 = \alpha qk - kp(\alpha + \beta + \gamma),$

$s_8 = rk\beta + kr\gamma,\ s_9 = \beta k^2 - p^2\gamma,\ s_{10} = k^2\beta - \gamma q^2,$

$s_{11} = s_6 s_{10} - s_9 s_7$, $s_{12} = s_5 s_9 - s_8 s_6$, $s_{13} = s_5 s_{10} - s_8 s_7$,

$$s_{14} = \frac{m\bar{\mu_0}(s_1 s_{11} - s_2 s_{12})}{i(\kappa k s_{11} s_3 s_{13} + s_4 s_{12}) + \frac{\nu}{2}\bar{\mu_0}(s_1 s_{11} - s_2 s_{12})},$$

$\xi_1 = (s_1 s_{11} - s_{12} s_2)(\mu_0 T_3 + \omega \eta_0 T_4), \xi_2 = (s_1 s_{11} - s_{12} s_2)(-\omega \eta_0 T_3 + \mu_0 T_4)$,

$\xi_3 = \frac{\mu_0 \nu}{2}(s_1 s_{11} - s_{12} s_2), \xi_4 = \kappa k s_{11} + s_3 s_{13} + s_4 s_{12} - \frac{\nu \omega \eta_0}{2}(s_1 s_{11} - s_{12} s_2)$,

$\xi_5 = \frac{\xi_1 \xi_3 + \xi_2 \xi_4}{\xi_3^2 + \xi_4^2}$, $\xi_6 = \frac{\xi_2 \xi_3 - \xi_1 \xi_4}{\xi_3^2 + \xi_4^2}$,

$\xi_9 = \nu \xi_5 + 2T_3$, $\xi_{10} = \nu \xi_6 + 2T_4$, $\xi_{11} = \nu + 2T_3 \xi_5 - 2T_4 \xi_6$, $\xi_{12} = 2T_4 \xi_5 + T_3 \xi_6$.

Equation (4.32) is the dispersion relation and equation (4.33) is damped velocity equation for the propagation of SH-wave in a vertically heterogeneous viscoelastic layer lying over a micropolar elastic half-space.

Apart from above we may consider vanishing of microrotation i.e.

$$\phi_1 = 0 \text{ at } z = 0, \tag{4.34}$$

$$\phi_3 = 0 \text{ at } z = 0, \tag{4.35}$$

instead of vanishing of couple stress (mentioned in (4.27) and (4.28)) at common interface of viscoelastic layered medium and micropolar elastic semi-infinite medium. In view of this fact, three conditions (4.21), (4.22) and (4.23) along with two conditions provided in (4.34) and (4.35) constitute five boundary conditions (Set-II) for the present problem.

Using equations (4.11) and (4.20) in the boundary condition (4.34) and (4.35), we get

$$kD - pF - qH = 0, \tag{4.36}$$

$$rD + kF + kH = 0. \tag{4.37}$$

Eliminating the arbitrary constants A, B, D, F and H from the equations (4.24), (4.25), (4.26), (4.36) and (4.37), we obtain the following equation

$$\tan(mH') = \frac{\nu m\bar{\mu_0} - 2ms_{16}}{2m^2\bar{\mu_0} + \nu s_{16}}, \tag{4.38}$$

where

$\xi_7 = \frac{\nu\mu_0}{2}$, $\xi_8 = \frac{\kappa k^2(q-p) + s_3(rq-k^2) - s_4(rp-k^2) - \frac{\nu}{2}\omega\eta_0 s_{15}}{s_15}$,

$s_{15} = s_1(-k^2+rq) - s_2(-k^2+rp)$, $s_{16} = \frac{i\kappa k^2(q-p) + is_3(rq-k^2) - is_4(rp-k^2) + \frac{\nu}{2}\bar{\mu_0}s_{15}}{s_{15}}$.

Comparing real and imaginary parts on both sides of equation (4.38), we get

$$\tan(T_3H') = \frac{\xi_{13} + \xi_{16}\tanh(T_4H)}{\xi_{15} + \xi_{14}\tanh(T_4H)}, \tag{4.39}$$

and

$$\tan(T_3H') = \frac{\xi_{14} - \xi_{15}\tanh(T_4H)}{\xi_{16} + \xi_{13}\tanh(T_4H)}, \tag{4.40}$$

where

$\xi_{13} = \nu(T_4\mu_0 + \omega\eta_0T_4) - 2(T_3\xi_7 - T_4\xi_8)$, $\xi_{14} = \nu(T_4\mu_0 - \omega\eta_0T_4) - 2(T_3\xi_8 + T_4\xi_7)$,

$\xi_{15} = \nu\xi_7 + 2(T_1\mu_0 + T_2\omega\eta_0)$, $\xi_{16} = -\nu\xi_8 + 2(T_2\mu_0 + T_1\omega\eta_0)$.

Equations (4.39) and (4.40) are the dispersion relation and damped velocity equation respectively, for the propagation of SH-wave in a vertically heterogeneous viscoelastic layer lying over a micropolar elastic half-space.

For further discussion, we have chosen the dispersion relation and damping equation obtained from the boundary conditions (Set-I). A similar analysis can also be done by considering dispersion relation (4.39) and damping equation (4.40) deduced with the help of boundary conditions (Set-II).

4.4 Particular cases

4.4.1 Case 1

When $\nu = 0$, dispersion equation (4.32) and damped velocity equation (4.33) reduce to

$$\tan(T_3'H') = \frac{\xi_9' + \xi_{11}' \tanh(T_4'H')}{\xi_{12}' + \xi_{10}' \tanh(T_4'H')}, \tag{4.41}$$

and

$$\tan(T_3'H') = \frac{\xi_{10}' - \xi_{11}' \tanh(T_4'H')}{\xi_{12}' + \xi_9' \tanh(T_4'H')}, \tag{4.42}$$

respectively, where

$T_1' = \dfrac{k^2c^2}{\beta_1^2\left(1 - \dfrac{\omega^2\eta_0^2}{\mu_0^2}\right)} - k^2$, $T_3'^2 = \dfrac{\sqrt{(T_1'^2 + T_2'^2)/2} + T_1'}{2}$, $T_4'^2 = \dfrac{\sqrt{(T_1'^2 + T_2'^2)/2} - T_1'}{2}$,

$\xi_4' = \kappa k s_{11} + s_3 s_{13} + s_4 s_{12}$, $\xi_5' = \dfrac{\xi_2}{\xi_4'}$, $\xi_6' = -\dfrac{\xi_1}{\xi_4'}$, $\xi_9' = 2T_3'$, $\xi_{10}' = 2T_4'$, $\xi_{11}' = 2T_3'\xi_5' - 2T_4'\xi_6'$,

$\xi_{12}' = 2T_4'\xi_5' + T_3'\xi_6'$.

Equations (4.41) and (4.42) are dispersion equation and damped velocity equation for the propagation of SH-wave in homogeneous viscoelastic layer lying over a micropolar elastic half-space respectively.

4.4.2 Case 2

When $\alpha = 0$, $\beta = 0$, $\kappa = 0$ and $\gamma \longrightarrow 0$, dispersion equation (4.32) and damped velocity equation (4.33) reduce to

$$\tan(T_3H') = \frac{\xi_9'' + \xi_{11}'' \tanh(T_4H')}{\xi_{12}'' + \xi_{10}'' \tanh(T_4H')}, \tag{4.43}$$

and

$$\tan(T_3H') = \frac{\xi_{10}'' - \xi_{11}'' \tanh(T_4H')}{\xi_{12}'' + \xi_9'' \tanh(T_4H')}, \tag{4.44}$$

where

$p'^2 = k^2(\frac{c^2}{\beta_2^2} - 1)$, $q' = ik$, $r' = ik$, $s_1'' = -\dfrac{k^2c^2}{\beta_2^2}$,

$s_3'' = \mu p' s_1'$, $s_4'' = \mu q' s_2'$, $s_{11}'' = -k^3p' - kp'^2q'$, $s_{12}'' = -k^2p'^2 - ik^3p'$, $s_{13}'' = -k^3p' - q'p'^2k$,

$\xi_1'' = s_1''s_{11}''(\mu_0 T_3 + \omega\eta_0 T_4), \xi_2'' = s_1''s_{11}''(-\omega\eta_0 T_3 + \mu_0 T_4)$,

$\xi_3'' = \frac{\mu_0\nu}{2}s_1''s_{11}'', \xi_4'' = s_3''s_{13}'' + s_4''s_{12}'' - \frac{\nu\omega\eta_0}{2}s_1''s_{11}'', \xi_5'' = \dfrac{\xi_1''\xi_3'' + \xi_2''\xi_4''}{\xi_3''^2 + \xi_4''^2}$, $\xi_6'' = \dfrac{\xi_2''\xi_3'' - \xi_1''\xi_4''}{\xi_3''^2 + \xi_4''^2}$,

$\xi_9'' = \nu\xi_5'' + 2T_3$, $\xi_{10}'' = \nu\xi_6'' + 2T_4$, $\xi_{11}'' = \nu + 2T_3\xi_5'' - 2T_4\xi_6''$, $\xi_{12}'' = 2T_4\xi_5'' + T_3\xi_6''$.

Equations (4.43) and (4.44) are dispersion equation and damped velocity equation for the propagation of SH-wave in vertically heterogeneous viscoelastic layer lying over an isotropic elastic half-space (without micropolarity) respectively.

4.4.3 Case 3

When $\nu = 0$, $\eta_0 = 0$, $\alpha = 0$, $\beta = 0$, $\kappa = 0$ and $\gamma \longrightarrow 0$, damped velocity equation (4.33) vanishes identically and dispersion equation (4.32) reduces to

$$\tan\left(kH'\sqrt{\frac{c^2}{\beta_1^2} - 1}\right) = \frac{\mu\sqrt{1 - \frac{c^2}{\beta_2^2}}}{\mu_0\sqrt{\frac{c^2}{\beta_1^2} - 1}}, \tag{4.45}$$

which is the classical Love wave equation [52]. This validates the study.

4.5 Numerical results and discussion

To study the effect of heterogeneity parameter (νH), wave number (kH), viscoelastic parameter ($\omega\eta_0/\mu_0$) and micropolar parameter ($\kappa H^2/\gamma$) on the phase velocity and damped velocity, we consider the following data:

(i) For vertically heterogeneous viscoelastic layer [62]:

$\mu_0 = 1.987 \times 10^{10}\ N/m^2$, $\rho_0 = 4705\ kg/m^3$.

(ii) For micropolar elastic half-space [56]:

$\rho = 2.19 \times 10^3\ kg/m^3$, $\mu = 1.89 \times 10^{10}\ N/m^2$, $\kappa = 0.0149 \times 10^{10}\ N/m^2$,

$\lambda = 7.59 \times 10^{10}\ N/m^2$, $j = 0.196 \times 10^{-4}\ m^2$, $\alpha = 0.01 \times 10^6\ N$, $\beta = 0.015 \times 10^6\ N$,

$\gamma = 0.268 \times 10^6\ N$.

For studying the case of vertically heterogeneous viscoelastic layer lying over a elastic half space, we consider the following data [62]:

$\mu = 6.34 \times 10^{10}\ N/m^2$, $\rho = 3364\ kg/m^3$.

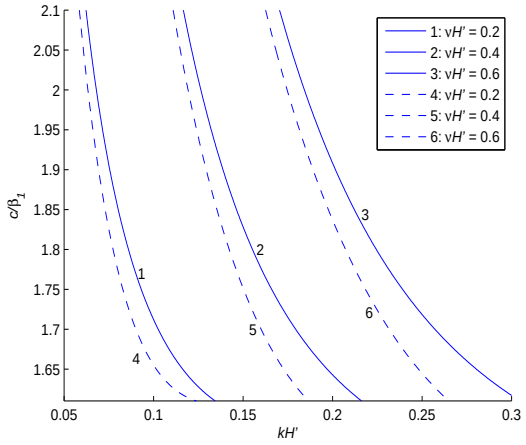

Figure 4.2: Variation of dimensionless phase velocity (c/β_1) against dimensionless wave number (kH') for different values of heterogeneity parameter ($\nu H'$) when half-space is comprised of micropolar elastic material (solid line curve) or elastic material without micropolarity (dashed line curve).

Dispersion equation and damping equation obtained from the boundary conditions of Set-I for SH-wave propagation in vertically heterogeneous viscoelastic layer lying over a micropolar elastic half-space have been established in closed form in equations (4.32) and (4.33) respectively. Phase velocity and damped velocity for the problem have been numerically computed and depicted by the means of graphs in Figs. (4.2) to (4.7). Moreover, to unravel the effect of anisotropy and micropolarity a comparative study is performed by comparing the phase velocity and damped

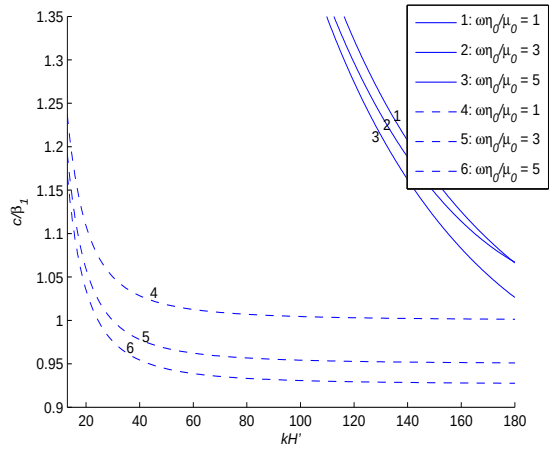

Figure 4.3: Variation of dimensionless phase velocity (c/β_1) against dimensionless wave number (kH') for different values of viscoelastic parameter ($\omega\eta_0/\mu_0$) when half-space is comprised of micropolar elastic material (solid line curve) or elastic material without micropolarity (dashed line curve).

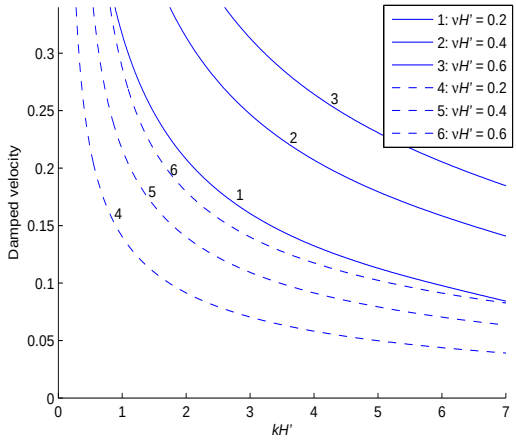

Figure 4.4: Variation of dimensionless damped velocity against dimensionless wave number (kH') for different values of heterogeneity parameter ($\nu H'$) when half-space is comprised of micropolar elastic material (solid line curve) or elastic material without micropolarity (dashed line curve).

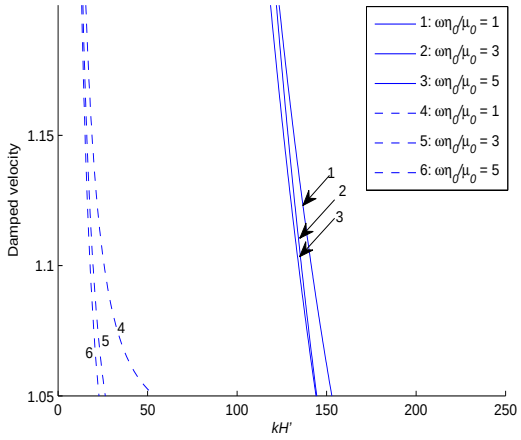

Figure 4.5: Variation of dimensionless damped velocity against dimensionless wave number (kH') for different values of viscoelastic parameter ($\omega\eta_0/\mu_0$) when half-space is comprised of micropolar elastic material (solid line curve) or elastic material without micropolarity (dashed line curve).

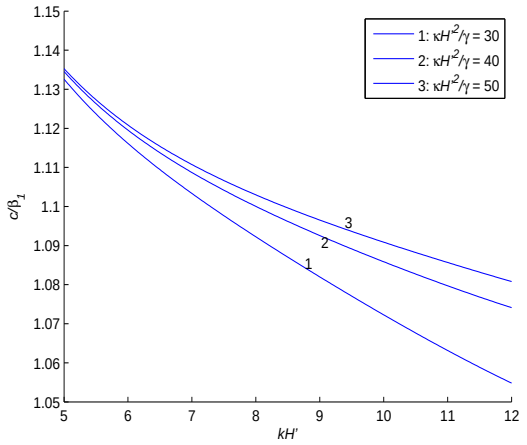

Figure 4.6: Variation of dimensionless phase velocity (c/β_1) against dimensionless wave number (kH') for different values of micropolar parameter ($\kappa H'^2/\gamma$) when a heterogeneous viscoelastic layer lies over a micropolar elastic half-space.

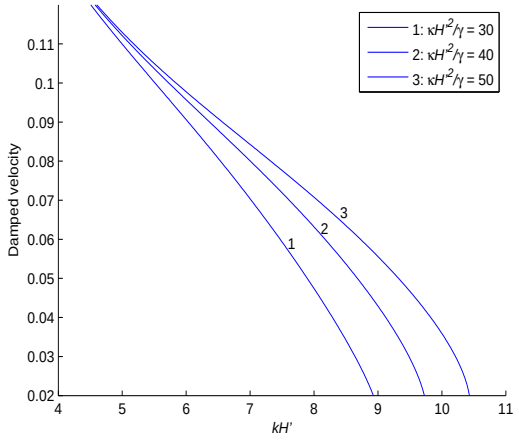

Figure 4.7: Variation of damped velocity against wave number (kH') for different values of micropolar parameter ($\kappa H'^2/\gamma$) when a heterogeneous viscoelastic layer lies over a micropolar elastic half-space.

velocity in the considered case (geometry) to the case when SH-wave is propagating in vertically heterogeneous viscoelastic layer lying over an elastic half-space without micropolarity.

Substantial effects of heterogeneity, viscoelasticity, anisotropy and micropolarity have been traced out and also highlighted by means of graphs. Distinct effects of heterogeneity over homogeneity; viscoelasticity over elasticity and micropolar elasticity over isotropic elasticity have also been exhibited through graphical comparison. Solid curves in all the figures represent the case when a vertically heterogeneous viscoelastic layer lying over a micropolar elastic half-space whereas dashed curves represent the case when a vertically heterogeneous viscoelastic layer lying over an elastic half-space without micropolarity. It is reported from all the figures that the phase velocity and damped velocity decrease with increase in wave number.

Figs. (4.2) and (4.3) represent the dispersion curves and reflect the effects of heterogeneity parameter (νH) and viscoelastic parameter ($\omega\eta_0/\mu_0$) respectively on phase velocity of SH-wave. Fig. (4.2) shows the effect of heterogeneity parameter of

the viscoelastic layer on phase velocity of SH-wave. It is worthy to note that curve 1 and curve 4 in Fig. (4.2) correspond to the case when viscoelastic layer is homogeneous whereas curves 2, 3, 5 and 6 correspond to the case when viscoelastic layer is heterogeneous. It is observed in this figure that inhomogeneity has significant effect on phase velocity of SH-wave. Phase velocity of SH-wave increases with increase in heterogeneity parameter of viscoelastic layer in both the cases when half-space is with or without micropolarity. More precisely as heterogeneity prevails in the medium phase velocity increases. Fig. (4.3) shows the effect of internal friction associated with viscoelastic layer on the phase velocity of SH-wave. Curves 1 and 4 are concerned with the case when layer is elastic (in absence of viscoelasticity) whereas curves 2, 3, 5 and 6 are concerned with the case when layer is viscoelastic. It is adduced from this figure that phase velocity of SH-wave decreases with increase in internal friction associated with viscoelastic layer in both the considered cases when half-space is with or without micropolarity.

In Figs. (4.4) and (4.5) variation of damped velocity of SH-wave against wave number is delineated and influence of heterogeneity and internal friction associated with viscoelastic layer are observed. In particular, Fig. (4.4) shows the effect of heterogeneity parameter on damped velocity. More specifically, in Fig. (4.4) curves 1 and 4 are associated with the case when layer is homogeneous viscoelastic whereas curves 2, 3, 5 and 6 are associated with the case layer is heterogeneous viscoelastic. It is evident from this figure that damped velocity increases with increase in heterogeneity parameter for a particular wave number in both considered cases. It can be concluded from Figs. (4.2) and (4.4) that heterogeneity has favoring effect on both phase and damped velocities regardless of the fact that micropolarity is

present or absent in the half-space. Effect of internal friction on damped velocity is depicted in Fig. (4.5) and it is found that damped velocity decreases with increase in internal friction associated with viscoelastic layer. Curves 2 and 3 in Fig. (4.5) correspond to the case of viscoelastic layer lying over a micropolar elastic half-space whereas curves 5 and 6 represent the case when of viscoelastic layer lying over an elastic half-space without micropolarity. Moreover, curves 1 and 4 in Fig. (4.5) correspond to the case of isotropic elastic layer (in absence of viscoelasticity) lying over a micropolar elastic half-space and elastic half-space without micropolarity. It is apparent from Figs. (4.3) and (4.6) that both phase and damped velocities decrease as viscoelasticity prevails in the layer medium. This is due to the fact that internal friction associated with viscoelastic layer acts as significant diminishing parameter for phase and damped velocity.

Figs. (4.6) and (4.7) delineate the influence of micropolarity present in the elastic half-space on the phase and damped velocities of SH-wave. These figures manifest favoring effect of micropolar parameter ($\kappa H^2/\gamma$) i.e. phase velocity of SH-wave increases with increase in the micropolar parameter of half-space. If we compare solid curves with dashed curves in Fig. (4.2) to Fig. (4.5) same effect can be analysed i.e. micropolarity of elastic half-space favors more to phase and damped velocity as compared to the elastic half-space without micropolarity regardless of the fact that viscoelasticity and heterogeneity are present in the layer medium or not.

4.6 Conclusion

This chapter emerges with meticulous study of propagation of horizontally polarised shear wave in vertically heterogeneous viscoelastic layer of finite width over a micropolar elastic half space. Dispersion equation and damping equation have been deduced in closed form. It has been instituted through the study that wave number, heterogeneity, viscoelasticity (internal friction) associated with viscoelastic layer, micropolarity associated with micropolar elastic half-space have a substantial effect on both phase velocity and damped velocity of SH-wave. Comparative study of the problem with isotropic case has been carried out to unreveal the effect due to presence of micropolarity in elastic half-space. The major highlights of the study may be pointed out as follows:

- Wave number affects the phase velocity and damped velocity of SH-wave substantially. Specifically, both phase velocity and damped velocity decrease with increases in wave number.

- Presence of heterogeneity in the layer medium favors the phase velocity and damped velocity of SH-wave significantly, regardless of the fact that micropolarity is present or absent in the half-space.

- Viscoelasticity associated with layer medium disfavors the phase velocity and damped velocity of SH-wave in the case when half-space is micropolar and simply isotropic substantially. This is due to the internal friction of the layer in viscoelastic medium.

- Phase velocity and damped velocity increase with increase in micropolar parameter.

- In the classical case (homogeneous isotropic layer lying over an homogeneous isotropic elastic half-space) deduced dispersion equation is found to be in well-agreement to the standard Love wave equation and deduced damping equation vanishes identically.

- The phenomenon exhibited by the rotation of particle at microscale leads to the increase in phase velocity of SH-wave. So consideration of this model will provide better results as compared to classical elasticity.

- Comparative study of the case when elastic half-space is with micropolarity to the case when elastic half-space is without micropolarity (simply isotropic) establishes that micropolarity in the medium of elastic half-space favors both phase velocity and damped velocity.

Chapter 5

Shear wave propagation at an imperfect interface between layer and half-space

5.1 Introduction

In the layered medium problems, it has been generally assumed that there is no slipping at the common interface between the layer and half-space. In such cases, phenomena of imperfect bonding play a crucial role in functionality and reliability of materials. It is evident that imperfectly bonded materials are characterized by weaker effective moduli than perfectly bonded ones. However, in the most practical cases, the weak interface response leads to the development of dislocations and voids, which dramatically decreases the strength of the whole material. Therefore, there have been considerable interests in imperfect interface problems as may be appropriate in the case of either pre-existing defects or interface damage. Imperfect bonding often occurs in SAW (surface acoustic wave) devices is due to the aging of glue applied to two conjunct solids, diffusion impurities, micro defects, and

The contents of section (5.2) are published in *Waves in Random and Complex Media, 26(4), 650-670, 2016, (SCI, Impact factor-0.952)* and contents of section (5.3) are communicated in SCI journal.

other forms of damages. Hence, common interface between two different materials cannot be perfectly bonded and transition or interphase with a thickness typically within the range of $30-240$ nm exists across the interface. To describe the physical conditions on the common interface with different mechanical boundary conditions a significant work has been done by different investigators. Notable among them are Jones and Whitter [67], Murty [90], Nayfeh and Nassar [92], Fan and Sze [53], Lavrentyev and Rokhlin [78], Wang and Zhong [139], Shodja et al. [121], Shariat and Eslami [112]. Sharma and Bhargava [117] has investigated the reflection and transmission of thermoelastic plane waves at an imperfect interface between a thermal conducting viscous-liquid and generalized thermoelastic solid half-space. Li and Jin [80] studied the propagation of shear horizontal waves in a piezoelectric layer imperfectly bonded to a metal or elastic substrate. Imperfect bonding considered in present study means that the components of stress are continuous and the small displacement field is not continuous. The small vector difference in the displacement is assumed to depend linearly on the traction vector. The state of boundary significantly affects elastic wave propagation phenomena.

In this chapter, we have considered two cases for the analysis, however the model can be extended for different types of half-spaces and layers involving imperfect bonding.

5.2 Influence of imperfectly bonded micropolar elastic half-space with non-homogeneous viscoelastic layer on propagation behavior of shear wave

In this section, a mathematical model is developed in which the effect of imperfect bonding between the constituents of layer and half-space on the phase velocity and damped velocity of SH-wave is discussed. The model consists of a micropolar elastic half-space bonded imperfectly with a heterogeneous viscoelastic layer. The dispersion equation and damping equation of SH-wave propagation in the said model is obtained in the closed form analytically. The effects of imperfect bonding, internal friction, heterogeneity, micropolarity and complex interface stiffness parameters are highlighted through numerical computation and graphical demonstrations. Standard Love-wave equation and dispersion equation as well as damping equation for perfectly bonded micropolar half-space with heterogeneous viscoelastic layer is obtained as a special case of the problem. Through comparative study of homogeneity with heterogeneity in the layer; imperfect bonding of layer and half-space with their welded (perfect) contact; and presence of micropolarity in half-space with its absence in half-space are studied meticulously.

5.2.1 Formulation of the problem

Following the imperfect bonded model as adopted by Li and Jin [80], we considered a viscoelastic layer of width H' (with vertical heterogeneity in exponential form) imperfectly bonded with a micropolar elastic half-space. The rectangular Cartesian

coordinate system is considered such that x-axis is along the direction of propagation of SH-wave and the z–axis is positive vertically downward, as shown in Fig. (5.1).

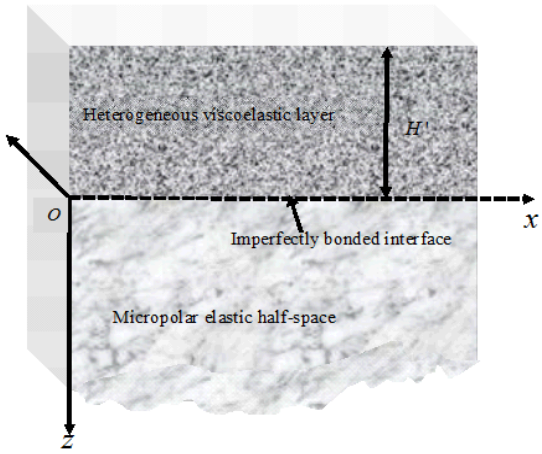

Figure 5.1: Geometry of the problem

Let us assume (u_1, v_1, w_1) and (u_2, v_2, w_2) as the displacement component caused due to propagation of SH-wave in upper layer and lower half-space respectively. Now, for the propagation of SH-wave in the $x-$direction and causing displacement only in $y-$direction, we shall assume that

$$u_i = 0,\ v_i = v_i(x, z, t),\ w_i = 0;\ (i = 1, 2). \tag{5.1}$$

Following the procedure adopted in sections 4.2.1 and 4.2.2 of Chapter-4, the displacement components of vertically heterogeneous viscoelastic layer and of micropolar elastic half-space are obtained as

$$v_1 = \frac{1}{\sqrt{\bar{\mu}_0}} e^{-\frac{\nu z}{2}} (A\cos(mz) + B\sin(mz)) e^{i(kx-\omega t)}, \tag{5.2}$$

$$v_2 = (Fe^{-ipz}s_1 + He^{-iqz}s_2) e^{i(kx-\omega t)},$$

$$\phi_1 = (De^{-irz}ik - ipFe^{-ipz} - iqHe^{-iqz}) e^{i(kx-\omega t)}, \tag{5.3}$$

$$\phi_3 = [-irDe^{-irz} - ik(Fe^{-ipz} + He^{-iqz})] e^{i(kx-\omega t)},$$

The notations and symbols are same as used in sections 4.2.1 and 4.2.2 of Chapter-4.

5.2.2 Boundary conditions

For the propagation of SH-wave in a vertically heterogeneous viscoelastic layer imperfectly bonded to a micropolar elastic half-space, the following boundary conditions are to be satisfied

(i) The upper most surface of heterogeneous viscoelastic layer is stress free, i.e.

$$p_{yz} = 0 \text{ at } z = -H'. \tag{5.4}$$

(ii) Common interface of layer and half-space is imperfectly bonded, i.e.

$$p_{yz} = R(v_2 - v_1) \text{ at } z = 0, \tag{5.5}$$

where R describes the degree of imperfectness at the common interface

(iii) Stresses are continuous at the common interface of layer and half-space, i.e.

$$p_{yz} = \tau_{yz} \text{ at } z = 0. \tag{5.6}$$

(iv) Couple stresses vanish at the common interface of layer and half-space, i.e.

$$\begin{aligned} m_{zz} &= 0 \text{ at } z = 0, \\ m_{zx} &= 0 \text{ at } z = 0. \end{aligned} \tag{5.7}$$

With the help of equations (5.2) and (5.3), the above boundary conditions (5.4)-(5.7) yield

$$A(2msin(mH') - \nu cos(mH')) + B(2mcos(mH') + \nu sin(mH')) = 0, \tag{5.8}$$

$$A(R - \frac{\nu\bar{\mu_0}}{2}) + \bar{\mu_0}mB = R\sqrt{\bar{\mu_0}}(Fs_1 + Hs_2), \tag{5.9}$$

$$\sqrt{\bar{\mu_0}}(-\frac{\nu A}{2} + Bm) = i\kappa kD - is_3F - is_4H, \tag{5.10}$$

$$s_5D + s_6F + s_7H = 0, \tag{5.11}$$

$$s_8D + s_9F + s_{10}H = 0, \tag{5.12}$$

where

$s_3 = (\mu s_1 + \kappa)p$, $s_4 = (\mu s_2 + \kappa)q$, $s_5 = -\alpha k^2 - r^2(\beta + \gamma + \alpha)$,

$s_6 = \alpha pk - kp(\beta + \gamma + \alpha)$, $s_7 = \alpha qk - kq(\beta + \gamma + \alpha)$,

$s_8 = rk\beta + kr\gamma$, $s_9 = \beta k^2 - \gamma p^2$, $s_{10} = \beta k^2 - \gamma q^2$.

Now, elimination of arbitrary constants A, B, F, H and D from the equations (5.8), (5.9), (5.10), (5.11), and (5.12) leads to

$$\tan(mH') = \frac{\nu s_{15} - 2m}{\nu + 2ms_{15}}, \tag{5.13}$$

where

$s_{11} = \dfrac{s_5s_{10} - s_7s_8}{s_8s_6 - s_5s_9}$, $s_{12} = \kappa ks_6 + s_3s_5$, $s_{13} = \kappa ks_7 + s_4s_5$,

$s_{15} = \xi_5 + i\xi_6$, $\xi_1 = Rs_5(s_1s_{11} + s_2)(\mu_0T_3 + \omega\eta_0T_4) - (s_{12}s_{11} + s_{13})(\mu_0T_4 - \omega\eta_0T_3)$,

$\xi_2 = Rs_5(s_1s_{11} + s_2)(\mu_0T_4 - \omega\eta_0T_3) - (s_{12}s_{11} + s_{13})(\mu_0T_3 + \omega\eta_0T_4)$,

$\xi_3 = \frac{\nu}{2}\mu_0Rs_5(s_1s_{11} + s_2) + \frac{\nu}{2}\omega\eta_0(s_{12}s_{11} + s_{13})$,

$\xi_4 = (R + \frac{\nu}{2}\mu_0)(s_{12}s_{11} + s_{13}) - \frac{\nu}{2}\omega\eta_0Rs_5(s_1s_{11} + s_2)$, $\xi_5 = \dfrac{\xi_1\xi_3 + \xi_2\xi_4}{\xi_3^2 + \xi_4^2}$, $\xi_6 = \dfrac{\xi_2\xi_3 - \xi_1\xi_4}{\xi_3^2 + \xi_4^2}$.

Comparing real and imaginary parts on both sides of equation (5.13), we get

$$\tan(T_3H') = \frac{\xi_{11}}{1 - \xi_{12}\tanh(T_4H')}, \tag{5.14}$$

and

$$\tan(T_3H') = \frac{\xi_{12} - \tanh(T_4H')}{\xi_{11}\tanh(T_4H')}, \tag{5.15}$$

where

$\xi_7 = \nu\xi_5 - 2T_3$, $\xi_8 = \nu\xi_6 - 2T_4$, $\xi_9 = \nu + 2(T_3\xi_5 - T_4\xi_6)$, $\xi_{10} = 2(T_4\xi_5 + T_3\xi_6)$,

$\xi_{11} = \dfrac{\xi_7\xi_9 + \xi_8\xi_{10}}{\xi_9^2 + \xi_{10}^2}$, $\xi_{12} = \dfrac{\xi_8\xi_9 - \xi_7\xi_{10}}{\xi_9^2 + \xi_{10}^2}$.

Equation (5.14) is the dispersion equation and equation (5.15) is damped velocity equation for the propagation of SH-wave in a vertically heterogeneous viscoelastic layer imperfectly bonded with a micropolar elastic half-space.

5.2.3 Particular cases

5.2.3.1 Case1

If we use a complex interface stiffness with an imaginary part that describes interface damping. So considering $R = R_1 + iR_2$, where both R_1 and R_2 are real. Hence,

$$\Gamma = \Gamma_1 - i\Gamma_2 = \frac{\mu k}{|R|^2}(R_1 - iR_2), \tag{5.16}$$

where Γ_1 and Γ_2 are real. Γ_1 corresponds to the flexibility imperfectness parameter of common interface, whereas Γ_2 is the viscoelastic imperfectness parameter of common interface.

When $R = R_1 + iR_2$, dispersion equation (5.14) and damped velocity equation (5.15) reduce to

$$\tan(T_3H') = \frac{\phi_{11}}{1 - \phi_{12}\tanh(T_4H')}, \tag{5.17}$$

and

$$\tan(T_3H') = \frac{\phi_{12} - \tanh(T_4H')}{\phi_{11}\tanh(T_4H')}, \tag{5.18}$$

where

$\phi_1 = R_1 s_5(s_1 s_{11} + s_2)(T_3\mu_0 + \omega\eta_0 T_4) - (T_4\mu_0 - \omega\eta_0 T_3)[R_2(s_1 s_{11} + s_2)s_5 + s_{12}s_{11} + s_{13}]$,

$\phi_2 = R_1 s_5(s_1 s_{11} + s_2)(T_4\mu_0 - \omega\eta_0 T_3) + (T_3\mu_0 + \omega\eta_0 T_4)[R_2(s_1 s_{11} + s_2)s_5 + s_{12}s_{11} + s_{13}]$,

$\phi_3 = -R_2(s_{12}s_{11} + s_{13}) + \dfrac{\nu}{2}\mu_0 R_1 s_5(s_1 s_{12} + s_2) + \dfrac{\nu\omega\eta_0}{2}[R_2 s_5(s_1 s_{11} + s_2) + s_{12}s_{11} + s_{13}]$,

$\phi_4 = R_1(s_{12}s_{11} + s_{13}) + \nu\mu_0[R_2 s_5(s_1 s_{11} + s_2) + s_{12}s_{11} + s_{13}] - \frac{\nu\omega\eta_0}{2} R_1 s_5(s_1 s_{12} + s_2)$,

$\phi_5 = \frac{\phi_1\phi_3 + \phi_2\phi_4}{\phi_3^2 + \phi_4^2}$, $\phi_6 = \frac{\phi_2\phi_3 - \phi_1\phi_4}{\phi_3^2 + \phi_4^2}$, $\phi_7 = \nu\phi_5 - 2T_3$, $\phi_8 = \nu\phi_6 - 2T_4$,

$\phi_9 = \nu + 2(T_3\phi_5 - T_4\phi_6)$, $\phi_{10} = 2(T_4\phi_5 + T_3\phi_6)$,

$\phi_{11} = \frac{\phi_7\phi_9 + \phi_8\phi_{10}}{\phi_9^2 + \phi_{10}^2}$, $\phi_{12} = \frac{\phi_8\phi_9 - \phi_7\phi_{10}}{\phi_9^2 + \phi_{10}^2}$.

Equations (5.23) and (5.18) are dispersion equation and damped velocity equation for the propagation of SH-wave in vertically heterogeneous viscoelastic layer lying over micropolar elastic half-space when common interface is complex.

5.2.3.2 Case2

When $R \to \infty$ or $\Gamma \to 0$, the common interface between layer and half-space becomes perfectly bonded and equations (5.14) and (5.15) reduce to

$$\tan(T_3 H') = \frac{\phi_5'}{1 - \phi_6' \tanh(T_4 H')}, \tag{5.19}$$

and

$$\tan(T_3 H') = \frac{\phi_6' - \tanh(T_4 H')}{\phi_5' \tanh(T_4 H')}, \tag{5.20}$$

where

$s_{16} = \frac{s_5(s_1 s_{11} + s_2)}{s_{12}s_{11} + s_{13}}$, $\phi_1' = \omega\eta_0\nu s_{16} - 2T_3$, $\phi_2' = \nu\mu_0 s_{16} - 2T_4$,

$\phi_3' = \nu + 2(T_3\omega\eta_0 s_{16} - \mu_0 s_{16} T_4)$, $\phi_4' = 2(T_3\mu - 0 s_{16} + 2\omega\eta_0 s_{16} T_4)$,

$\phi_5' = \frac{\phi_1'\phi_3' + \phi_2'\phi_4'}{\phi_3'^2 + \phi_4'^2}$, $\phi_6' = \frac{\phi_2'\phi_3' - \phi_1'\phi_4'}{\phi_3'^2 + \phi_4'^2}$.

Equations (5.19) and (5.20) are dispersion equation and damped velocity equation for the propagation of SH-wave when vertically heterogeneous viscoelastic layer and micropolar elastic half-space are perfectly bonded.

5.2.3.3 Case3

When $\nu = 0$, dispersion equation (5.14) and damped velocity equation (5.15) reduce to

$$\tan(T_3'H') = \frac{\xi_{11}'}{1 - \xi_{12}' \tanh(T_4'H')}, \tag{5.21}$$

and

$$\tan(T_3'H') = \frac{\xi_{12}' - \tanh(T_4'H')}{\xi_{11}' \tanh(T_4'H')}, \tag{5.22}$$

where

$m' = T_3' + iT_4'$, $T_1' = \dfrac{k^2c^2}{\beta_1^2\left(1 - \dfrac{\omega^2\eta_0^2}{\mu_0^2}\right)} - k^2$, $T_3'^2 = \dfrac{T_5' + T_1'}{2}$, $T_4'^2 = \dfrac{T_5' - T_1'}{2}$, $T_5'^2 = T_1'^2 + T_2^2$ $\xi_1' = s_{14}(\mu_0 T_3' + \omega\eta_0 T_4')$, $\xi_2' = s_{14}(-\omega\eta_0 T_3' + \mu_0 T_4')$,

$\xi_4' = R(s_{12}s_{11} + s_{13})$, $\xi_9' = 2\dfrac{T_3\xi_2' + T_4'\xi_1'}{\xi_4'}$, $\xi_{10}' = 2\dfrac{T_4'\xi_2' - T_3'\xi_1'}{\xi_4'}$,

$\xi_{11}' = -2\dfrac{T_3'\xi_9' + T_4'\xi_{10}'}{\xi_9'^2 + \xi_{10}'^2}$, $\xi_{12}' = 2\dfrac{-2T_4'\xi_9' + 2T_3'\xi_{10}'}{\xi_9'^2 + \xi_{10}'^2}$.

Equations (5.21) and (5.22) are dispersion equation and damped velocity equation for the propagation of SH-wave in homogeneous viscoelastic layer imperfectly bonded with a micropolar elastic half-space respectively.

5.2.3.4 Case4

When $\nu = 0$, $\eta_0 = 0$, $\alpha = 0$, $\beta = 0$, $\kappa = 0$ and $\gamma \longrightarrow 0$, damped velocity equation (5.15) vanishes identically and dispersion equation (5.14) reduces to

$$\tan\left(kH'\sqrt{\frac{c^2}{\beta_1^2} - 1}\right) = \frac{\mu\sqrt{1 - \dfrac{c^2}{\beta_2^2}}}{\mu_0\sqrt{\dfrac{c^2}{\beta_1^2} - 1}}, \tag{5.23}$$

which is the classical Love wave equation [52].

5.2.4 Numerical results and discussion

To study the effect of imperfectly bonded layer and half-space, heterogeneity, wave number, internal friction of viscoelastic layer, and micropolar parameter on the phase velocity and damped velocity of SH-wave propagating in a vertically heterogeneous viscoelastic layer imperfectly bonded with a micropolar elastic half-space, we consider the following data:

(i) For viscoelastic layer [62]:

$\mu_0 = 1.987 \times 10^{10}\ N/m^2$, $\rho_0 = 4705\ kg/m^3$.

(ii) For micropolar elastic half-space [56]:

$\rho = 2.19 \times 10^3\ kg/m^3$, $\mu = 1.89 \times 10^{10}\ N/m^2$, $\kappa = 0.0149 \times 10^{10}\ N/m^2$,

$\lambda = 7.59 \times 10^{10}\ N/m^2$, $j = 0.196 \times 10^{-4}\ m^2$, $\alpha = 0.01 \times 10^6\ N$, $\beta = 0.015 \times 10^6\ N$,

$\gamma = 0.268 \times 10^6\ N$.

For comparative study, we consider the case of vertically heterogeneous viscoelastic layer lying over and imperfectly bonded to an isotropic elastic half space and the following data is taken into account [62]:

$\mu = 6.34 \times 10^{10}\ N/m^2$, $\rho = 3364\ kg/m^3$.

Dispersion and damping equations of SH-wave propagating in vertically heterogeneous viscoelastic layer imperfectly bonded with a micropolar elastic half-space have been established in closed form in equations (5.14) and (5.15) respectively. Figures 2 to 13 graphically demonstrate phase velocity and damped velocity of SH-wave through numerical computations. Moreover, to unravel the effect of presence and absence of micropolarity on phase velocity and damped velocity, a comparative study is performed by comparing the considered case (when SH-wave is propagating

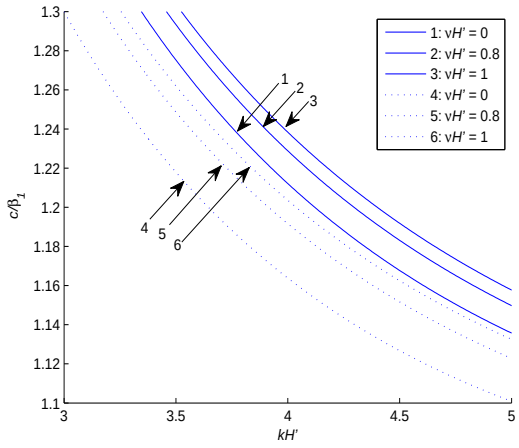

Figure 5.2: Variation in dimensionless phase velocity (c/β_1) against dimensionless wave number (kH') for different values of heterogeneity parameter of layer ($\nu H'$) .

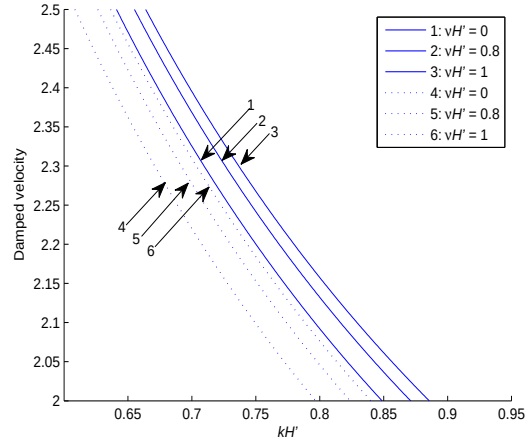

Figure 5.3: Variation in dimensionless damped velocity against dimensionless wave number (kH') for different values of heterogeneity parameter of layer ($\nu H'$) .

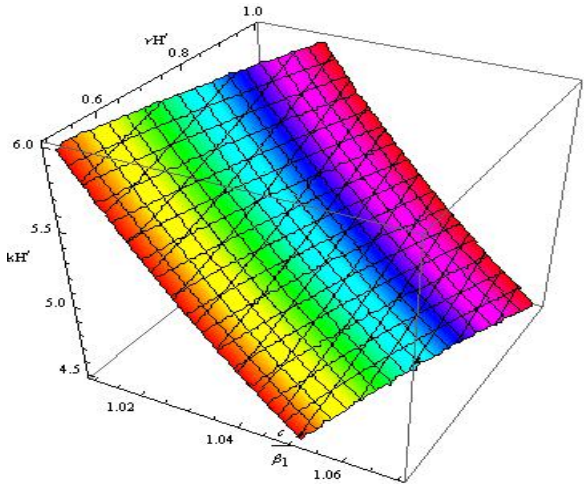

Figure 5.4: Surface plot of dimensionless phase velocity (c/β_1) against dimensionless wave number (kH') and non-dimensional heterogeneity parameter ($\nu H'$).

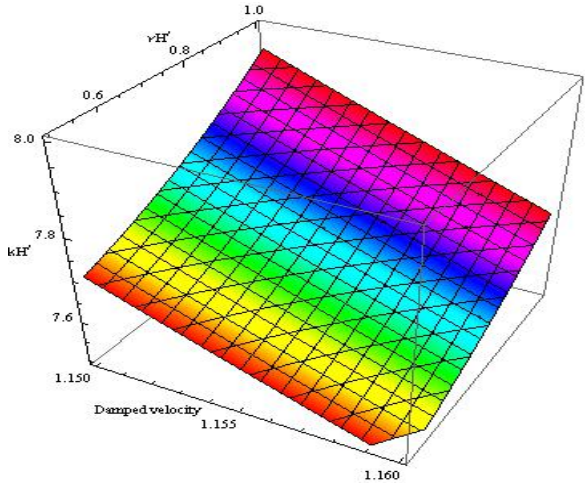

Figure 5.5: Surface plot of dimensionless damped velocity against dimensionless wave number (kH') and non-dimensional heterogeneity parameter ($\nu H'$).

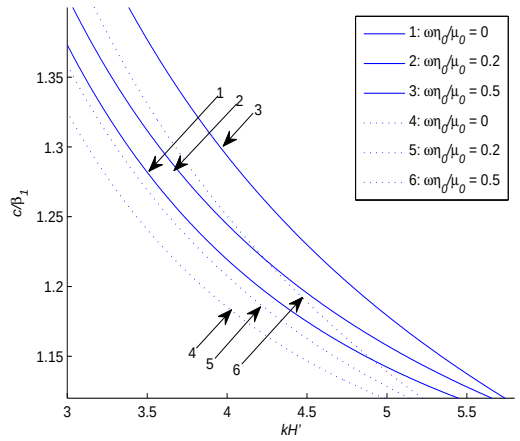

Figure 5.6: Variation in dimensionless phase velocity (c/β_1) against dimensionless wave number (kH') for different values of viscoelasticity of the layer ($\omega\eta_0/\mu_0$).

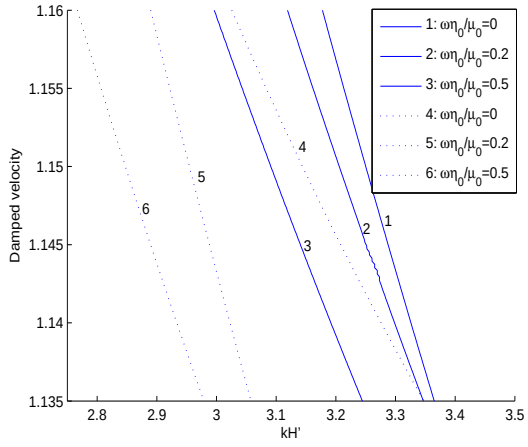

Figure 5.7: Variation in dimensionless damped velocity against dimensionless wave number (kH') for different values of viscoelasticity of the layer ($\omega\eta_0/\mu_0$).

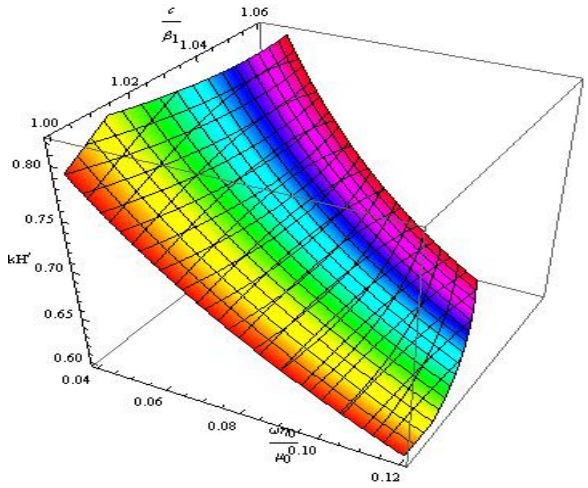

Figure 5.8: Surface plot of dimensionless phase velocity (c/β_1) against dimensionless wave number (kH') and non-dimensional viscoelasticity of the layer ($\omega\eta_0/\mu_0$).

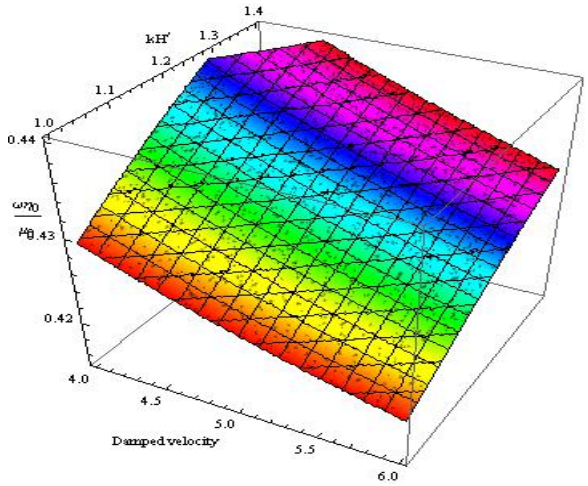

Figure 5.9: Surface plot of dimensionless damped velocity against dimensionless wave number (kH') and non-dimensional viscoelasticity of the layer ($\omega\eta_0/\mu_0$).

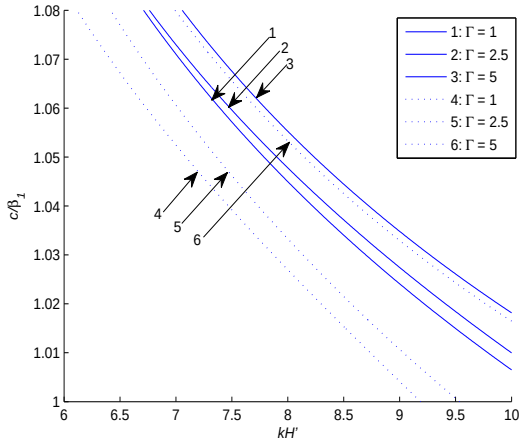

Figure 5.10: Variation in dimensionless phase velocity (c/β_1) for different values of imperfectness parameter ($\Gamma = \frac{k\mu}{R}$) of complex common interface.

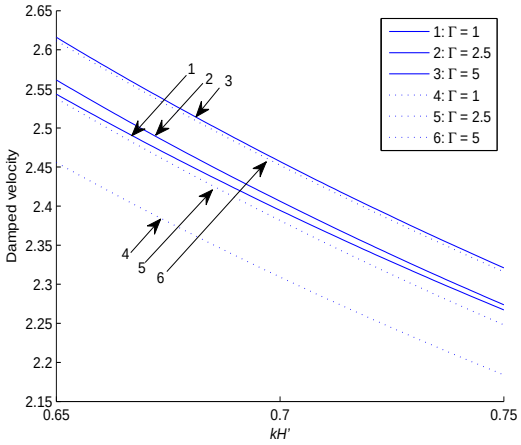

Figure 5.11: Variation in dimensionless damped velocity against dimensionless wave number (kH') for different values of imperfectness parameter ($\Gamma = \frac{k\mu}{R}$) of complex common interface.

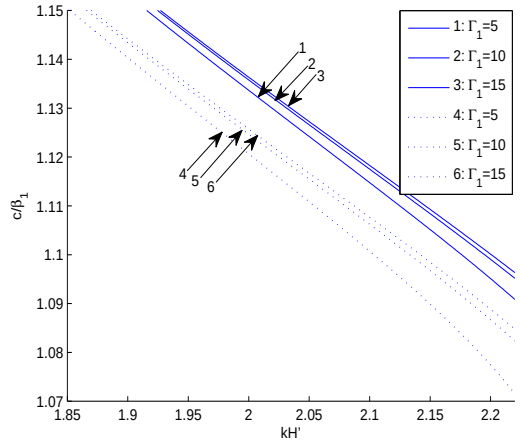

Figure 5.12: Variation in dimensionless phase velocity (c/β_1) for different values of non-dimensional flexibility imperfectness parameter ($\Gamma_1 = \frac{k\mu}{R_1}$) of complex common interface.

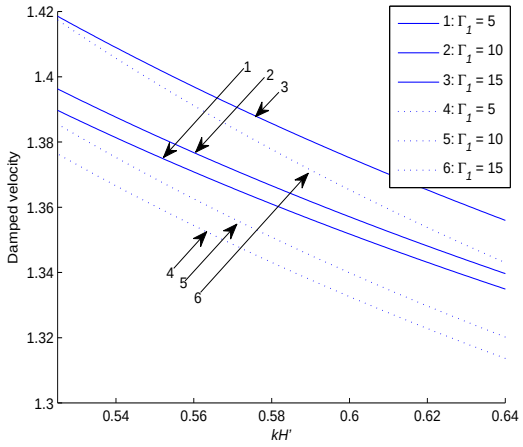

Figure 5.13: Variation in dimensionless damped velocity against dimensionless wave number (kH') for different values of non-dimensional flexibility imperfectness parameter ($\Gamma_1 = \frac{k\mu}{R_1}$) of complex common interface.

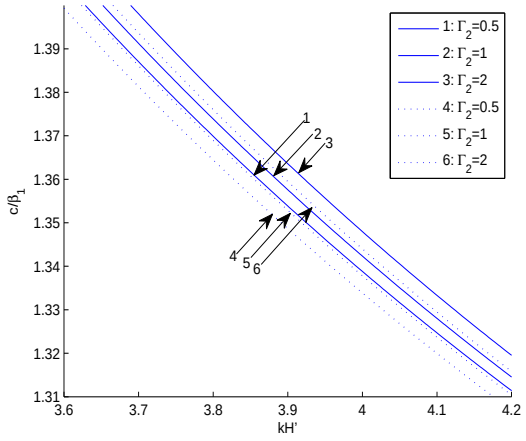

Figure 5.14: Variation in dimensionless phase velocity (c/β_1) against dimensionless wave number (kH') for different values of non-dimensional viscoelastic imperfectness parameter ($\Gamma_2 = \frac{k\mu}{R_2}$) of complex common interface.

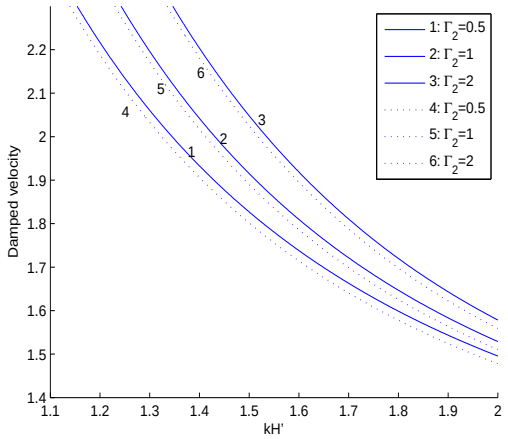

Figure 5.15: Variation in dimensionless damped velocity against dimensionless wave number (kH') for different values of non-dimensional viscoelastic imperfectness parameter ($\Gamma_2 = \frac{k\mu}{R_2}$) of complex common interface.

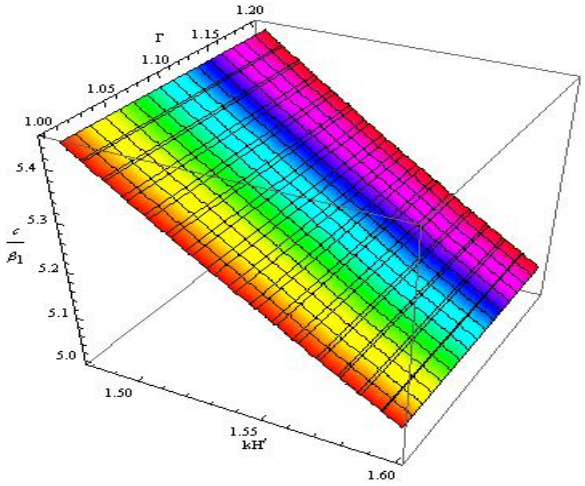

Figure 5.16: Surface plot of dimensionless phase velocity (c/β_1) against dimensionless wave number (kH') and non-dimensional imperfectness parameter ($\Gamma = \frac{k\mu}{R}$) of complex common interface.

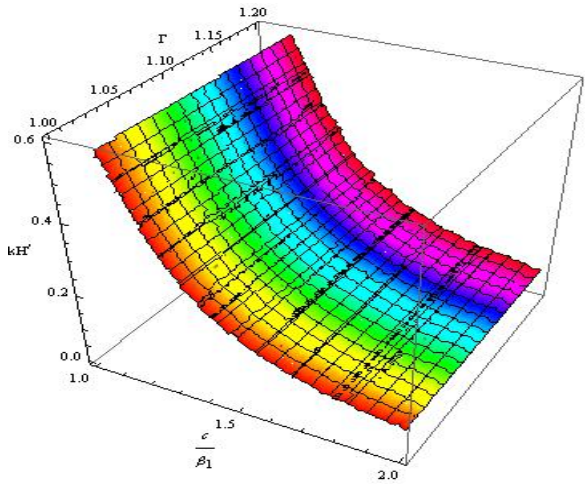

Figure 5.17: Surface plot of dimensionless damped velocity against dimensionless wave number (kH') and non-dimensional imperfectness parameter ($\Gamma = \frac{k\mu}{R}$) of complex common interface.

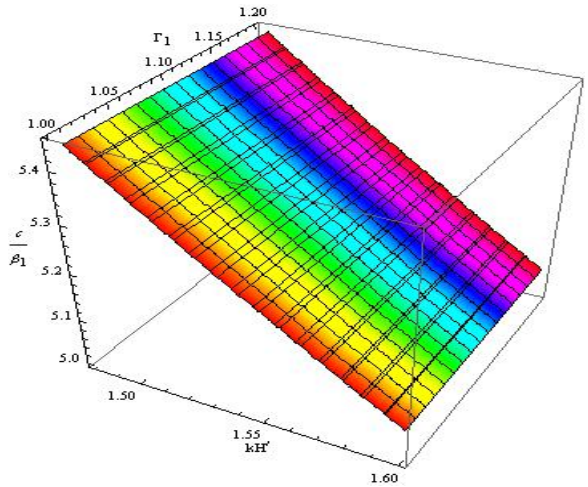

Figure 5.18: Surface plot of dimensionless phase velocity (c/β_1) against dimensionless wave number (kH') and non-dimensional flexibility imperfectness parameter ($\Gamma_1 = \frac{k\mu}{R_1}$) of complex common interface.

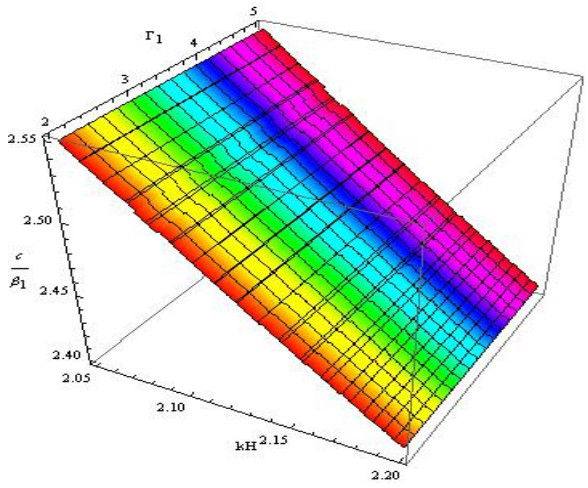

Figure 5.19: Surface plot of dimensionless damped velocity against dimensionless wave number (kH') and non-dimensional flexibility imperfectness parameter ($\Gamma_1 = \frac{k\mu}{R_1}$) of complex common interface.

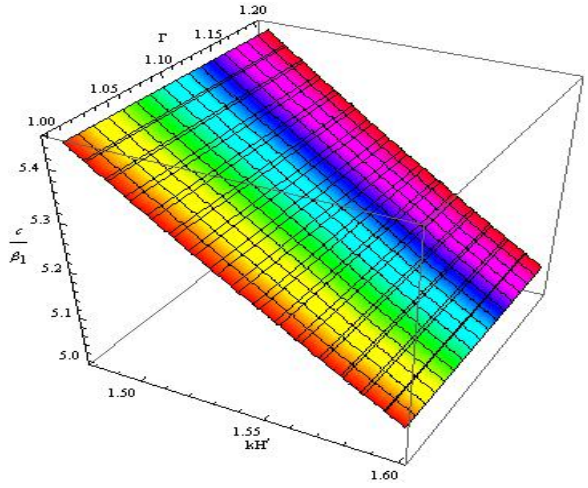

Figure 5.20: Surface plot of dimensionless phase velocity (c/β_1) against dimensionless wave number (kH') and non-dimensional viscoelastic imperfectness parameter ($\Gamma_2 = \frac{k\mu}{R_2}$) of complex common interface.

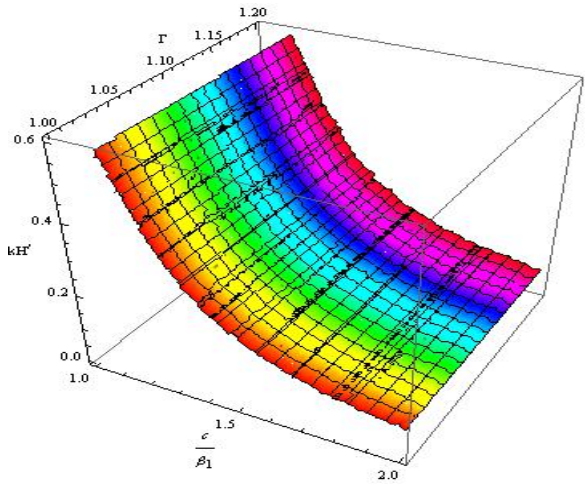

Figure 5.21: Surface plot of dimensionless damped velocity against dimensionless wave number (kH') and non-dimensional viscoelastic imperfectness parameter ($\Gamma_2 = \frac{k\mu}{R_2}$) of complex common interface.

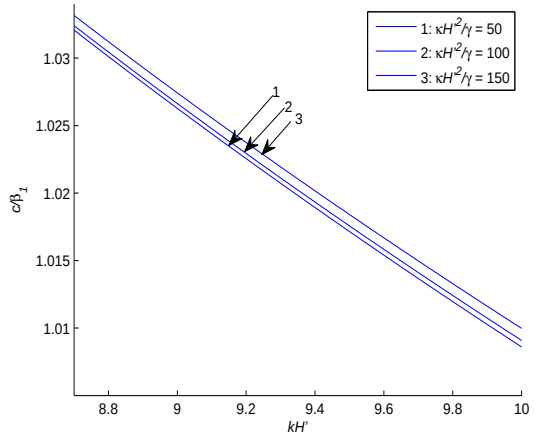

Figure 5.22: Variation in dimensionless phase velocity (c/β_1) against dimensionless wave number (kH') for different values of micropolar parameter ($\kappa H'^2/\gamma$) of micropolar elastic half-space.

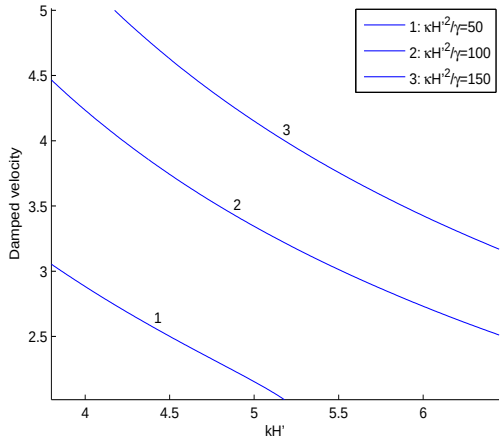

Figure 5.23: Variation in and dimensionless damped velocity against dimensionless wave number (kH') for different values of micropolar parameter ($\kappa H'^2/\gamma$) of micropolar elastic half-space.

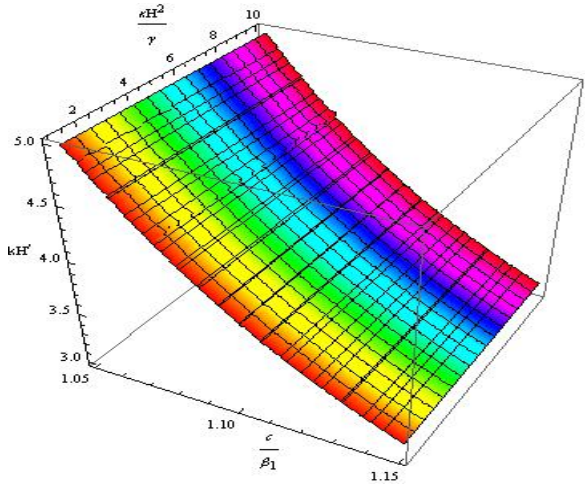

Figure 5.24: Surface plot of dimensionless phase velocity (c/β_1) against dimensionless wave number (kH') and non-dimensional micropolar parameter ($\kappa H'^2/\gamma$).

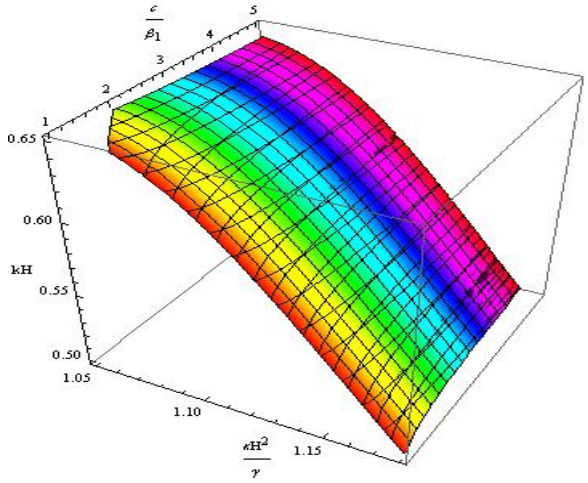

Figure 5.25: Surface plot of dimensionless damped velocity against dimensionless wave number (kH') and non-dimensional micropolar parameter ($\kappa H'^2/\gamma$).

in a vertically heterogeneous viscoelastic layer imperfectly bonded with a micropolar half-space) to the case when SH-wave is propagating in a vertically heterogeneous viscoelastic layer imperfectly bonded with an isotopic elastic half-space.

Distinct effects of heterogeneity over homogeneity; viscoelasticity over elasticity and micropolar elasticity over isotropic elasticity have also been exhibited through numerical computation and graphical comparison. Solid curves in figures 2, 4, 6, 7, 8 and 12 represent the case when a vertically heterogeneous viscoelastic layer is imperfectly bonded with a micropolar elastic half-space and dotted curves represent the case when a vertically heterogeneous viscoelastic layer is imperfectly bonded with an isotropic elastic half-space. From all these figures 2 to 13 it can be concluded that both phase velocity and damped velocity decrease with increase in dimensionless wave number.

Effect of heterogeneity

Figs. 2 (a) and 3 (a) show the effect of heterogeneity parameter associated with material constants on dimensionless phase velocity, whereas Figs. 2 (b) and 3 (b)

reveal the influence of heterogeneity parameter associated with material constants on dimensionless damped velocity. It is worthy to note that curve 1 and curve 4 in Figs. 2 (a) and 2 (b) correspond to the case when viscoelastic layer is homogeneous whereas curves 2, 3, 5 and 6 correspond to the case when viscoelastic layer is heterogeneous. It can be seen from these figures that both phase and damped velocities increase as the value of heterogeneity parameter increases in both the considered cases. It can be seen form these figures that as heterogeneity prevails in the layer medium, phase velocity and damped velocity increase.

Effect of viscoelasticity

Effect of internal friction associated with viscoelastic layer on phase velocity of SH-wave has been shown in Figs. 4 (a) and 5 (a) and on damped velocity of SH-wave has been elucidated through Figs. 4 (b) and 5 (b). It can be seen from these figures that internal friction of viscoelastic layer has disfavoring effect on both phase and damped velocities. Curve 1 and curve 4 in both the figures correspond to the case when layer medium is isotropic (without viscoelasticity) whereas curves 2, 3, 5 and 6 represent the case when layer medium is viscoelastic. It is adduced from these figures that both phase and damped velocities increase as the value of viscoelastic parameter decreases.

Influence of imperfectly bonded layer and half-space

In order to show the influence of the imperfect bonding at the common interface of layer and half-space on the dispersion and damping curves different values of imperfectness parameter associated to common interface are considered in Figs. 6 (a) and 6 (b). Figures 6 (a), 6 (b), 9 (a) and 9 (b) suggest that both phase velocity and

damped velocity increase as the value of imperfectness interface parameter increases. More noticeably, when the common interface of layer and half-space is imperfect then both phase velocity and damped velocity are more as compared to the case when common interface of layer and half-space is smooth and perfectly welded (i.e. $\Gamma = 0$ or $R \longrightarrow \infty$). The effect of flexibility imperfectness parameter associated to complex common interface has been shown in Figs. 7 (a), 7 (b), 10 (a) and 10 (b) and influence of viscoelastic imperfectness parameter associated to complex common interface has been shown in Figs. 8 (a), 8 (b), 11 (a) and 11 (b). It can be noticed from figures 7, 8, 9 and 10 that with increase in both flexibility and viscoelastic imperfectness parameters associated to complex common interface both phase and damped velocities increase. Meticulous examination of figures 6, 7, 8, 9 and 10 reveal that both phase and damped velocities are favored by imperfect bonding of layer and half-space. As bonding between layer and half-space approaches towards a perfect one (welded contact), phase and damped velocity decreases.

Effect of micropolarity

Effect of micropolarity present in half-space on phase velocity has been shown in Figs. 12 (a) and 13 (a) and on damped velocity through Figs. 12 (b) and 13 (b). It can be seen from these figures that micropolarity has favoring effect on both phase and damped velocities. If we compare solid line curves with dotted line curves in Figs. 2, 4, 6, 7 and 8 same effect can be analysed i.e. micropolarity of elastic half-space favors more to phase and damped velocity as compared to the isotropic elastic half-space without microploarity regardless of the fact that viscoelasticity and heterogeneity are present in the layer medium or not.

5.2.5 Conclusion

Propagation of horizontally polarised shear wave in a vertically heterogeneous viscoelastic layer of finite width imperfectly bonded with a micropolar elastic half space has been investigated analytically. The closed form expressions of dispersion equation and damping equation have been deduced. It has been established through the study that wave number, heterogeneity, imperfectness associated with complex common interface, viscoelasticity (internal friction) associated with viscoelastic layer, micropolarity associated with micropolar elastic half-space have a substantial effect on both phase velocity and damped velocity of SH-wave. To unravel the effect of presence and absence of micropolarity in elastic half-space, a comparative study of the problem with that of isotropic case has been carried out. The major highlights of the study may be pointed out as follows:

- Wave number affects the phase velocity and damped velocity of SH-wave substantially. Specifically, both phase velocity and damped velocity decrease with increases in wave number regardle-ss of homogeneity or heterogeneity in the layer; imperfect or perfect bonding of layer and half-space; and presence or absence of micropolarity in half-space.

- The imperfect interface strongly influences both phase velocity and damped velocity of SH-wave. When the common interface of layer and half-space is imperfect bonded both the phase velocity and damped velocity are more as compared to the case when common interface of layer and half-space is smooth and perfectly welded. Moreover, complex interface stiffness is considered and

it is observed that flexibility and viscoelasticity imperfectness parameters associated to the common interface of layer and half-space have favoring effect on both phase and damped velocities irrespective of the situation that homogeneity or heterogeneity in the layer; and presence or absence of micropolarity in half-space.

- Presence of heterogeneity in the layer medium favors the phase velocity and damped velocity of SH-wave significantly, regardless of the fact that micropolarity is present or absent in the half-space ; bonding of the layer and half-space is imperfect or perfect; and viscoelasticity is present or absent in the layer.

- Viscoelasticity associated with layer medium disfavors the phase velocity and damped velocity of SH-wave in both the cases when half-space is micropolar elastic or simply isotropic elastic. This is due to internal friction of the layer in viscoelastic medium.

- Micropolarity associated with micropolar elastic half-space has a substantial effect on both phase and damped velocities. It is noticed that both phase velocity and damped velocity increases with increase in micropolar parameter.

- In the classical case (homogeneous isotropic layer lying over and perfectly bonded to a homogeneous isotropic elastic half-space) deduced dispersion equation is found in well-agreement to the standard Love wave equation and the deduced damping equation vanishes identically.

- The phenomenon exhibited by the rotation of particle at microscale leads to the increase in phase velocity of SH-wave. So, consideration of this model will

provide better results as compared to classical elasticity.

- Comparative study of the case when elastic half-space is with micropolarity to the case when elastic half-space is without micropolarity (simply isotropic) establishes that as micropolarity prevails in the medium of elastic half-space both phase velocity and damped velocity are favored.

5.3 Propagation of Love type wave in a vertically heterogeneous fibre-reinforced layer imperfectly bonded to a micropolar elastic half-space

In this section, dispersion of Love type wave is studied in a vertically heterogeneous fibre-reinforced layer lying over a micropolar elastic half-space. The imperfect interfacial bonding between fibre-reinforced layer and micropolar half-space is proposed. An analytical expression of dispersion equation of Love type wave has been established. The study reveals that imperfectness, heterogeneity, reinforcement, micropolarity and coupling factor have significant effect on phase velocity and these effects are displayed by graphs. The effect of complex interface on phase velocity is analysed as a particular case of the problem.

5.3.1 Formulation of the problem

Following the geometry as shown in Fig. (5.1), we consider an imperfect bonded model of fibre-reinforced layer of width H' (with vertical heterogeneity in exponential form) and micropolar elastic half-space.

Let us assume (u_1, v_1, w_1) and (u_2, v_2, w_2) as the displacement component caused due to propagation of Love type wave in upper layer and lower half-space respectively. Now, for the propagation of Love type wave in the $x-$direction and causing displacement only in $y-$direction, we shall assume that

$$u_i = 0,\ v_i = v_i(x, z, t),\ w_i = 0;\ (i = 1, 2). \tag{5.24}$$

5.3.2 Solution for heterogeneous fibre-reinforced layer

The constitutive equations for a fibre-reinforced linearly elastic medium are given (1.15) in Chapter-1.

The heterogeneity in fibre-reinforced layer is considered as

$$\mu_L = \mu_L^0 e^{\nu(z+H')},\ \mu_T = \mu_T^0 e^{\nu(z+H')} \text{ and } \rho_1 = \rho_1^0 e^{\nu(z+H')}, \tag{5.25}$$

where ν is a heterogeneity parameter for fibre-reinforced layer having dimension inverse of length.

In the absence of body forces, the only non-vanishing equation of motion for small elastic disturbance in fibre-reinforced layer is

$$\frac{\partial \tau_{21}}{\partial x} + \frac{\partial \tau_{23}}{\partial z} = \rho_1 \frac{\partial^2 v_2}{\partial t^2}, \tag{5.26}$$

where

$$\begin{aligned} \tau_{21} &= \left[\mu_T \frac{\partial v_1}{\partial x} + (\mu_L - \mu_T) a_1 \left(a_1 \frac{\partial v_1}{\partial x} + a_3 \frac{\partial v_1}{\partial z}\right)\right] e^{\nu(z+H')}, \\ \tau_{23} &= \left[\mu_T \frac{\partial v_1}{\partial z} + (\mu_L - \mu_T) a_3 \left(a_1 \frac{\partial v_1}{\partial x} + a_3 \frac{\partial v_1}{\partial z}\right)\right] e^{\nu(z+H')}. \end{aligned} \tag{5.27}$$

Using equations (5.24) and (5.25) together with stresses (5.27), the equation of motion (5.26) for the propagation of Love type wave in fibre-reinforced layer reduces

to

$$P'\frac{\partial^2 v_1}{\partial x^2} + Q'\frac{\partial^2 v_1}{\partial x \partial z} + R'\frac{\partial^2 v_1}{\partial z^2} + S'\frac{\partial v_1}{\partial x} + T'\frac{\partial v_1}{\partial z} = \rho_1^0 \frac{\partial^2 v_1}{\partial t^2}, \tag{5.28}$$

where

$P' = \mu_T^0 + a_1^2(\mu_L^0 - \mu_T^0)$, $Q' = 2a_1a_3(\mu_L^0 - \mu_T^0)$, $R' = \mu_T^0 + a_3^2(\mu_L^0 - \mu_T^0)$,

$S' = \nu a_1 a_3(\mu_L^0 - \mu_T^0)$ and $T' = \nu(\mu_L^0 + a_3^2(\mu_L^0 - \mu_T^0))$.

Solution of (5.28) may be assumed as

$$v_1 = V_1(z)e^{i(kx-\omega t)}, \tag{5.29}$$

where k is the wave number and $\omega(= kc)$ is circular frequency.

In view of (5.29), equation (5.28) gives,

$$R'\frac{d^2V_1}{dz^2} + (ikQ' + T')\frac{dV_1}{dz} + (ikS' - P'k^2 + \rho_1^0\omega^2)V_1(z) = 0. \tag{5.30}$$

Solution of equation (5.30) is

$$v_1(z) = (Ae^{m_1 z} + Be^{m_2 z})e^{i(kx-\omega t)}, \tag{5.31}$$

where

$m_1 = m_3 + im_4$, $m_2 = m_5 + im_6$, $m_3 = \dfrac{-T' - r'^{1/2}\sin(\frac{\theta}{2})}{2R'}$, $m_4 = \dfrac{r'^{1/2}\cos(\frac{\theta}{2}) - kQ'}{2R'}$,

$m_5 = \dfrac{-T' + r'^{1/2}\sin(\frac{\theta}{2})}{2R'}$, $m_6 = \dfrac{-r'^{1/2}\cos(\frac{\theta}{2}) - kQ'}{2R'}$,

$\theta = \tan^{-1}\left(\dfrac{4R'S'k - 2kQ'T'}{k^2Q'^2 + 4R'\rho_1^0\omega^2 - T'^2 - 4R'P'k^2}\right)$,

$r' = \sqrt{(4R'S'k - 2kQ'T')^2 + (k^2Q'^2 + 4R'\rho_1^0\omega^2 - T'^2 - 4R'P'k^2)^2}$.

5.3.3 Solution for micropolar elastic half-space

Using same procedure as in section 4.2.2 in Chapter-4, the displacement components for micropolar elastic half-space are obtained as

$$v_2 = (Fe^{-ipz}s_1 + He^{-iqz}s_2)e^{i(kx-\omega t)}, \tag{5.32}$$

$$\phi_1 = (ikD'e^{-irz} - ipFe^{-ipz} - iqHe^{-iqz})e^{i(kx-\omega t)}, \tag{5.33}$$

$$\phi_3 = [-irD'e^{-irz} - ik(Fe^{-ipz} + He^{-iqz})]e^{i(kx-\omega t)}. \tag{5.34}$$

5.3.4 Boundary Conditions

For the propagation of Love type wave in vertically heterogeneous fibre-reinforced layer imperfectly welded with a micropolar elastic half-space, the following boundary conditions are to be satisfied

(i) The upper most surface of vertically heterogeneous fibre-reinforced layer is stress free, i.e.

$$\tau_{yz} = 0 \text{ at } z = -H'. \tag{5.35}$$

(ii) Layer and half-space are imperfectly welded, i.e.

$$\tau_{yz} = L(v_2 - v_1) \text{ at } z = 0, \tag{5.36}$$

where L is the degree of imperfectness of common interface.

(iii) Stresses are continuous at the common interface of layer and half-space, i.e.

$$\tau_{yz} = \sigma_{yz} \text{ at } z = 0. \tag{5.37}$$

(iv) Couple stresses vanishes at the common interface of layer and half-space, i.e.

$$\begin{aligned} m_{zz} &= 0 \text{ at } z = 0, \\ m_{zx} &= 0 \text{ at } z = 0. \end{aligned} \tag{5.38}$$

Using equations (5.29), (5.32), (5.33) and (5.34) together with the boundary conditions (5.36), (5.36), (5.37), and (5.38), we get

$$e^{-m_1 H'} s_3 A + e^{-m_2 H'} s_4 B = 0, \tag{5.39}$$

$$e^{\nu H'}(s_3A + s_4B) = i\kappa kD - is_5F - is_6H, \tag{5.40}$$

$$(e^{\nu H'}s_3 + L)A + (e^{\nu H'}s_4 + L)B = FLs_1 + HLs_2, \tag{5.41}$$

$$s_5D + s_6F + s_7H = 0, \tag{5.42}$$

$$s_8D + s_9F + s_{10}H = 0, \tag{5.43}$$

where

$s_3 = t_1+it_2$, $t_1 = m_3\mu_t^0+m_3a_3^2(\mu_L^0-\mu_T^0)$, $t_2 = m_4\mu_t^0+a_1a_3(\mu_L^0-\mu_T^0)k+m_4a_3^2(\mu_L^0-\mu_T^0)$,

$s_4 = t_3+it_4$, $t_3 = m_5\mu_t^0+m_5a_3^2(\mu_L^0-\mu_T^0)$, $t_4 = m_6\mu_t^0+a_1a_3(\mu_L^0-\mu_T^0)k+m_6a_3^2(\mu_L^0-\mu_T^0)$,

$s_5 = \mu s_1 + \kappa$, $s_6 = \mu s_2 + \kappa$, $s_7 = -\alpha(k^2 - r^2) - r^2(\beta + \gamma)$, $s_8 = -kp(\beta + \gamma)$,

$s_9 = -kq(\beta + \gamma)$, $s_{10} = (-\beta k^2 + \gamma rk)$.

Now, elimination of arbitrary constants A, B, D, F and H from the equations (5.39), (5.40), (5.41), (5.42) and (5.43) leads to

$$\tan(m_6H') = \frac{\xi_3\cos(m_4H') + \xi_4\sin(m_4H') - \xi_5\cos(m_6H')}{\xi_6\cos(m_6H')}, \tag{5.44}$$

where

$\xi_1 = (t_1t_4 + t_2t_3)(Ls_{13} + s_{14})e^{\nu H'}$, $\xi_2 = (t_1t_3 - t_2t_4)(Ls_{13} + s_{14})e^{\nu H'}$,

$\xi_3 = (\xi_2 + Lt_1s_{14})e^{-m_3H'}$,

$\xi_4 = (\xi_1 + Lt_2s_{14})e^{-m_3H'}$,

$\xi_5 = (\xi_2 + Lt_3s_{14})e^{-m_5H'}$, $\xi_6 = (\xi_1 + Lt_4s_{14})e^{-m_5H'}$,

$s_{11} = (-kr\beta - p^2\gamma)$, $s_{12} = (-kq\beta - q^2\gamma)$, $s_{13} = s_1(s_8s_{12} - s_{11}s_9) - s_2(s_7s_{11} - s_{10}s_8)$,

$s_{14} = \kappa k(s_8s_{12} - s_9s_{11}) - s_5(s_7s_{12} - s_9s_{10}) + s_6(s_7s_{11} - s_8s_{10})$.

Equation (5.44) is the dispersion equation for Love type wave in a vertically heterogeneous fiber-reinforced layer imperfectly welded with a micropolar elastic half-space.

5.3.5 Particular Cases

5.3.3.1 Case 1

To describe interface damping, we use a complex interface stiffness with an imaginary part given in (5.16).

Using complex interface stiffness, dispersion equation (5.44) reduces to

$$\tan(m_6 H') = \frac{\chi_{13}\chi_{15} + \chi_{14}\chi_{16}}{\chi_{15}^2 + \chi_{16}^2}, \tag{5.45}$$

where

$\chi_1 = (t_1 t_4 + t_2 t_3)(L_1 s_{13} + s14)e^{\nu H'}$, $\chi_2 = (t_1 t_4 + t_2 t_3)L_2 s_{13} e^{\nu H'}$,

$\chi_3 = (t_1 t_3 - t_2 t_4)(L_1 s_{13} + s14)e^{\nu H'}$, $\chi_4 = (t_1 t_3 - t_2 t_4)L_1 s_{13} e^{\nu H'}$,

$\chi_5 = (\chi_3 + L_1 t_1 s_{14})e^{-m_3 H'}$, $\chi_6 = (\chi_4 + L_2 t_1 s_{14})e^{-m_3 H'}$, $\chi_7 = (\chi_1 + L_1 t_2 s_{14})e^{-m_3 H'}$,

$\chi_8 = (\chi_2 + L_2 t_2 s_{14})e^{-m_3 H'}$, $\chi_9 = (\chi_3 + L_1 t_3 s_{14})e^{-m_5 H'}$, $\chi_{10} = (\chi_4 + L_2 t_3 s_{14})e^{-m_5 H'}$,

$\chi_{11} = (\chi_1 + L_1 t_4 s_{14})e^{-m_5 H'}$, $\chi_{12} = (\chi_2 + L_2 t_4 s_{14})e^{-m_5 H'}$,

$\chi_{13} = \chi_5 \cos(m_4 H') + \chi_7 \sin(m_4 H') - \chi_9 \cos(m_6 H')$,

$\chi_{14} = \chi_6 \cos(m_4 H') + \chi_8 \sin(m_4 H') - \chi_{10} \cos(m_6 H')$,

$\chi_{15} = \chi_{11} \cos(m_6 H')$, $\chi_{16} = \chi_{12} \cos(m_6 H')$.

Equation (5.45) is dispersion equation for the propagation of Love type wave in vertically heterogeneous fibre-reinforced layer lying over a micropolar elastic half-space when interface is complex.

5.3.3.2 Case 2

When $L \to \infty$ or $\Gamma \to 0$ dispersion equation (5.44) reduces to

$$\tan(m_6 H') = \frac{\chi_3' \cos(m_4 H') + \chi_4' \sin(m_4 H') - \chi_5' \cos(m_6 H')}{\chi_6' \cos(m_6 H')}, \tag{5.46}$$

where

$\chi_3' = t_1 s_{14} e^{-m_3 H'}$, $\chi_4' = t_2 s_{14} e^{-m_3 H'}$, $\chi_5' = t_3 s_{14} e^{-m_5 H'}$, $\chi_6' = t_4 s_{14} e^{-m_5 H'}$.

Equation (5.46) is dispersion equation for the propagation of Love type wave in vertically heterogeneous fibre-reinforced layer perfectly welded with micropolar elastic half-space.

5.3.3.3 Case 3

When $\nu = 0$ dispersion equation (5.44) reduces to

$$\tan(m_6' H') = \frac{\xi_2' \cos(m_4 H') + \xi_4' \sin(m_4 H') - \xi_2' \cos(m_6 H')}{\xi_6' \cos(m_6 H')}, \tag{5.47}$$

where

$r'' = k^2 Q'^2 + 4R'\rho_1^0\omega^2 - 4R'P'k^2$, $m_4' = \dfrac{r''^{1/2}}{2R'}$, $m_6' = -\dfrac{r''^{1/2}}{2R'}$,

$t_2' = m_4'\mu_T^0 + a_1 a_3(\mu_L^0 - \mu_T^0)k + m_4' a_3^2(\mu_L^0 - \mu_T^0)$,

$t_4' = m_6'\mu_T^0 + a_1 a_3(\mu_L^0 - \mu_T^0)k + m_6' a_3^2(\mu_L^0 - \mu_T^0)$,

$\xi_2' = -t_2' t_4'(s_{13} + s_{14})$, $\xi_4' = L t_2' s_{14}$, $\xi_6' = L t_4' s_{14}$,

Equation (5.47) is dispersion equation for the propagation of Love type wave in homogeneous fibre-reinforced layer imperfectly welded with micropolar elastic half-space.

5.3.3.4 Case 4

When $\mu_L^0 = \mu_T^0 = \mu_1^0$ and $a_1 = a_3 = 0$ dispersion equation (5.44) reduces to

$$\tan(m_6'' H') = \frac{\xi_3'' \cos(m_4'' H') + \xi_4'' \sin(m_4'' H') - \xi_5'' \cos(m_6'' H')}{\xi_6'' \cos(m_6'' H')}, \tag{5.48}$$

where

$r_1' = 4\mu_1^0\rho_1^0\omega^2 - \nu^2\mu_1^{0\,2} - 4\mu_1^{0\,2}k^2$, $m_3'' = -\frac{\nu}{2}$, $m_4'' = \dfrac{r_1'^{\,1/2}}{2\mu_1^0}$,

$m_5'' = -\frac{\nu}{2}$, $m_6'' = -\frac{r_1'^{1/2}}{2\mu_1^0}$, $t_1'' = -\frac{\nu\mu_1^0}{2}$, $t_2'' = m_4''\mu_1^0$, $t_3'' = -\frac{\nu\mu_1^0}{2}$, $t_4'' = m_6''\mu_1^0$,

$\xi_1'' = (t_1''t_4'' + t_2''t_3'')(Ls_{13} + s_{14})e^{\nu H'}$, $\xi_2'' = (t_1''t_3'' - t_2''t_4'')(Ls_{13} + s_{14})e^{\nu H'}$,

$\xi_3'' = (\xi_2'' + Lt_1''s_{14})e^{-m_3H'}$, $\xi_4'' = (\xi_1'' + Lt_2''s_{14})e^{-m_3H'}$,

$\xi_5'' = (\xi_2'' + Lt_3''s_{14})e^{-m_5H'}$, $\xi_6'' = (\xi_1 + Lt_4''s_{14})e^{-m_5H'}$.

Equation (5.48) is dispersion equation for the propagation of Love type wave in vertically heterogeneous reinforced-free layer imperfectly welded with micropolar elastic half-space.

5.3.3.5 Case 5

When $\nu = 0$, $\mu_L^0 = \mu_T^0 = \mu_1^0$ and $a_1 = a_3 = 0$ dispersion equation (5.44) reduces to

$$\tan(m_6'''H') = \frac{\xi_2'''\cos(m_4'''H') + \xi_4'''\sin(m_4'''H') - \xi_2'''\cos(m_6'''H')}{\xi_6'''\cos(m_6'''H')}, \tag{5.49}$$

where

$r_1'' = 4\mu_1^0\rho_1^0\omega^2 - 4\mu_1^{0^2}k^2$, $m_4''' = \frac{r_1''^{1/2}}{2\mu_1^0}$, $m_6''' = -\frac{r_1''^{1/2}}{2\mu_1^0}$, $t_2''' = m_4'''\mu_1^0$,

$t_4''' = m_6'''\mu_1^0$, $\xi_2''' = -t_2'''t_4'''(s_{13} + s_{14})$, $\xi_4''' = Lt_2'''s_{14}$, $\xi_6''' = Lt_4'''s_{14}$.

Equation (5.49) is dispersion equation for the propagation of Love type wave in homogeneous reinforced-free layer imperfectly welded with micropolar elastic half-space.

5.3.6 Numerical results and discussion

To perform numerical computation and to unravel the impact of heterogeneity prevailing in the layer, micropolarity associated with layer, imperfectness of common interface and reinforcement on phase velocity of Love type wave, following data is taken into account for graphical illustration.

(i) For heterogeneous fibre-reinforced layer (Chattopadhyay [25]):

$\mu_L^0 = 4.4 \times 10^9\ N/m^2$, $\mu_T^0 = 1.89 \times 10^9\ N/m^2$, $\rho_0 = 5600\ kg/m^3$.

(ii) For micropolar elastic half-space (Gauthier [56]):

$\rho_2 = 2.19 \times 10^3\ kg/m^3$, $\mu = 1.89 \times 10^{10}\ N/m^2$, $\kappa = 0.0149 \times 10^{10}\ N/m^2$,

$\lambda = 7.59 \times 10^{10}\ N/m^2$, $j = 0.196 \times 10^{-4}\ m^2$, $\alpha = 0.01 \times 10^6\ N$, $\beta = 0.015 \times 10^6\ N$,

$\gamma = 0.268 \times 10^6\ N$.

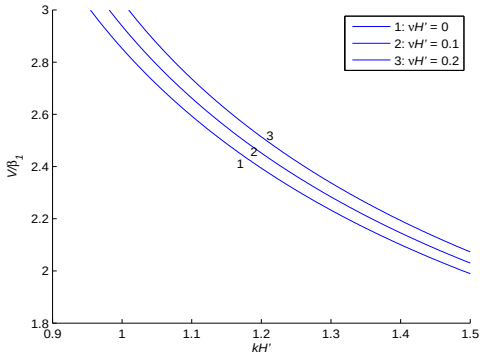

Figure 5.26: Variation of dimensionless phase velocity (c/β_1) against dimensionless wave number (kH') for different values of heterogeneity parameter $(\nu H')$ when when $N = 0.1$, $\frac{\kappa H'^2}{\gamma} = 50$ and $\Gamma = 1$.

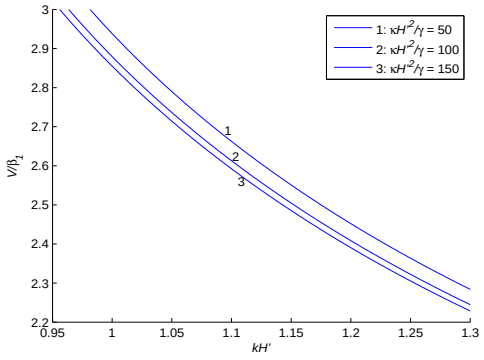

Figure 5.27: Variation of dimensionless phase velocity (c/β_1) against dimensionless wave number (kH') for different values of micropolarity parameter $(\frac{\kappa H'^2}{\gamma})$ when $\nu H' = 0.1$, $N = 0.1$ and $\Gamma = 1$.

The effects of imperfect common interface, reinforcement, heterogeneity, micropolarity and coupling factor on the dimensionless phase velocity of Love type

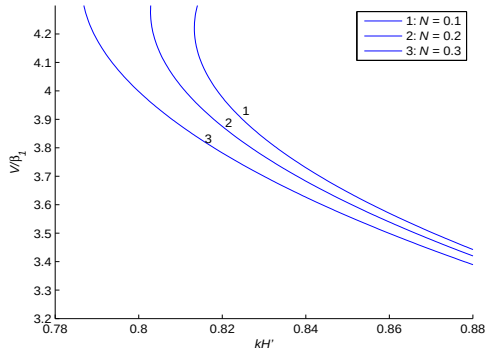

Figure 5.28: Variation of dimensionless phase velocity (c/β_1) against dimensionless wave number (kH') for different values of coupling factor (N) when $\nu H' = 0.1$, $\frac{\kappa H'^2}{\gamma} = 50$ and $\Gamma = 1$.

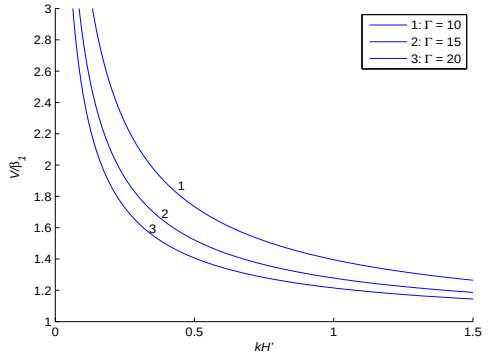

Figure 5.29: Variation of dimensionless phase velocity (c/β_1) against dimensionless wave number (kH') for different values of imperfect factor $(\Gamma = \frac{k\mu}{L})$ when $\nu H' = 0.1$, $\frac{\kappa H'^2}{\gamma} = 50$ and $N = 0.1$.

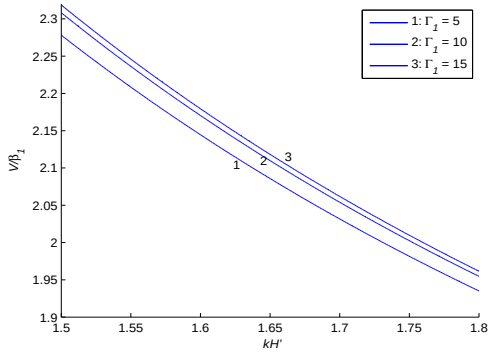

Figure 5.30: Variation of dimensionless phase velocity (c/β_1) against dimensionless wave number (kH') for different values of flexibility parameter of imperfect common interface $(\Gamma_1 = \frac{k\mu}{L_1})$ when $\nu H' = 0.1$, $\frac{\kappa H'^2}{\gamma} = 50$, $N = 0.1$ and $\Gamma_2 = 0.5$.

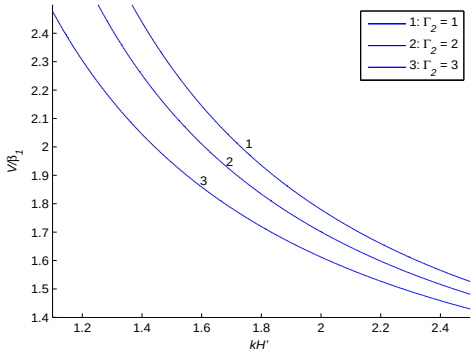

Figure 5.31: Variation of dimensionless phase velocity (c/β_1) against dimensionless wave number (kH') for different values of viscoelastic parameter of common imperfect interface $(\Gamma_2 = \frac{k\mu}{L_2})$ when $\nu H' = 0.1$, $\frac{\kappa H'^2}{\gamma} = 50$, $N = 0.1$ and $\Gamma_2 = 5$.

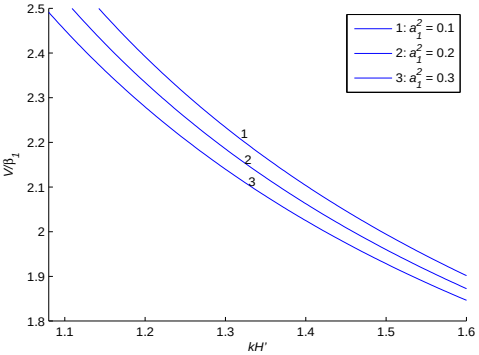

Figure 5.32: Variation of dimensionless phase velocity (c/β_1) against dimensionless wave number (kH') for different values of reinforcement parameter a_1 when $\nu H' = 0.1$, $\frac{\kappa H'^2}{\gamma} = 50$, $N = 0.1$ and $\Gamma = 1$.

wave in a fiber-reinforced layer and reinforced-free layer over a micropolar elastic half-space have been presented by graphs. From the above figures it is observed that with increase in wave number phase velocity of Love type wave decreases.

Effect of heterogeneity:

The effect of different values of heterogeneity parameter $\nu H'$ prevailing in the layer on phase velocity of Love type wave has been studied in Fig. (5.26). It can be observed from the phase velocity profiles of Love type wave that with increase in heterogeneity parameter of layer the phase velocity increases i.e. phase velocity increases as heterogeneity prevails in the layer. More precisely, curve 1 correspond to the case of homogeneous layer lying over a micropolar elastic half-space.

Effect of micropolarity:

Fig. (5.27) delineate the influence of micropolar parameter present in the elastic half-space on the phase velocity of SH-wave. This figure manifests disfavoring effect of micropolar parmeter $(\kappa H^2/\gamma)$ i.e. phase velocity of SH-wave decreases with increase in the micropolar parameter of half-space.

Effect of coupling factor:

The micropolar theory of elasticity offers more advantage over classical elasticity in the prediction of stresses in materials with microstructure. Fatemi et al. [54] defined the characteristic length and coupling factor (N) for these types of materials as

$$\gamma = 4l^2\mu, \kappa = 2N^2\mu/(1-N^2),$$

where $0 \leq N < 1$. Here $N = 0$ corresponds to a classical elastic materials and $N = 1$ refers to famous coupled stress theory. In Fig. (5.28) it is observed that phase velocity profiles of Love type wave are affected by microstructure properties of half-space. It is evident from this figure that increase in value of coupling factor results in the decrease in dimensionless phase velocity of Love type wave in fibre-reinforced layer lying over a micropolar elastic half-space.

Effect of nature of imperfectly bonded common interface:

The effect of imperfectly bonded common interface on the phase velocity of Love type wave is investigated by taking the imperfectness factor. Moreover, a particular case of complex imperfectness factor is also analyzed by taking the imperfectness factor to be complex. Fig. (5.29) shows the variation of dimensionless phase velocity under the impact of real imperfectness parameter of common interface. It is noted from this figure that as imperfectness of common interface increases, phase velocity of Love type wave decreases in the considered case. Figs. (5.30) and (5.31) show the effect of complex imperfectness factors i.e. flexibility and viscoelastic of common interface respectively. It can be seen from these figures that phase velocity increases with increase in flexibility parameter of the imperfect common interface whereas with increase in viscoelastic parameters of the imperfect common interface phase velocity decreases.

Effect of reinforcement:

The effect of reinforcement can be seen in Fig. (5.32). It is evidently reflected from Fig. 8 that increasing value of the reinforcement parameter corresponds to decreasing phase velocity. More precisely, presence of reinforcement in the layer

decreases phase velocity.

5.3.7 Conclusion

In this section, propagation of Love type wave in a fibre-reinforced lying over a micropolar elastic half-space has been studied. Dispersion equation has been established in closed form and the effects of heterogeneity in layer, micropolarity associated with half-space and imperfectness of common interface on the phase velocity of Love type wave have been observed and depicted graphically. Following points can be outlined as an outcome of the study:

- Wave number affects the phase velocity of Love type wave substantially. In reinforced layer lying over a micropolar elastic half-space phase velocity decreases with increases in wave number.

- Presence of heterogeneity in the layer medium favors the phase velocity of Love type wave significantly.

- Substantial effect of micropolar parameter is observed on phase velocity of Love type wave. With increasing value of micropolar parameter phase velocity decreases.

- It is observed that micropolarity has remarkable effect on phase velocity of Love type wave. Phase velocity of Love type wave increases with increase in coupling factor in both the considered cases.

- Imperfectness associated with common interface has significant effect on phase velocity of Love type wave. Imperfectness factor is taken as real and complex. Real imperfectness factor and viscoelastic parameter of common imperfect

interface disfavors the phase velocity of Love type wave whereas flexibility parameter of imperfect common interface favors the phase velocity of Love type wave.

- Reinforcement parameter of layer disfavors phase velocity of Love type wave i.e. as reinforcement prevails in the medium phase velocity decreases.

Chapter 6

Propagation of shear wave at a loosely bonded corrugated interface between a fibre-reinforced layer and an isotropic half-space

6.1 Introduction

It might not always be possible to cover all the mechanics of a material medium by assuming the constituent layers of it to be isotropic and homogeneous. The presence of various types of elements and compounds give rise to anisotropy and heterogeneity in it. Other than anisotropy and heterogeneity, initial stress is also a trivial characteristic as well as an important factor which affects the propagation of surface waves through the concerned material. Facts like overburdening of layers, atmospheric pressure, gravitational field slow process of creep, variation in temperature etc. are responsible for generating a huge amount of initial stress in the material medium. This initial stress is liable to alterations of physical properties of the medium and hence conceivably influences the propagation of waves through the mediums. Moreover, their presence in the media causes the formation of natural

The contents of this chapter are communicated in *SCI journal*.

reinforcement in it. Chattopadhyay et al. [31] studied the effect of heterogeneity, anisotropy and initial stress on the propagation of torsional surface wave in heterogeneous anisotropic half-space under initial stress. Gupta et al. [64] found the dispersion relation and then briefly discussed the impact of heterogeneity, anisotropy and initial stress on Love wave propagation in non-homogeneous substratum over initially stressed heterogeneous half-space.

Further, the constituent layers of material may not be always perfectly bonded i.e. the interfaces of the layers may be smooth, welded or loosely bonded in accordance with the individual properties of the mediums. Therefore, it is worthy to consider the effect of not only corrugated but also loosely bonded interface of layers in the study of mechanics of solids. The effects of loose bonding and viscoelasticity on amplitude ratios obtained by solving the problem of reflection and transmission of elastic waves at a loosely bonded interface between an elastic solid and a viscoelastic porous solid saturated by viscous liquid was studied by Singh [124]. Singh and Kumar [122] explored the problem of a reflection and refraction of micropolar elastic waves at a loosely bonded interface between a viscoelastic solid and a micropolar elastic solid. The partition of incident energy among the reflected and refracted waves for each incidence at an imperfectly bonded interface between poroelastic solid and cracked elastic solid was studied by Nandal and Saini [91]. Khurana and Vashisth [73] briefly discussed the influence of loose bonding on the propagation of Love waves in an elastic layer overlying a poroelastic solid half-space. Besides these, some notable work considering smooth irregularity (corrugated) at the boundary surfaces of considered media includes Singh and Tomar [125], Kaur et al. [70], Tomar and Kaur [131, 132, 69], Singh [124]. Till date researcher have paid their

attention to study the effect of corrugated boundaries on reflection, refraction as well as transmission of seismic waves; but the problems dealing with dispersion characteristics of surface waves propagating through anisotropic and heterogeneous stratum with corrugated boundary surfaces bearing different characteristics still needs to be attended.

This chapter aims to investigate the propagation of SH-wave in a heterogeneous fibre-reinforced composite layer lying over an initially stressed isotropic elastic half-space with corrugated and loose bonded interface. The effect of reinforcement, anisotropy, heterogeneity, initial stress, loose bonding, undulation parameter and position parameter on phase velocity of SH-wave have been examined. Comparative studies which are performed for various cases are among the major highlights of the study. With a view to unravel the hidden facts, numerical computation along with graphical demonstration has been carried out extensively for the present problem.

6.2 Formulation of the problem

Following the corrugated interface model adopted by Tomar and Kaur [132], we considered a heterogeneous fibre-reinforced layer of average finite thickness H_1 lying over an isotropic elastic half-space under initial stress. Rectangular Cartesian Coordinate system has been taken into consideration with origin O, at the corrugated as well as loosely bonded common interface of layer and half-space. x-axis is taken in the direction of wave propagation and y-axis is taken in horizontal plane of rectangular coordinate system and z-axis is positive vertically downwards as shown in Fig. (6.1).

Let the equation of upper planar boundary surface be $z = -H_1$ and the equation

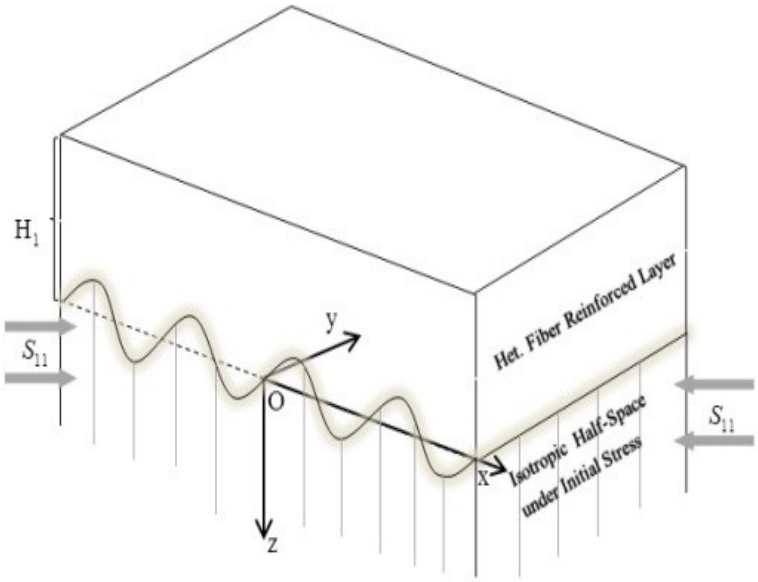

Figure 6.1: Geometry of the problem

of corrugated interface between layer and half-space be $z = g(x)$, where $g(x)$ is a periodic function and independent of y. Taking a suitable origin of coordinates we can represent Trigonometric Fourier series of $g(x)$, as follows [13]:

$$g = \sum_{n=1}^{\inf} \left[g_n e^{inbx} + g_{-n} e^{-inbx} \right], \tag{1}$$

where g_n and g_{-n} are Fourier expansion coefficients and n is series expansion order. Let us introduce the constants a, R_n, I_n as follows:

$g_{\pm 1} = \dfrac{a}{2}$, $g_{\pm n} = \dfrac{R_n + iI_n}{2}$, $n = 2, 3, ...$

and

$g = a\cos(bx) + R_2\cos(2bx) + I_2\sin(2bx) + ... + R_n\cos(nbx) + I_n\sin(nbx) + ...,$

where R_n, I_n are are the cosine and sine Fourier coefficients, respectively and $i = \sqrt{-1}$.

As far as the present problem is concerned, the common interface may be expressed with the aid of cosine terms i.e.

$g = a\cos(bx)$, where b is the wave number of corrugation, a is the amplitude of

corrugation and the wavelength of the corrugation is $2\pi/b$.

Let us assume (u_1, v_1, w_1) and (u_2, v_2, w_2) as the displacement components of upper heterogeneous fibre-reinforced layer and lower isotropic elastic half-space under initial stress respectively.

For the propagation of SH-wave, we consider

$$u_i = 0, w_i = 0, v_i = v_i(x, z, t), i = 1, 2. \tag{6.1}$$

6.2.1 Dynamics of the upper heterogeneous fibre-reinforced composite layer

The constitutive equation for a fibre-reinforced linearly elastic anisotropic composite medium with preferred direction $\vec{a}$ is given by equation (1.15) in Chapter-1.

The heterogeneity in the fibre-reinforced composite layer is considered as

$$\mu_T = e^{\alpha_1(z+H_1)}\mu_T^0, \mu_L = e^{\alpha_1(z+H_1)}\mu_L^0, \rho_1 = e^{\alpha_1(z+H_1)}\rho_1^0, \tag{6.2}$$

where α_1 is the heterogeneity parameter having dimension inverse of length.

$\mu_T^0, \mu_L^0, \rho_1^0$ are the values of μ_T, μ_L, ρ_1 respectively at $z = -H_1$.

The only non-vanishing equation of motion for the propagation of SH wave as per equation (6.1) is obtained as

$$\frac{\partial \tau_{21}}{d\partial x} + \frac{\partial \tau_{23}}{\partial z} = \rho_1 \frac{\partial^2 v_1}{\partial t^2}, \tag{6.3}$$

where

$$\tau_{12} = e^{\alpha_1(z+H_1)}\left[\mu_T^0 \frac{\partial v_1}{\partial x} + (\mu_L^0 - \mu_T^0)a_1\left(a_1\frac{\partial v_1}{\partial x} + a_3\frac{\partial v_1}{\partial z}\right)\right], \tag{6.4}$$

$$\tau_{23} = e^{\alpha_1(z+H_1)}\left[\mu_T^0 \frac{\partial v_1}{\partial z} + (\mu_L^0 - \mu_T^0)a_3\left(a_1\frac{\partial v_1}{\partial x} + a_3\frac{\partial v_1}{\partial z}\right)\right]. \tag{6.5}$$

In view of equations (6.4) and (6.5), equation (6.3) leads to

$$P\frac{\partial^2 v_1}{\partial z^2}+Q\frac{\partial^2 v_1}{\partial x^2}+R\frac{\partial^2 v_1}{\partial x\partial z}+\frac{\alpha_1 R}{2}\frac{\partial v_1}{\partial x}+\alpha_1 P\frac{\partial v_1}{\partial z}=\frac{1}{\beta_1^2}\frac{\partial^2 v_1}{\partial t^2}, \tag{6.6}$$

where

$P=1+\left(\frac{\mu_L^0}{\mu_T^0}-1\right)a_3^2$, $Q=1+\left(\frac{\mu_L^0}{\mu_T^0}-1\right)a_1^2$, $R=2a_1a_3\left(\frac{\mu_L^0}{\mu_T^0}-1\right)$, $\beta_1=\sqrt{\frac{\mu_T^0}{\rho_1^0}}$.

Let us assume the harmonic wave solution of the equation (6.6) in the form

$$v_1(x,z,t)=V_1(z)e^{ik(x-ct)}, \tag{6.7}$$

k being the wave number and c is the common wave velocity.

Substituing (6.7) in equation (6.6), we get

$$\frac{d^2V_1}{dz^2}+\left(\frac{ikR\alpha_1 P}{P}\right)\frac{dV_1}{dz}-\frac{1}{P}\left(Qk^2-\frac{ikR\alpha_1}{2}-\frac{c^2k^2}{\beta_1^2}\right)V_1=0. \tag{6.8}$$

The solution of (6.8) gives the expression for the non-vanishing displacement component of layer as

$$v_1(x,z,t)=e^{-\frac{\phi_1 z}{2}}(A_1\cos(Tz)+B_1\sin(Tz))e^{ik(x-ct)}, \tag{6.9}$$

where

$\phi_1=\frac{ikR+\alpha_1 P}{P}, T=\sqrt{\frac{c^2k^2}{\beta_1^2 P}-\frac{\alpha_1^2}{4}-\frac{Qk^2}{P}+\frac{k^2R^2}{4P^2}}$.

6.2.2 Dynamics of lower isotropic initially stressed half-space

The lowermost half-space is isotropic with horizontal initial stress (S_{11}). In view of equation (6.1), non-vanishing equation of motion for propagation of SH-wave in initially stressed isotropic half-space may be written as [18]

$$\frac{\partial\tau_{12}^*}{\partial x}+\frac{\partial\tau_{22}^*}{\partial y}+\frac{\partial\tau_{23}^*}{\partial z}-\frac{S_{11}\partial\omega_{21}}{2\partial x}=\rho_2\frac{\partial^2 v_1}{\partial t^2}, \tag{6.10}$$

where τ_{ij}^* are stress components, ω_{ij} are rotational components and ρ_2 is the density of the half-space. The components τ_{ij}^* of stress tensor of isotropic half-space used in (6.10) are:

$$\tau_{12}^* = \mu_2 \frac{\partial v_2}{\partial x},\ \tau_{22}^* = 0,\ \tau_{23}^* = \mu \frac{\partial v_2}{\partial z}, \tag{6.11}$$

Substituting (6.11) in (6.10), we obtain

$$\left(\mu_2 - \frac{S_{11}}{2}\right) \frac{\partial^2 v_2}{\partial x^2} = \mu_2 \frac{\partial^2 v_2}{\partial z^2} = \rho_2 \frac{\partial^2 v_2}{\partial t^2}. \tag{6.12}$$

Considering

$$v_2(x, z, t) = V_2(z) e^{ik(x-ct)}, \tag{6.13}$$

Using (6.13) in (6.12), we get

$$\frac{d^2 V_2}{dz^2} + k^2 \left[\frac{c^2}{\beta_2^2} + \xi - 1\right] V_2 = 0, \tag{6.14}$$

where

$\xi = \dfrac{S_{11}}{2\mu_2}$, $\beta_2 = \sqrt{\dfrac{\mu_2}{\rho_2}}$.

Equation (6.14) can be rewritten in the form,

$$\frac{d^2 V_2}{dz^2} - s^2 V_2 = 0, \tag{6.15}$$

where

$s^2 = k^2 \left(1 - \dfrac{c^2}{\beta_2^2} - \xi\right)$.

Keeping in mind that SH-wave dies out with increase in depth, the appropriate solution of (6.15) can be written as

$$V_2 = B_2 e^{-sz}, \tag{6.16}$$

which on substituting in (6.13) gives

$$v_2 = B_2 e^{-sz} e^{ik(x-ct)}. \tag{6.17}$$

6.3 Boundary conditions and dispersion relation

The boundary conditions at the stress free surface of heterogeneous fibre-reinforced composite layer and at the corrugated loosely bonded common interface between layer and half-space are as follows:

(i) Upper surface of the layer is traction free i.e.

$$\tau_{23} = 0 \text{ at } z = -H_1.$$

(ii) At the corrugated loosely bonded interface of layer and half-space,

$$\tau_{23} - g'\tau_{21} = ik\mu_2 \frac{\psi}{1-\psi}(v_1 - v_2) \text{ at } z = g(x),$$

where ψ is loosely bonded parameter.

(iii) Stresses are continuous at the corrugated loosely bonded interface between the layer and half-space i.e.,

$$\tau_{23} - g'\tau_{21} = \tau_{23}^* - g'\tau_{12}^* \text{ at } z = g(x),$$

g' is the derivative of g with respect to x.

Using equations (6.9) and (6.17) in the boundary conditions (i), (ii), (iii), we get

$$A_1(t_1\cos(TH_1) + t_2\sin(TH_1)) + B_1(-t_1\sin(TH_1 + t_2\cos(TH_1)) = 0, \tag{6.18}$$

$$e^{t_3 g+\alpha_1 H_1}(1-\psi)\mu_T^0[A_1(t_4\cos(Tg) - t_5\sin(Tg)) + B_1(t_4\sin(Tg) + t_5\cos(Tg))]$$

$$= ik\mu_2\psi[e^{-\phi_1 g/2}(A_1\cos(Tg) + B_1\sin(Tg)) - B_2 e^{-sg}], \tag{6.19}$$

$$B_2\mu_2(-s - g'ik)e^{-sg} = e^{t_3 g+\alpha_1 H_1}\mu_T^0[A_1(t_4\cos(Tg) - t_5\sin(Tg)) + B_1(t_4\sin(Tg) + t_5\cos(Tg))], \tag{6.20}$$

where

$$t_1 = \frac{R}{2}ik - \frac{\phi_1}{2}P,\ t_2 = PT,\ t_3 = \alpha_1 - \frac{\phi_1}{2},$$

$t_4 = \left(\frac{R}{2} - g'Q\right) ik - \frac{\phi_1}{2}\left(P - g'\frac{R}{2}\right)$, $t_5 = \left(P - g'\frac{R}{2}\right) T$.

Eliminating the arbitrary constants A_1, B_1, B_2 from equations (6.18), (6.19) and (6.20), we obtain

$$\tan[T(g + H_1)] = \frac{t_2 - \Omega(t_1 t_5 - t_2 t_4)}{t_1 - \Omega(t_1 t_4 - t_2 t_5)}, \tag{6.21}$$

where

$\Omega = e^{-t_3 g - \alpha_1 H_1 + \frac{\phi_1 g}{2}} \frac{\mu_T^0}{ik\mu_2\psi} \frac{ik\psi - (1-\psi)(s + g'ik)}{s + g'ik}$.

Equation (6.21) represents the dispersion relation for SH-wave propagation in a heterogeneous fibre-reinforced composite layer over an initially stressed isotropic elastic half-space with corrugated as well as loosely bonded common interface. It is worthy to be note that the dispersion relation depends on the wave number, anisotropy, loose bonding, reinforcement, heterogeneity parameter, initial stress and corrugation of the common interface ($z = g(x)$).

6.4 Particular cases

6.4.1 Case 1

When heterogeneity of the layer vanishes i.e. $\alpha_1 = 0$, the dispersion relation (6.21) reduces to

$$\tan\left[\sqrt{\frac{c^2k^2}{\beta_1^2 P} - \frac{Qk^2}{P} + \frac{k^2R^2}{4p^2}}(g + H_1)\right] = \frac{1 + \Omega^{(1)} t_4^{(1)}}{\Omega^{(1)} t_2^{(1)}}, \tag{6.22}$$

where

$\Omega^{(1)} = e^{\frac{ikRg}{P}} \frac{\mu_T}{ik\mu_2\psi} \frac{ik\psi - (1-\psi)(s + g'ik)}{s + g'ik}$, $t_2^{(1)} = P\sqrt{\frac{c^2k^2}{\beta_1^2 P} - \frac{Qk^2}{P} + \frac{k^2R^2}{4P^2}}$,

$t_4^{(1)} = \left(\frac{R}{2} - g'Q\right) ik - \frac{ikR}{2P}\left(P - \frac{g'R}{2}\right)$.

Equation (6.22) is the dispersion equation for homogeneous fibre-reinforced composite layer lying over an initially stressed isotropic elastic half-space with corrugated

and loosely bonded interface.

6.4.2 Case 2

When heterogeneity of the layer and initial stress acting in the half-space vanishes i.e. S_{11} and $\alpha_1 = 0$, the dispersion relation (6.21) takes the form

$$\tan\left[\sqrt{\frac{c^2k^2}{\beta_1^2 P} - \frac{Qk^2}{P} + \frac{k^2R^2}{4p^2}}(g + H_1)\right] = \frac{1 + \Omega^{(2)}t_4^{(1)}}{\Omega^{(2)}t_2^{(1)}}, \tag{6.23}$$

where

$$\Omega^{(2)} = e^{\frac{ikRg}{P}}\frac{\mu_T}{ik\mu_2\psi}\frac{i\psi - (1-\psi)\left(\sqrt{1 - \frac{c^2}{\beta_2^2}} + g'i\right)}{\sqrt{1 - \frac{c^2}{\beta_2^2}} + g'ik}.$$

Equation (6.23) is the dispersion equation for homogeneous fibre-reinforced composite layer lying over an isotropic elastic half-space without initial stress having corrugated and loosely bonded interface.

6.5.3 Case 3

When the layer is without reinforcement as well as heterogeneity and initial stress acting in the half-space vanishes i.e. $S_{11} = 0, \alpha_1 = 0$ and $\mu_L = \mu_T$, the dispersion relation (6.21) takes the form

$$\tan\left[k\sqrt{\frac{c^2}{\beta_1^2} - 1}(g + H_1)\right] = \frac{1 - \Omega^{(3)}g'ik}{\Omega^{(3)}k\sqrt{\frac{c^2}{\beta_1^2} - 1}}, \tag{6.24}$$

where

$$\Omega^{(3)} = -\frac{\mu_T}{ik\mu_2\psi}\frac{i\psi - (1-\psi)\left(\sqrt{1 - \frac{c^2}{\beta_2^2}} + g'i\right)}{\sqrt{1 - \frac{c^2}{\beta_2^2}} + g'ik}.$$

Equation (6.24) represents the dispersion equation for an isotropic elastic layer lying over an isotropic elastic half-space without initial stress and having corrugated as well as loosely bonded common interface.

6.4.4 Case 4

When the layer is without reinforcement, as well as heterogeneity and initial stress acting in the half space vanishes and the mediums are under welded contact (perfectly bonded) i.e. $S_{11} = 0, \alpha_1 = 0, \mu_L = \mu_T$ and $\psi = 0$, the dispersion relation (6.21) reduces to

$$\tan\left[k\sqrt{\frac{c^2}{\beta_1^2} - 1}(g + H_1)\right] = \frac{1 - \Omega^{(4)} g' ik}{\Omega^{(4)} k\sqrt{\frac{c^2}{\beta_1^2} - 1}}, \tag{6.25}$$

where

$$\Omega^{(4)} = \frac{\mu_T}{k\mu_2} \frac{1}{\sqrt{1 - \frac{c^2}{\beta_2^2}} + g' ik}.$$

Equation (6.25) represents the dispersion equation for an isotropic layer lying over an isotropic elastic half-space without initial stress having corrugated and welded common interface.

6.4.5 Case 5

When the layer is without reinforcement as well as heterogeneity and initial stress acting in the half-space vanishes and also both the mediums are under welded contact with planar common interface i.e. $S_{11} = 0, \alpha_1 = 0, \mu_L = \mu_T, \psi = 0$ and $g = 0$, the dispersion relation (6.21) reduces to

$$\tan\left[kH_1\sqrt{\frac{c^2}{\beta_1^2} - 1}\right] = \frac{\mu_2}{\mu_T} \frac{\sqrt{1 - \frac{c^2}{\beta_2^2}}}{\sqrt{\frac{c^2}{\beta_1^2} - 1}}, \tag{6.26}$$

which is the classical Love wave equation [52].

6.5 Numerical results and discussion

We perform numerical computation in order to study the effect of reinforcement, anisotropy, horizontal initial stress, heterogeneity, bonding parameter, corrugation, position parameter and undulatory parameter on the phase velocity of SH-wave propagating in a heterogeneous fibre-reinforced composite layer lying over an initially stressed isotropic elastic half-space with corrugated and loosely bonded interface. The following material constants have been considered in this context:

For the heterogeneous fibre-reinforced composite layer [83]

$\mu_L^0 = 7.07 \times 10^9\ N/m^2$, $\mu_T^0 = 3.50 \times 10^9\ N/m^2$, $\rho_1^0 = 1600\ kg/m^3$, $a_1 = 0.00316227$, $a_3 = 0.999995$.

For the isotropic elastic half-space under initial stress [62]

$\mu_2 = 32.3 \times 10^9\ N/m^2, \rho_2 = 2802\ kg/m^3$.

For the sake of comparative study of the considered model to that of the case when SH-wave propagates in an isotropic heterogeneous layer over an initially stressed half-space, we take $a_1 = 0, a_3 = 0$.

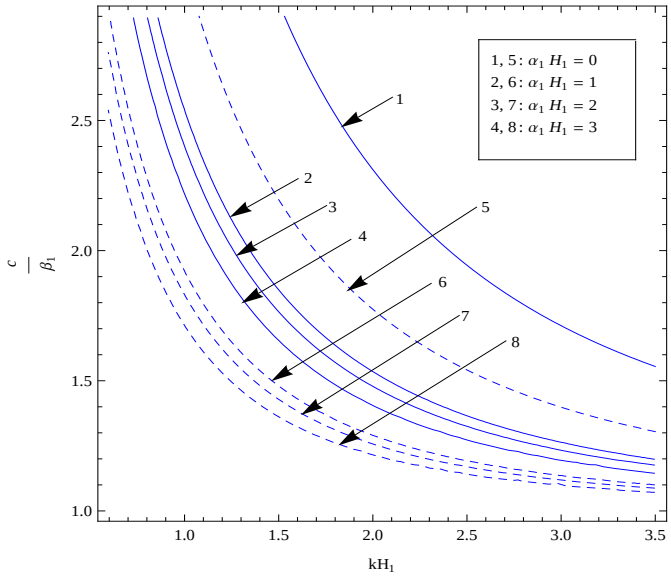

Figure 6.2: Variation of phase velocity (c/β_1) against wave number (kH_1) for different values of heterogeneity parameter (αH_1) when $\xi = 0.2, \psi = 0.2, ab = 0.1, bH_1 = 1.4, x/H_1 = 0.04$.

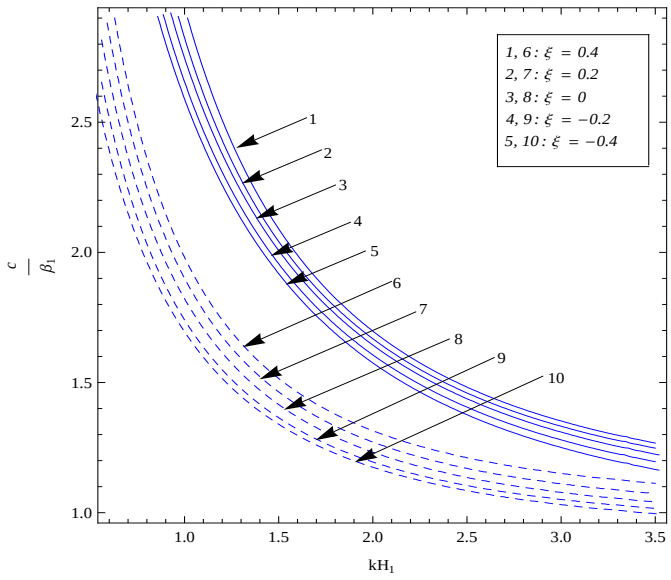

Figure 6.3: Variation of phase velocity (c/β_1) against wave number (kH_1) for different values of horizontal initial stress (ξ) when $\alpha_1 H_1 = 1, \psi = 0.2, ab = 0.1, bH_1 = 1.4, x/H_1 = 0.04$.

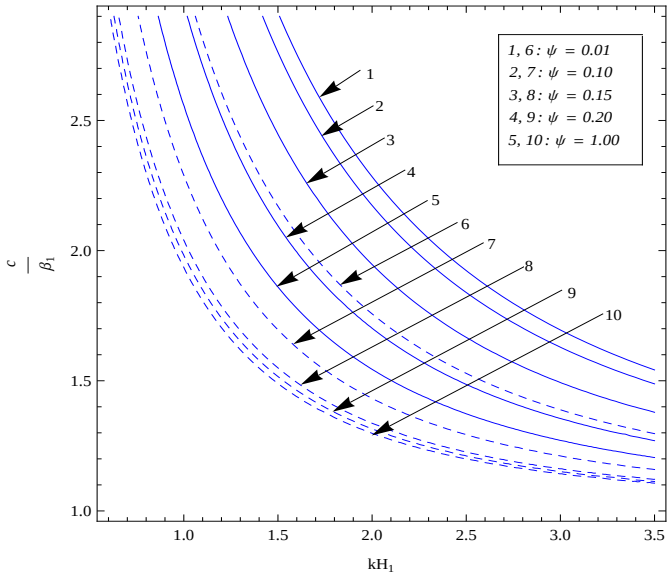

Figure 6.4: Variation of phase velocity (c/β_1) against wave number (kH_1) for different values of bonding parameter (ψ) when $\xi = 0.2, \alpha_1 H_1 = 1, \xi = 0.2, ab = 0.1, bH_1 = 1.4, x/H_1 = 0.04$.

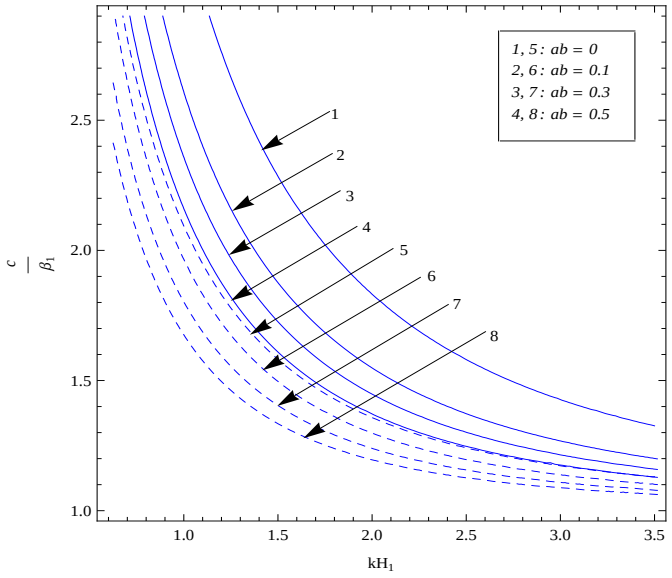

Figure 6.5: Variation of phase velocity (c/β_1) against wave number (kH_1) for different values of corrugation parameter (ab) when $\xi = 0.2, \alpha_1 H_1 = 1, \xi = 0.2, \psi = 0.2, bH_1 = 1.4, x/H_1 = 0.04$.

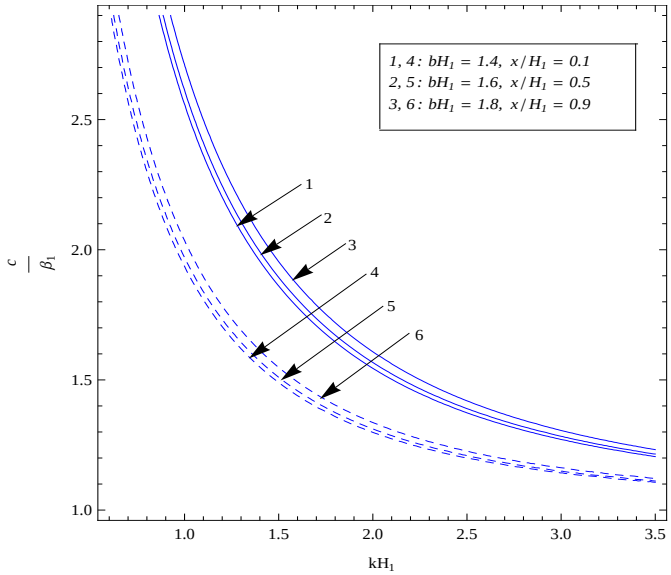

Figure 6.6: Variation of phase velocity (c/β_1) against wave number (kH_1) for different values of undulatory parameter (bH_1) when $\alpha H_1 = 1, \xi = 0.2, \psi = 0.2, ab = 0.1, x/H_1 = 0.04$.

In Figs. (6.2) to (6.6), curves have been plotted with a view to exhibit the effect of heterogeneity, initial stress, bonding parameter and corrugation on the dispersion curve i.e. variation of phase velocity against wave number. In each of the figures, comparison has been made between the cases when the upper layer is reinforced (anisotropic) to the case when upper layer is reinforced free (isotropic). It has been observed through meticulous observation of all the figures that the phase velocity of SH-wave decreases with increase in wave number. Moreover, an overview of all the figures establish that the curves corresponding to the reinforced case lie above the curves corresponding to reinforced free case i.e. presence of reinforcement in the upper layer supports more to phase velocity as compared to the case of absence of reinforcement in the layer.

Fig. (6.2) shows the influence of heterogeneity on the phase velocity of SH-wave. Curves 1 and 5 in the concerned figure depict the case when there is no heterogeneity in the layer i.e. the SH-wave is propagating in a homogeneous layer lying over an

initially stressed half-space. It can be marked from the figure that phase velocity of SH-wave decreases with increase in heterogeneity of layer for both reinforced and reinforced free cases. In addition to this, it can be quoted that homogeneity of the layer supports more to phase velocity as compared to heterogeneity of layer i.e. the presence of heterogeneity in the layer resists the phase velocity of SH-wave propagating through it in comparison to a homogeneous layer. The phase velocity of SH-wave is found to be very high when the layer is homogeneous and reinforced than that of homogeneous/heterogeneous and reinforced free case or heterogeneous and reinforced case.

Fig. (6.3) represents the effect of horizontal initial stress on the phase velocity of SH-wave. Curves 1, 2, 6 and 7 in the figure correspond to the case when half-space is under horizontal compressive initial stress; curves 3 and 8 represent the dispersion curve corresponding to the case when half-space is without initial stress; and curves 4, 9, 5 and 10 correspond to the case when half-space is under horizontal tensile initial stress. It has been notified that phase velocity of SH-wave increases with increase in horizontal initial stress for both reinforced and reinforced free cases. More precisely, phase velocity of SH-wave increases with increase in horizontal compressive initial stress whereas it decreases with increase in horizontal tensile initial stress. The effect of horizontal initial stress acting in the half-space is found to be more on the dispersion curve corresponding to the case of reinforced free layer as compared to the case of reinforced layer.

Fig. (6.4) delineates the effect of bonding parameter on the dispersion curve. Curves 1 and 6 in the figure particularize the state when layer and half-space are almost under smooth contact, curves 2, 3, 4, 7, 8 and 9 indicate that the mediums

are loosely bonded and curves 5 and 10 depict that they are under welded contact. This figure manifests that the phase velocity of SH-wave decreases with increase in the magnitude of bonding parameter for both reinforced and reinforced free cases. Moreover, it has been noticed that lower magnitude of bonding parameter significantly affects the dispersion curve as compared to higher magnitude of bonding parameter. Further, effect of bonding parameter on the curves corresponding to reinforced case is more prominent than that of the curves corresponding to reinforced free case. The phase velocity is found to be in its peak when layer and half-space are under smooth contact and at its bottom when they are under welded contact for both reinforced and reinforced free cases.

The effect of corrugation existing at the interface of layer and half-space on phase velocity of SH-wave has been shown in Fig. (6.5). Curves 1 and 5 in Fig. (6.5) represent the dispersion curve for the case when interface of layer and half-space is not corrugated but planar. The figure interprets that phase velocity decreases with increase in corrugation parameter of the interface of layer and half-space for both reinforced and reinforced free cases. The influence of non-corrugated interface on the phase velocity of SH-wave for reinforced case is more pronounced than that of the reinforced free case. More specifically, the phase velocity of SH-wave seems to be high when the interface of layer and half-space is planar whereas corrugated interface of the layer and half-space acts as hindrance to the phase velocity of SH-wave.

Fig. (6.6) unravels the effect of undulation parameter along with position parameter on the dispersion curve. The figure exhibits that undulation at the interface of the mediums support phase velocity for both reinforced and reinforced free cases. In other words, the phase velocity of SH-wave increases with increase in undulation

parameter along with position parameter for both reinforced and reinforced free cases.

Meticulous examination of all figures establish that lower magnitude of bonding parameter associated with the interface of layer and half-space has the most significant effect on dispersion curve as compared to all other affecting parameters; whereas effect of undulation along with position parameter is the least on it.

6.6 Conclusion

The current study deals with the propagation of SH-wave in a heterogeneous fibre-reinforced composite layer lying over an initially stressed isotropic elastic half-space with corrugated and loosely bonded common interface. The dispersion relation has been found analytically in closed form. The effect of presence and absence of corrugation and loose bonding at common surface on the dispersion curves have been meticulously examined. Moreover, the substantial effects of anisotropy, reinforcement, heterogeneity, initial stress, corrugation, undulation parameter and position parameter on phase velocity of SH-wave have been traced out through numerical computation and graphical demonstration. Comparative study is also performed to compared reinforced case with reinforced free case, heterogeneous case with homogeneous case and loosely bonded corrugated interface case with perfectly bonded planar interface case. The upshots of the current study are summarized as follows:

- The phase velocity decreases with increase of wave number for both reinforced composite (anisotropic) and reinforced free (isotropic) case.

- The phase velocity is always more for the case when layer is reinforced composite (anisotropic) as compared to the case when layer is reinforced free (isotropic).

- The phase velocity of SH-wave decreases as heterogeneity grows in the layer for both cases when the layer is reinforced and reinforced free.

- Phase velocity increases with increase in horizontal compressive initial stress whereas phase velocity decrease with increase in horizontal tensile initial stress acting in the half-space for both cases when the layer is reinforced (anisotropic) and reinforced free (isotropic).

- The dispersion curve shifts downward as the magnitude of bonding parameter increases at the interface i.e. phase velocity decreases with increase in the magnitude of bonding parameter for both cases when the layer is reinforced (anisotropic) and reinforced free (isotropic).

- Phase velocity decreases with increase in corrugation parameter of the interface of the mediums for both reinforced (anisotropic) and reinforced free (anisotropic) layer.

- With increase in position parameter along with undulatory parameter, the phase velocity increases.

- The effect of lower magnitude of bonding parameter on dispersion curve has been found to be most significant and effect of undulation along with position parameter is the least significant as compared to all other affecting parameters.

- As a particular case of the problem, the obtained dispersion relation is found to be in well-agreement to the classical Love wave equation.

Nowadays, composite materials are among the basic requirements of large scale architectural designs and constructions. Therefore, the present problem may find its worthy applications in the field of construction, space, aviation, geophysics, geomechanics, retaining structures, embankments to subgrade stabilization beneath footings and pavements, etc. The presence of reinforcement, anisotropy, initial stress, heterogeneity and corrugation in a material medium significantly affects the propagation of elastic waves through them. Moreover, the chapter concludes that a mild change in the nature of bonding between two mediums bearing different properties may be responsible for a pronounced effect on phase velocity of the elastic wave propagating through it. Non-destructive testing may also be a great application of the present problem.

Bibliography

[1] Abd-Alla, A. M. and Ahmed, S. M. [1996], 'Rayleigh waves in an orthotropic thermoelastic medium under gravity field and initial stress', *Earth, Moon, and Planets* **75**(3), 185–197.

[2] Abd-Alla, A. M. and Ahmed, S. M. [2003], 'Stonley and rayleigh waves in a non-homogeneous orthotropic elastic medium under the influence of gravity', *Applied Mathematics and Computation* **135**, 187–200.

[3] Achenbach, J. D. [1969], 'Free vibrations of a layer of micropolar continuum', *International Journal of Engineering Science* **7**(10), 1025–1040.

[4] Achenbach, J. D. [1976], *Wave Propagation in Elastic Solids*, North Holland Publication Company, New York.

[5] Achenbach, J. D., Keshava, S. P. and Herrmann, G. [1967], 'Moving load on a plate resting on an elastic half space', *Journal of Applied Mechanics* **34**(4), 910–914.

[6] Adkins, J. E. [1956], 'Finite plane deformation of thin elastic sheets reinforced with inextensible cords', *Philosophical Transactions of the Royal Society of London A: Mathematical, Physical and Engineering Sciences* **249**(961), 125–150.

[7] Adkins, J. E. and Rivlin, R. S. [1955], 'Large elastic deformations of isotropic materials x. reinforcement by inextensible cords', *Philosophical Transactions of the Royal Society of London A: Mathematical, Physical and Engineering Sciences* **248**(944), 201–223.

[8] Aero, E. L. and Kuvshinskii, E. V. [1961], 'Fundamental equations of the theory

of elastic media with rotationally interacting particles', *Soviet Physics-Solid State* **2**(7), 1272–1281.

[9] Aki, K. and Richards, P. G. [1980], 'Quantitative seismology', *Theory and Methods* **1**, 557.

[10] Alekseyeva, L. A. [2007], 'The dynamics of an elastic half-space under the action of a moving load', *Journal of Applied Mathematics and Mechanics* **71**(4), 511–518.

[11] Altenbach, H. and Eremeyev, V. A. [2014], 'Strain rate tensors and constitutive equations of inelastic micropolar materials', *International Journal of Plasticity* **63**, 3–17.

[12] Anderson, W. B. and Lakes, R. S. [1994], 'Size effects due to cosserat elasticity and surface damage in closed-cell polymethacrylimide foam', *Journal of Materials Science* **29**(24), 6413–6419.

[13] Asano, S. [1966], 'Reflection and refraction of elastic waves at a corrugated interface', *Bulletin of the Seismological Society of America* **56**(1), 201–221.

[14] Belfield, A. J., Rogers, T. G. and Spencer, A. J. M. [1983], 'Stress in elastic plates reinforced by fibres lying in concentric circles', *Journal of the Mechanics and Physics of Solids* **31**(1), 25–54.

[15] Biot, M. A. [1955], 'Theory of elasticity and consolidation for a porous anisotropic solid', *Journal of Applied Physics* **26**(2), 182–185.

[16] Biot, M. A. [1956], 'Theory of deformation of a porous viscoelastic anisotropic solid', *Journal of Applied Physics* **27**, 459.

[17] Biot, M. A. [1962], 'Mechanics of deformation and acoustic propagation in porous media', *Journal of Applied Physics* **33**, 1482.

[18] Biot, M. A. [1965], *Mechanics of Incremental Deformation*, Wiley, New York.

[19] Bose, S. K. [1962], 'Wave propagation in marine sediments and water saturated soils', *Pure and applied geophysics* **52**, 27–40.

[20] Brekhovskikh, L. M. [1960], *Waves in Layered Media*, Academic Press, New York.

[21] Bromwich, T. J. [1898], 'On the influence of gravity on elastic waves, and, in particular on the vibrations of an elastic globe', *Proceedings of the London Mathematical Society* **1**(1), 98–120.

[22] Burridge, R. and Vargas, C. A. [1979], 'The fundamental solution in dynamic poro-elasticity', *Geophysical Journal of the Royal Astronomical Society* **58**, 61–90.

[23] Červenỳ, V. [2004], 'Inhomogeneous harmonic plane waves in viscoelastic anisotropic media', *Studia geophysica et geodaetica* **48**(1), 167–186.

[24] Chattopadhyay, A. and Choudhury, S. [1990], 'Propagation, reflection and transmission of magnetoelastic shear waves in a self-reinforced medium', *International Journal of Engineering Science* **28**(6), 485–495.

[25] Chattopadhyay, A. and Choudhury, S. [1995], 'Magnetoelastic shear waves in an infinite self-reinforced plate', *International journal for numerical and analytical methods in geomechanics* **19**(4), 289–304.

[26] Chattopadhyay, A., Gupta, S., Sahu, S. A. and Singh, A. K. [2011], 'Dispersion equation of magnetoelastic shear waves in irregular monoclinic layer', *Applied mathematics and mechanics* **32**(5), 571–586.

[27] Chattopadhyay, A., Gupta, S., Sahu, S. A. and Singh, A. K. [2012], 'Dispersion of horizontally polarized shear waves in an irregular non-homogeneous self-reinforced crustal layer over a semi-infinite self-reinforced medium', *Journal of Vibration and Control* p. doi.1077546311430699.

[28] Chattopadhyay, A., Gupta, S., Sharma, V. K. and Kumari, P. [2011], 'Stresses produced on a rough irregular half-space by a moving load', *Acta mechanica* **221**(3-4), 271–280.

[29] Chattopadhyay, A., Gupta, S. and Singh, A. K. [2010], 'The dispersion of shear wave in multilayered magnetoelastic self-reinforced media', *International Journal of Solids and Structures* **47**(9), 1317–1324.

[30] Chattopadhyay, A. and Saha, S. [2006], 'Dynamic response of normal moving load in the plane of symmetry of a monoclinic half-space', *Tamkang Journal of Science and Engineering* **9**(4), 307–312.

[31] Chattopadhyay, A., Sahu, S. A. and Singh, A. K. [2013], 'Dispersion of sh waves in an irregular non homogeneous self-reinforced crustal layer over a semi-infinite self-reinforced medium', *Journal of Vibration and Control* **19**, 109–119.

[32] Chattopadhyay, A. and Venkateswarlu, R. L. K. [1998], 'Stresses produced in a fibre-reinforced half space due to moving load', *Bulletin of Calcutta Mathematical Society* **90**, 337–342.

[33] Chaudhary, S., Kauhsik, V. P. and Tomar, S. K. [2006], 'Plane sh-wave response from elastic slab interposed between two different self-reinforced elastic solids', *Applied Mechanics and Engineering* **11**(4), 787.

[34] Chaudhary, S., Kaushik, V. P. and Tomar, S. K. [2005], 'Transmission of shear waves through a self-reinforced layer sandwiched between two inhomogeneous viscoelastic half-spaces', *International journal of mechanical sciences* **47**(9), 1455–1472.

[35] Chonan, S. [1976], 'Moving load on a pre-stressed plate resting on a fluid half-space', *Ingenieur-Archiv* **45**(3), 171–178.

[36] Cole, J. and Huth, J. [1958], 'Stresses produced in a half plane by moving loads', *Journal of Applied Mechanics* **25**, 433–436.

[37] Cooper Jr, H. F. [1967], 'Reflection and transmission of oblique plane waves at a plane interface between viscoelastic media', *The Journal of the Acoustical Society of America* **42**(5), 1064–1069.

[38] Cosserat, E. and Cosserat, F. [1909], 'The'orie des corps deformables', *Hermann, Paris* .

[39] Das, S. C., Acharya, D. P. and Sengupta, P. R. [1992], 'Surface waves in an inhomogeneous elastic medium under the influence of gravity', *Revue roumaine des sciences techniques. Série de mécanique appliquée* **37**(5), 539–551.

[40] Datta, B. K. [1986], 'Some observations on interactions of rayleigh waves in an elastic solid medium with the gravity field', *Revue roumaine des sciences techniques. Série de mécanique appliquée* **31**(4), 369–374.

[41] De, S. N. and Sen-Gupta, P. R. [1974], 'Influence of gravity on wave propagation in an elastic layer', *The Journal of the Acoustical Society of America* **55**(5), 919–921.

[42] De, S. N. and Sengupta, P. R. [1973], 'Plane lambs problem under the influence of gravity', *Gerlands Beitr. Geophys* **82**, 421–426.

[43] De, S. N. and Sengupta, P. R. [1976], 'Surface waves under the influence of gravity', *Gerlands Beitr. Geophys* **85**, 311–318.

[44] Eringen, A. C. [1962], *Nonlinear theory of continuous media*, McGraw-Hill, New York.

[45] Eringen, A. C. [1964], 'Simple microfluids', *International Journal of Engineering Science* **2**(2), 205–217.

[46] Eringen, A. C. [1966], 'Linear theory of micropolar elasticity', *Journal of Mathematics and Mechanics* **15**, 909–923.

[47] Eringen, A. C. [1978], *Micropolar theory of liquid crystals. Liquid Crystals and Ordered Fluids*, Vol. 3, Plenum Press, New York.

[48] Eringen, A. C. [1980], *Mechanics of Continua*, 2nd ed. krieger edn, Melbourne, Florida.

[49] Eringen, A. C. [1990], 'Theory of thermo-microstretch elastic solids', *International Journal of Engineering Science* **28**(12), 1291–1301.

[50] Eringen, A. C. [2001], *Microcontinuum Field Theories, Fluent Media*, Springer-Verlag, New York.

[51] Eringen, A. C. and Suhubi, E. S. [1964], 'Nonlinear theory of simple micro-elastic solidsi', *International Journal of Engineering Science* **2**(2), 189–203.

[52] Ewing, W. M., Jardetsky, W. S. and Press, F. [1957], *Elastic Waves in Layered Media*, McGraw-Hill, New York.

[53] Fan, H. and Sze, K. Y. [2001], 'A micro-mechanics model for imperfect interface in dielectric materials', *Mechanics of Materials* **33**(6), 363–370.

[54] Fatemi, J., Keulen, F. V. and Onck, P. R. [2002], 'Generalized continuum theories: Application to stress analysis in bone', *Meccanica* **37**(4-5), 385–396.

[55] Galilei, G. [1638], *Dialogues Concerning Two New Sciences*, number ISBN 0-486-60099-8, crew, henry; de salvio, alfonso, eds. edn, Dover Publications, New York.

[56] Gauthier, R. D. [1982], 'Experimental investigations on micropolar media', *Mechanics of micropolar media* pp. 395–463.

[57] Ghosh, B. C. [1985], 'Steady-response of moving loads in the micropolar solid media', **51**(3), 586–597.

[58] Ghosh, N. C., Nath, S. and Debnath, L. [2001], 'Propagation of waves in micropolar solid-solid semispaces in the presence of a compressional wave source in the upper solid substratum', *Mathematical and computer modelling* **34**(5), 557–563.

[59] Gogna, M. L. and Chander, S. [1985], 'Reflection and transmission of sh-waves at an interface between anisotropic inhomogeneous elastic and viscoelastic half-spaces', *Acta Geophys. Pol* **33**(4), 357–375.

[60] Graff, K. F. [1991], *Wave Motion Elastic Solids*, (Oxford engineering science series), Dover Publications; New ed., New York.

[61] Grioli, G. [1960], 'Elasticità asimmetrica', *Annali di matematica pura ed applicata* **50**(1), 389–417.

[62] Gubbins, D. [1990], *Seismology and plate tectonics*, Cambridge University Press.

[63] Günther, W. [1958], 'Zur statik und kinematik des cosseratschen kontinuums', *Abh. Braunschweig. Wiss. Ges* **10**(213), 1.

[64] Gupta, S., Majhi, D. K., Kundu, S. and Vishwakarma, S. K. [2013], 'Propagation of love waves in non-homogeneous substratum over initially stressed heterogeneous half-space', *Applied Mathematics and Mechanics* **34**(2), 249–258.

[65] Hashin, Z. and Rosen, B. W. [1964], 'The elastic moduli of fiber-reinforced materials', *Journal of Applied Mechanics* **31**(2), 223–232.

[66] Ieşan, D. [1981], 'Some applications of micropolar mechanics to earthquake problems', *International Journal of Engineering Science* **19**(6), 855–864.

[67] Jones, J. P. and Whittier, J. S. [1967], 'Waves at a flexibly bonded interface', *Journal of Applied Mechanics* **34**(4), 905–909.

[68] Kanai, K. [1950], 'The effect of solid viscosity of surface layer on the earthquake movements', *Bulletin of the Earthquake Research Institute* **28**, 31.

[69] Kaur, J. and Tomar, S. K. [2004], 'Reflection and refraction of sh-waves at a corrugated interface between two monoclinic elastic half-spaces', *International journal for numerical and analytical methods in geomechanics* **28**(15), 1543–1575.

[70] Kaur, J., Tomar, S. K. and Kaushik, V. P. [2005], 'Reflection and refraction of sh-waves at a corrugated interface between two laterally and vertically heterogeneous viscoelastic solid half-spaces', *International Journal of Solids and Structures* **42**(13), 3621–3643.

[71] Kaushik, V. P. and Chopra, S. D. [1983], 'Reflection and transmission of general plane sh-waves at the plane interface between two heterogeneous and homogeneous viscoelastic media', *Geophys. Res. Bull* **20**, 1–20.

[72] Khoshgoftar, M., Najarian, S., Farmanzad, F., Vahidi, B. and Ghomshe, F. T. [2007], 'A biomechanical composite model to determine effective elastic moduli of the cns gray matter', *American Journal of Applied Sciences* **4**(11), 918–924.

[73] Khurana, P. and Vashisth, A. K. [2001], 'Love wave propagation in a pre-stressed medium', *Indian Journal of Pure and Applied Mathematics* **32**(8), 1201–1208.

[74] Koiter, W. T. [1964], 'Couple-stresses in the linear theory of elasticity', *Proceedings KoninKlije Nederlandse Akademie van Wetenshappen* **67**(17-29), 30–44.

[75] Kumar, R. and Deswal, S. [2000], 'Steady-state response of a micropolar generalized thermoelastic half-space to the moving mechanical/thermal loads', **110**(4), 449–465.

[76] Kumar, R. and Gogna, M. L. [1992], 'Steady-state response to moving loads in micropolar elastic medium with stretch', *International journal of engineering science* **30**(6), 811–820.

[77] Kumar, S., Sharma, J. N. and Sharma, Y. D. [2011], 'Generalized thermoelastic waves in microstretch plates loaded with fluid of varying temperature', *International Journal of Applied Mechanics* **3**(03), 563–586.

[78] Lavrentyev, A. I. and Rokhlin, S. I. [1998], 'Ultrasonic spectroscopy of imperfect contact interfaces between a layer and two solids', *The Journal of the Acoustical Society of America* **103**(2), 657–664.

[79] Lee, H. P. and Ng, T. Y. [1994], 'Dynamic response of a cracked beam subject to a moving load', *Acta mechanica* **106**(3-4), 221–230.

[80] Li, P. and Jin, F. [2015], 'Excitation and propagation of shear horizontal waves in a piezoelectric layer imperfectly bonded to a metal or elastic substrate', *Acta Mechanica* **226**(2), 267–284.

[81] Love, A. E. H. [1911], *Some problems of Geodynamics*, Cambridge University Press, London.

[82] Love, A. E. H. [2013], *A treatise on the mathematical theory of elasticity*, Vol. 1, Cambridge University Press, New York.

[83] Markham, M. F. [1969], 'Measurement of the elastic constants of fibre composites by ultrasonics', *Composites* **1**(2), 145–149.

[84] Maugin, G. A. [1981], 'Wave motion in magnetisable deformable solids', *International Journal of Engineering Science* **19**(3), 321–388.

[85] Meissner, R. [2002], *The little book of planet earth*, Springer-Verlag, New York.

[86] Miles, J. W. [1966], 'Response of a layered half-space to a moving load', *Journal of Applied Mechanics* **33**(3), 680–681.

[87] Mindlin, R. D. and Tiersten, H. F. [1962], 'Effects of couple-stresses in linear elasticity', *Archive for Rational Mechanics and Analysis* **11**(1), 415–448.

[88] Mukherjee, S. [1969], 'Stresses produced by a load moving over the rough boundary of a semi-infinite transversely isotropic solid', *Pure and Applied Geophysics* **72**(1), 45–50.

[89] Mukhopadhyay, A. [1965], 'Stresses produced by a normal load moving over a transversely isotropic layer of ice lying on a rigid foundation', *pure and applied geophysics* **60**(1), 29–41.

[90] Murty, G. S. [1975], 'A theoretical model for the attenuation and dispersion of stoneley waves at the loosely bonded interface of elastic half spaces', *Physics of the Earth and Planetary Interiors* **11**(1), 65–79.

[91] Nandal, J. S. and Saini, T. N. [2013], 'Reflection and refraction at an imperfectly bonded interface between poroelastic solid and cracked elastic solid', *Journal of seismology* **17**(2), 239–253.

[92] Nayfeh, A. H. and Nassar, E. A. M. [1978], 'Simulation of the influence of bonding materials on the dynamic behavior of laminated composites', *Journal of Applied Mechanics* **45**(4), 822–828.

[93] Nowacki, W. [1974], 'Micropolar elasticity', *International Center for Mechanical Sciences* **Courses and Lectures No. 151,**. Udine, Springer-Verlag, Wien-New York.

[94] Olsson, M. [1991], 'On the fundamental moving load problem', *Journal of Sound and Vibration* **145**(2), 299–307.

[95] Pabst, W. [2005], 'Micropolar materials', *Ceramics- Silikaty* **49**(3), 170–180.

[96] Palmov, V. A. [1964], 'Basic equations of the theory of asymmetric elasticity', *Prikladnaya Matematika i Mekhanika* **28**, 401–408.

[97] Park, H. C. and Lakes, R. S. [1986], 'Cosserat micromechanics of human bone: strain redistribution by a hydration sensitive constituent', *Journal of biomechanics* **19**(5), 385–397.

[98] Pradhan, A., Samal, S. and Mahanti, N. [2003], 'Influence of anisotropy on the love waves in a self-reinforced medium', *Tamkang Journal of Science and Engineering* **6**(3), 173–178.

[99] Prakash, J., Ogulu, A. and Zhandire, E. [2008], 'Mhd free convection and mass transfer flow of a micro-polar thermally radiating and reacting fluid with time dependent suction', *Indian Journal of Pure and Applied Physics* **46**, 679–684.

[100] Rajagopal, E. S. [1960], 'The existence of interfacial couples in infinitesimal elasticity', *Annalen der Physik* **461**(3-4), 192–201.

[101] Ravindra, R. [1968], 'Usual assumptions in the treatment of wave propagation in heterogeneous elastic media', *pure and applied geophysics* **70**(1), 12–17.

[102] Rayleigh, L. [1885], 'On waves propagation on the plane surface of an elastic solid', *Proceedings of the London Mathematical Society* **17**, 4–11.

[103] Romeo, M. [2003], 'Interfacial viscoelastic sh waves', *International journal of solids and structures* **40**(9), 2057–2068.

[104] Roy, A. [2008], Sh-wave propagation in laterally heterogeneous medium, *in* 'Vibration Problems ICOVP-2007', Springer, pp. 335–338.

[105] Sackman, J. L. [1961], 'Uniformly moving load on a layered half plane', *Journal of the Engineering Mechanics Division* **87**(4), 75–90.

[106] Sahu, A. R. [1995], The effects of resisting media and other rotating beam parameter changes on the fundamental frequency of bending vibrations, *in* 'Computational Mechanics 95', Springer, pp. 1274–1278.

[107] Sahu, A. R. [2001], 'Theoretical frequency equation of bending vibrations of an exponentially tapered beam under rotation', *Journal of Vibration and Control* **7**(6), 775–780.

[108] Sahu, S. A., Saroj, P. K. and Dewangan, N. [2014], 'Sh-waves in viscoelastic heterogeneous layer over half-space with self-weight', *Archive of Applied Mechanics* **84**(2), 235–245.

[109] Schoenberg, M. [1971], 'Transmission and reflection of plane waves at an elastic-viscoelastic interface', *Geophysical Journal International* **25**(1-3), 35–47.

[110] Selim, M. M. [2007], 'Static deformation of an irregular initially stressed medium', *Applied mathematics and computation* **188**(2), 1274–1284.

[111] Sengupta, P. R. and Acharya, D. [1979], 'The influence of gravity on the propagation of waves in a thermoelastic layer', *Revue Roumaine des Sciences Techniques - Srie de Mcanique Applique* **24**, 395–406.

[112] Shariat, B. A. S. and Eslami, M. R. [2006], 'Thermal buckling of imperfect functionally graded plates', *International Journal of Solids and Structures* **43**(14), 4082–4096.

[113] Sharma, J. N. and Kumar, S. [2009], 'Lamb waves in micropolar thermoelastic solid plates immersed in liquid with varying temperature', *Meccanica* **44**(3), 305–319.

[114] Sharma, J. N., Kumar, S. and Sharma, Y. D. [2007], 'Propagation of rayleigh surface waves in microstretch thermoelastic continua under inviscid fluid loadings', *Journal of Thermal Stresses* **31**(1), 18–39.

[115] Sharma, J. N. and Pathania, V. [2003], 'Generalized thermoelastic lamb waves in a plate bordered with layers of inviscid liquid', *Journal of sound and vibration* **268**(5), 897–916.

[116] Sharma, J. N. and Pathania, V. [2005], 'Propagation of leaky surface waves in thermoelastic solids due to inviscid fluid loadings', *Journal of Thermal Stresses* **28**(5), 485–519.

[117] Sharma, K. and Bhargava, R. R. [2014], 'Propagation of thermoelastic plane waves at an imperfect boundary of thermal conducting viscous liquid/generalized thermoelastic solid', *Afrika Matematika* **25**(1), 81–102.

[118] Sharma, K., Sharma, S. and Bhargava, R. R. [2013], 'Propagation of waves in micropolar thermoelastic solid with two temperatures bordered with layers or half-spaces of inviscid liquid', *Materials Physics and Mechanics* **16**, 66–81.

[119] Sharma, V. and Kumar, S. [2014], 'Velocity dispersion in an elastic plate with microstructure: effects of characteristic length in a couple stress model', *Meccanica* **49**(5), 1083–1090.

[120] Shaw, R. P. and Bugl, P. [1969], 'Transmission of plane waves through layered linear viscoelastic media', *The Journal of the Acoustical Society of America* **46**(3B), 649–654.

[121] Shodja, H. M., Tabatabaei, S. M. and Kamali, M. T. [2006], 'A piezoelectric-inhomogeneity system with imperfect interface', *International journal of engineering science* **44**(5), 291–311.

[122] Singh, B. and Kumar, R. [1998], 'Reflection and refraction of micropolar elastic waves at a loosely bonded interface between viscoelastic solid and micropolar elastic solid', *International journal of engineering science* **36**(2), 101–117.

[123] Singh, B. and Singh, S. [2014], 'Reflection and transmission of elastic waves at a loosely bonded interface between an elastic solid and a viscoelastic porous solid saturated by viscous liquid', *Global Journal of Researches In Engineering* **14**(3), 35–46.

[124] Singh, S. [2011], 'Love wave at a layer medium bounded by irregular boundary surfaces', *Journal of Vibration and Control* **17**(5), 789–795.

[125] Singh, S. S. and Tomar, S. K. [2008], 'qp-wave at a corrugated interface between two dissimilar pre-stressed elastic half-spaces', *Journal of Sound and Vibration* **317**(3), 687–708.

[126] Sivaraj, R., Kumar, B. R. and Prakash, J. [2012], 'Mhd mixed convective flow of viscoelastic and viscous fluids in a vertical porous channel', *Applications Appl Math* **7**, 99–116.

[127] Sneddon, I. N. [1952], 'The stress produced by a pulse of pressure moving along the surface of a semi-infinite solid', *Rendiconti del Circolo Matematico di Palermo* **1**(1), 57–62.

[128] Sokolnikoff, I. [1956], *Mathematical theory of Elasticity*, McGraw Hill, New York.

[129] Spencer, A. J. M. [1972], *Deformation of Fibre-reinforced Material*, Oxford University, United Kingdom.

[130] Spencer, A. J. M. [1974], 'Boundary layers in highly anisotropic plane elasticity', *International Journal of Solids and Structures* **10**(10), 1103–1123.

[131] Tomar, S. K. and Kaur, J. [2003], 'Reflection and transmission of sh-waves at a corrugated interface between two laterally and vertically heterogeneous anisotropic elastic solid half-spaces', *Earth, planets and space* **55**(9), 531–547.

[132] Tomar, S. K. and Kaur, J. [2007], 'Sh-waves at a corrugated interface between a dry sandy half-space and an anisotropic elastic half-space', *Acta Mechanica* **190**(1-4), 1–28.

[133] Toupin, R. A. [1962], 'Elastic materials with couple-stresses', *Archive for Rational Mechanics and Analysis* **11**(1), 385–414.

[134] Udias, A. [1999], *Principles of Seismology*, Cambridge University Press, Cambridge, England.

[135] Ungar, A. [1976], 'Wave generation in an elastic half-space by a normal point load moving uniformly over the free surface', *International Journal of Engineering Science* **14**(10), 935–945.

[136] Verma, P. D. S. and Rana, O. H. [1983], 'Rotation of a circular cylindrical tube reinforced by fibres lying along helices', *Mechanics of Materials* **2**(4), 353–359.

[137] Voigt, W. [1887], 'Theoretische studien fiber die elastizitatsverhiltnisse der kristalle (theoretical studies on the elasticity relationships of crystals)', *Abh. Gesch. Wissenschaften* **34**, 3–51.

[138] Wang, C. D., Wang, W. J., Lin, Y. T. and Ruan, Z. W. [2012], 'Wave propagation in an inhomogeneous transversely isotropic material obeying the generalized power law model', *Archive of Applied Mechanics* **82**(7), 919–936.

[139] Wang, X. and Zhong, Z. [2003], 'Three-dimensional solution of smart laminated anisotropic circular cylindrical shells with imperfect bonding', *International journal of solids and structures* **40**(22), 5901–5921.

[140] Wu, J. and Zhu, Z. [1992], 'The propagation of lamb waves in a plate bordered with layers of a liquid', *The Journal of the Acoustical Society of America* **91**(2), 861–867.

[141] Yang, J. F. C. and Lakes, R. S. [1981], 'Transient study of couple stress effects in compact bone: torsion', *Journal of biomechanical engineering* **103**(4), 275–279.

[142] Yang, J. F. C. and Lakes, R. S. [1982], 'Experimental study of micropolar and couple stress elasticity in compact bone in bending', *Journal of biomechanics* **15**(2), 91–98.